

BPC-01-300-1
Revision 0
January 1984

HOPE CREEK GENERATING STATION
PLANT UNIQUE ANALYSIS REPORT
VOLUME 1
GENERAL CRITERIA AND
LOADS METHODOLOGY

Prepared for:
Public Service Electric and Gas Company

Prepared by:
NUTECH Engineers, Inc.
San Jose, California

Prepared by:

Robert A. Lehnert

R. A. Lehnert, P.E.
Project Manager

Reviewed by:

R. A. Sanchez

R. A. Sanchez, P.E.
Principal Engineer

Approved by:

N. W. Edwards

N. W. Edwards, P.E.
President

Issued by:

Robert A. Lehnert

R. A. Lehnert, P.E.
Project Manager

8402230101 840210
PDR ADOCK 05000354
A PDR

nutech
ENGINEERS

TITLE: Hope Creek Generating
Station
Plant Unique Analysis
Report
Volume 1

DOCUMENT NUMBER: BPC-01-300-1
Revision 0

Robert A. Lehnert
R. A. Lehnert/Project Manager

RAL
Initials

Robert D. Quinn
R. D. Quinn/Senior Engineer

RDQ
Initials

R. A. Sanchez
R. A. Sanchez/Principal Engineer

RAS
Initials

D. K. Yoshida
D. K. Yoshida/Engineer

DKY
Initials

PAGE(S)	REV	PREPARED BY / DATE	ACCURACY CHECK BY / DATE	CRITERIA CHECK BY / DATE	REMARKS
ii	0	RAL / 1-17-84	DKY / 1-18-84	DKY / 1-18-84	
iii	0				
iv	0				
v	0				
vi	0				
vii	0				
viii	0				
ix	0				
x	0				
xi	0				
xii	0				
xiii	0				
xiv	0				
1-1.1	0				
1-1.2	0				
1-1.3	0				
1-1.4	0				
1-1.5	0				
1-1.6	0				
1-1.7	0				
1-1.8	0				
1-1.9	0	RAL / 1-17-84	DKY / 1-18-84	DKY / 1-18-84	

REVISION CONTROL SHEET
(CONTINUATION)

Hope Creek Generating Station
TITLE: Plant Unique Analysis Report
 Volume 1

REPORT NUMBER: BPC-01-300-1
Revision 0

PAGE(S)	REV	PREPARED BY / DATE	ACCURACY CHECK BY / DATE	CRITERIA CHECK BY / DATE	REMARKS
1-1.10	0	RAL/1-17-84	APK/1-18-84	ADKY/1-18-84	
1-1.11	0				
1-1.12	0				
1-1.13	0				
1-1.14	0				
1-1.15	0				
1-1.16	0				
1-1.17	0				
1-1.18	0				
1-1.19	0				
1-1.20	0				
1-1.21	0				
1-1.22	0				
1-1.23	0		ADKY/1-18-84	ADKY/1-18-84	
1-2.1	0		ROQ/1-18-84	ROQ/1-18-84	
1-2.2	0				
1-2.3	0				
1-2.4	0				
1-2.5	0				
1-2.6	0				
1-2.7	0				
1-2.8	0				
1-2.9	0				
1-2.10	0				
1-2.11	0				
1-2.12	0				
1-2.13	0				
1-2.14	0				
1-2.15	0				
1-2.16	0				
1-2.17	0		ROQ/1-18-84	ROQ/1-18-84	
1-2.18	0	RAL/1-17-84	RAS/1/18/84	RAS/1/18/84	

Hope Creek Generating
Station
TITLE: Plant Unique Analysis
Report
Volume 1

REVISION CONTROL SHEET
(CONTINUATION)

REPORT NUMBER: BPC-01-300-1
Revision 0

PAGE(S)	REV	PREPARED BY / DATE	ACCURACY CHECK BY / DATE	CRITERIA CHECK BY / DATE	REMARKS
1-2.19	0	RAL / 1-17-84	RAS 1/18/84	RAS 1/18/84	
1-2.20	0		RAS 1/18/84	RAS 1/18/84	
1-3.1	0		WKY / 1-18-84	WKY / 1-18-84	
1-3.2	0				
1-3.3	0				
1-3.4	0				
1-3.5	0				
1-3.6	0		WKY / 1-18-84	WKY / 1-18-84	
1-3.7	0		RDQ / 1-18-84	RDQ / 1-18-84	
1-3.8	0				
1-3.9	0				
1-3.10	0				
1-3.11	0				
1-3.12	0				
1-3.13	0				
1-3.14	0				
1-3.15	0		RDQ / 1-18-84	RDQ / 1-18-84	
1-3.16	0		WKY / 1-18-84	WKY / 1-18-84	
1-4.1	0	RAL / 1-17-84	RAS 1/18/84	RAS 1/18/84	
1-4.2	0		WKY / 1-18-84	WKY / 1-18-84	
1-4.3	0				
1-4.4	0				
1-4.5	0				
1-4.6	0				
1-4.7	0				
1-4.8	0				
1-4.9	0				
1-4.10	0				
1-4.11	0		WKY / 1-18-84	WKY / 1-18-84	
1-4.12	0		RAS 1/18/84	RAS 1/18/84	
1-4.13	0		RAS 1/18/84	RAS 1/18/84	
1-4.14	0				
1-4.15	0		WKY / 1-18-84	WKY / 1-18-84	

REVISION CONTROL SHEET
(CONTINUATION)

Hope Creek Generating Station
TITLE: Plant Unique Analysis
 Report
 Volume 1

REPORT NUMBER: BPC-01-300-1
 Revision 0

PAGE(S)	REV	PREPARED BY / DATE	ACCURACY CHECK BY / DATE	CRITERIA CHECK BY / DATE	REMARKS
1-4.16	0	RAL/1-17-84	RAS 1/18/84	RAS 1/18/84	
1-4.17	0		RAS 1/18/84	RAS 1/18/84	
1-4.18	0		WKY/1-18-84	WKY/1-18/84	
1-4.19	0		↓	↓	
1-4.20	0		WKY/1-18-84	WKY/1-18-84	
1-4.21	0		RAS 1/18/84	RAS 1/18/84	
1-4.22	0		RAS 1/18/84	RAS 1/18/84	
1-4.23	0		WKY/1-18-84	WKY/1-18/84	
1-4.24	0		↓	↓	
1-4.25	0		WKY/1-18-84	WKY/1-18-84	
1-4.26	0		↓	↓	
1-4.27	0		↓	↓	
1-4.28	0		↓	↓	
1-4.29	0		WKY/1-18-84	WKY/1-18-84	
1-4.30	0		RAS 1/18/84	RAS 1/18/84	
1-4.31	0		RAS 1/18/84	RAS 1/18/84	
1-4.32	0		WKY/1-18-84	WKY/1-18-84	
1-4.33	0		WKY/1-18-84	WKY/1-18-84	
1-4.34	0		RAS 1/18/84	RAS 1/18/84	
1-4.35	0		WKY/1-18-84	WKY/1-18-84	
1-4.36	0		↓	↓	
1-4.37	0		WKY/1-18-84	WKY/1-18-84	
1-4.38	0		↓	↓	
1-4.39	0		WKY/1-18-84	WKY/1-18-84	
1-4.40	0		RAS 1/18/84	RAS 1/18/84	
1-4.41	0		↓	↓	
1-4.42	0		↓	↓	
1-4.43	0		↓	↓	
1-4.44	0		↓	↓	
1-4.45	0		↓	↓	
1-4.46	0		RAS 1/18/84	RAS 1/18/84	
1-4.47	0		WKY/1-18-84	WKY/1-18-84	
1-4.48	0	RAL/1-17-84	WKY/1-18-84	WKY/1-18-84	

REVISION CONTROL SHEET

Hope Creek Generating (CONTINUATION)
Station
Plant Unique Analysis
Report
Volume 1

TITLE:

REPORT NUMBER: BPC-01-300-1
Revision 0

PAGE(S)	REV	PREPARED BY / DATE	ACCURACY CHECK BY / DATE	CRITERIA CHECK BY / DATE	REMARKS
1-4.49	0	RAL / 1-17-84	WKY / 1-18-84	WKY / 1-18-84	
1-4.50	0		WKY / 1-18-84	WKY / 1-18-84	
1-4.51	0		RAS 1/18/84	RAS 1/18/84	
1-4.52	0				
1-4.53	0				
1-4.54	0				
1-4.55	0				
1-4.56	0				
1-4.57	0				
1-4.58	0				
1-4.59	0				
1-4.60	0		RAS 1/18/84	RAS 1/18/84	
1-4.61	0		WKY / 1-18-84	WKY / 1-18-84	
1-4.62	0				
1-4.63	0		WKY / 1-18-84	WKY / 1-18-84	
1-4.64	0		RAS 1/18/84	RAS 1/18/84	
1-4.65	0		WKY / 1-18-84	WKY / 1-18-84	
1-4.66	0		RAS 1/18/84	RAS 1/18/84	
1-4.67	0		WKY / 1-18-84	WKY / 1-18-84	
1-4.68	0				
1-4.69	0		WKY / 1-18-84	WKY / 1-18-84	
1-4.70	0		RAS 1/18/84	RAS 1/18/84	
1-4.71	0				
1-4.72	0				
1-4.73	0				
1-4.74	0		RAS 1/18/84	RAS 1/18/84	
1-4.75	0		WKY / 1-18-84	WKY / 1-18-84	
1-4.76	0				
1-4.77	0		WKY / 1-18-84	WKY / 1-18-84	
1-4.78	0		RAS 1/18/84	RAS 1/18/84	
1-4.79	0		WKY / 1-18-84	WKY / 1-18-84	
1-4.80	0		WKY / 1-18-84	WKY / 1-18-84	
1-4.81	0	RAL / 1-17-84	RAS 1/18/84	RAS 1/18/84	

REVISION CONTROL SHEET

TITLE: Hope Creek Generating (CONTINUATION)
Station
Plant Unique Analysis
Report
Volume 1

REPORT NUMBER: BPC-01-300-1
Revision 0

PAGE(S)	REV	PREPARED BY / DATE	ACCURACY CHECK BY / DATE	CRITERIA CHECK BY / DATE	REMARKS
1-4.82	0	RAL/1-17-84	RAS 1/18/84	RAS 1/18/84	
1-4.83	0		WKY/1-18-84	WKY/1-18-84	
1-4.84	0		WKY/1-18-84	WKY/1-18-84	
1-4.85	0		RAS 1/18/84	RAS 1/18/84	
1-4.86	0		RAS 1/18/84	RAS 1/18/84	
1-4.87	0		WKY/1-18-84	WKY/1-18-84	
1-4.88	0		↓	↓	
1-4.89	0				
1-4.90	0		↓	↓	
1-4.91	0		WKY/1-18-84	WKY/1-18-84	
1-4.92	0		RAS 1/18/84	RAS 1/18/84	
1-4.93	0		WKY/1-18-84	WKY/1-18-84	
1-4.94	0		↓	↓	
1-4.95	0		WKY/1-18-84	WKY/1-18-84	
1-4.96	0		RAS 1/18/84	RAS 1/18/84	
1-4.97	0		RAS 1/18/84	RAS 1/18/84	
1-4.98	0		WKY/1-18-84	WKY/1-18-84	
1-4.99	0		↓	↓	
1-4.100	0		WKY/1-18-84	WKY/1-18-84	
1-4.101	0		RAS 1/18/84	RAS 1/18/84	
1-4.102	0		↓	↓	
1-4.103	0		RAS 1/18/84	RAS 1/18/84	
1-4.104	0		WKY/1-18-84	WKY/1-18-84	
1-4.105	0		↓	↓	
1-4.106	0		WKY/1-18-84	WKY/1-18-84	
1-4.107	0		RAS 1/18/84	RAS 1/18/84	
1-4.108	0		WKY/1-18-84	WKY/1-18-84	
1-4.109	0		WKY/1-18-84	WKY/1-18-84	
1-4.110	0		RAS 1/18/84	RAS 1/18/84	
1-4.111	0		WKY/1-18-84	WKY/1-18-84	
1-4.112	0		RAS 1/18/84	RAS 1/18/84	
1-4.113	0		↓	↓	
1-4.114	0	RAL/1-17-84	RAS 1/18/84	RAS 1/18/84	

Hope Creek Generating
Station
TITLE: Plant Unique Analysis
Report
Volume 1

REVISION CONTROL SHEET
(CONTINUATION)

REPORT NUMBER: BPC-01-300-1
Revision 0

PAGE(S)	REV	PREPARED BY / DATE	ACCURACY CHECK BY / DATE	CRITERIA CHECK BY / DATE	REMARKS
1-4.115	0	RAL/1-17-84	RAS 1/18/84	RAS 1/18/84	
1-4.116	0		RAS 1/18/84	RAS 1/18/84	
1-4.117	0		WKY/1-18-84	WKY/1-18-84	
1-4.118	0		RAS 1/18/84	RAS 1/18/84	
1-4.119	0		WKY/1-18-84	WKY/1-18-84	
1-4.120	0		RAS 1/18/84	RAS 1/18/84	
1-5.1	0		WKY/1-18-84	WKY/1-18-84	
1-5.2	0	RAL/1-17-84	WKY/1-18-84	WKY/1-18-84	

ABSTRACT

The primary containment for the Hope Creek Generating Station was designed, erected, pressure-tested, and N-stamped in accordance with the ASME Boiler and Pressure Vessel Code, Section III, 1974 Edition with addenda up to and including Winter 1974. These activities were performed for the Public Service Electric and Gas Company (PSE&G) by the Pittsburgh Des Moines Steel Company. Since then, new requirements which affect the design and operation of the primary containment system have been established. These requirements are defined in the Nuclear Regulatory Commission's (NRC) Safety Evaluation Report, NUREG-0661. The NUREG-0661 requirements define revised containment design loads postulated to occur during a loss-of-coolant accident or a safety-relief valve discharge event which are to be evaluated. In addition, NUREG-0661 requires that an assessment of the effects that these postulated events have on the operation of the containment system be performed.

This plant unique analysis report (PUAR) documents the efforts undertaken to address and resolve each of the applicable NUREG-0661 requirements for Hope Creek. It demonstrates, in accordance with NUREG-0661 acceptance criteria, that the design of the primary containment system is adequate and that original design safety margins have been restored. The Hope Creek PUAR is composed of the following six volumes:

- o Volume 1 - GENERAL CRITERIA AND LOADS METHODOLOGY
- o Volume 2 - SUPPRESSION CHAMBER ANALYSIS
- o Volume 3 - VENT SYSTEM ANALYSIS
- o Volume 4 - INTERNAL STRUCTURES ANALYSIS
- o Volume 5 - SAFETY RELIEF VALVE DISCHARGE PIPING ANALYSIS
- o Volume 6 - TORUS ATTACHED PIPING AND SUPPRESSION CHAMBER PENETRATION ANALYSES

Major portions of all volumes of this report have been prepared by NUTECH Engineers, Incorporated (NUTECH), acting as a consultant responsible to the Public Service Electric and Gas Company. Selected sections of Volumes 5 and 6 have been prepared by the Bechtel Power Corporation (acting as an agent responsible to the Public Service Electric and Gas Company).

This volume, Volume 1, provides introductory and background information regarding the reevaluation of the primary containment system including torus attached piping. It includes a description of the Hope Creek containment system, a description of the structural and mechanical acceptance criteria, and the hydrodynamic loads methodology used in the analyses presented in Volumes 2 through 6.

NOTE: Identification of the volume number precedes each page, section, subsection, table, and figure number.

TABLE OF CONTENTS

	<u>Page</u>
ABSTRACT	1-ii
LIST OF ACRONYMS	1-vii
LIST OF TABLES	1-x
LIST OF FIGURES	1-xii
1-1.0 INTRODUCTION	1-1.1
1-1.1 Containment System General Description	1-1.7
1-1.2 Review of Phenomena	1-1.9
1-1.2.1 LOCA-Related Phenomena	1-1.10
1-1.2.2 SRV Discharge Phenomena	1-1.12
1-1.3 Scope of Analysis	1-1.14
1-1.4 Evaluation Philosophy	1-1.16
1-2.0 PLANT UNIQUE CHARACTERISTICS	1-2.1
1-2.1 Plant Configuration	1-2.2
1-2.1.1 Suppression Chamber	1-2.5
1-2.1.2 Vent System	1-2.6
1-2.1.3 Internal Structures	1-2.8
1-2.1.4 SRV Discharge Piping	1-2.9
1-2.1.5 Torus Attached Piping and Penetrations	1-2.11
1-2.2 Operating Parameters	1-2.18
1-3.0 PLANT UNIQUE ANALYSIS CRITERIA	1-3.1
1-3.1 Hydrodynamic Loads: NRC Acceptance Criteria	1-3.2
1-3.1.1 LOCA-Related Load Applications	1-3.3
1-3.1.2 SRV Discharge Load Applications	1-3.5
1-3.1.3 Other Considerations	1-3.7

TABLE OF CONTENTS
(Continued)

	<u>Page</u>
1-3.2 Component Analysis: Structural Acceptance Criteria	1-3.8
1-3.2.1 Classification of Components	1-3.9
1-3.2.2 Service Level Assignments	1-3.10
1-3.2.3 Other Considerations	1-3.15
1-4.0 HYDRODYNAMIC LOADS METHODOLOGY AND EVENT SEQUENCE SUMMARY	1-4.1
1-4.1 LOCA-Related Loads	1-4.3
1-4.1.1 Containment Pressure and Temperature Response	1-4.5
1-4.1.2 Vent System Discharge Loads	1-4.6
1-4.1.3 Pool Swell Loads on Torus Shell	1-4.8
1-4.1.4 Pool Swell Loads on Elevated Structures	1-4.10
1-4.1.4.1 Impact and Drag Loads on the Vent System	1-4.11
1-4.1.4.2 Impact and Drag Loads on Other Structures	1-4.15
1-4.1.4.3 Pool Swell Froth Impingement Loads	1-4.18
1-4.1.4.4 Pool Fallback Loads	1-4.24
1-4.1.5 LOCA Water Jet Loads on Submerged Structures	1-4.27
1-4.1.6 LOCA Bubble-Induced Loads on Submerged Structures	1-4.33
1-4.1.7 Condensation Oscillation Loads	1-4.36
1-4.1.7.1 CO Loads on Torus Shell	1-4.37
1-4.1.7.2 CO Loads on Downcomers and Vent System	1-4.47
1-4.1.7.3 CO Loads on Submerged Structures	1-4.61
1-4.1.8 Chugging Loads	1-4.65
1-4.1.8.1 Chugging Loads on Torus Shell	1-4.67
1-4.1.8.2 Chugging Downcomer Lateral Loads	1-4.75
1-4.1.8.3 Chugging Loads on Submerged Structures	1-4.79

TABLE OF CONTENTS
(Concluded)

	<u>Page</u>
1-4.2 Safety Relief Valve Discharge Loads	1-4.83
1-4.2.1 SRV Actuation Cases	1-4.87
1-4.2.2 SRV Discharge Line Clearing Loads	1-4.93
1-4.2.3 SRV Loads on Torus Shell	1-4.98
1-4.2.4 SRV Loads on Submerged Structures	1-4.104
1-4.3 Event Sequence	1-4.108
1-4.3.1 Design Basis Accident	1-4.111
1-4.3.2 Intermediate Break Accident	1-4.117
1-4.3.3 Small Break Accident	1-4.119
1-5.0 LIST OF REFERENCES	1-5.1

LIST OF ACRONYMS

ACI	American Concrete Institute
ADS	Automatic Depressurization System
AISC	American Institute of Steel Construction
ASME	American Society of Mechanical Engineers
ATWS	Anticipated Transients Without Scram
BDC	Bottom Dead Center
BWR	Boiling Water Reactor
CDF	Cumulative Distribution Function
CO	Condensation Oscillation
DBA	Design Basis Accident
DC	Downcomer
DLF	Dynamic Load Factor
ECCS	Emergency Core Cooling System
FSAR	Final Safety Analysis Report
FSI	Fluid-Structure Interaction
FSTF	Full-Scale Test Facility
HNWL	High Normal Water Level
HPCI	High Pressure Coolant Injection
IBA	Intermediate Break Accident
I&C	Instrumentation and Control
ID	Inside Diameter
IR	Inside Radius
LDR	Load Definition Report (Mark I Containment Program)
LOCA	Loss-of-Coolant Accident

LIST OF ACRONYMS

(Continued)

LPCI	Low Pressure Coolant Injection
LTP	Long-Term Program
MC	Midcylinder
MCF	Modal Correction Factor
MJ	Mitered Joint
MVA	Multiple Valve Actuation
NEP	Non-Exceedance Probability
NOC	Normal Operating Conditions
NRC	Nuclear Regulatory Commission
NSSS	Nuclear Steam Supply System
NVB	Non-Vent Line Bay
OBE	Operating Basis Earthquake
OD	Outside Diameter
PSD	Power Spectral Density
PSE&G	Public Service Electric and Gas Company
PUA	Plant Unique Analysis
PUAAG	Plant Unique Analysis Application Guide
PUAR	Plant Unique Analysis Report
PULD	Plant Unique Load Definition
QSTF	Quarter-Scale Test Facility
RCIC	Reactor Core Isolation Cooling
RHR	Residual Heat Removal
RPV	Reactor Pressure Vessel

LIST OF ACRONYMS

(Concluded)

RSEL	Resultant Static-Equivalent Load
SBA	Small Break Accident
SBP	Small Bore Piping
SER	Safety Evaluation Report
SORV	Stuck-Open Safety Relief Valve
SRSS	Square Root of the Sum of the Squares
SRV	Safety Relief Valve
SRVDL	Safety Relief Valve Discharge Line
SSE	Safe Shutdown Earthquake
STP	Short-Term Program
SVA	Single Valve Actuation
TAP	Torus Attached Piping
VB	Vent Line Bay
VH	Vent Header
VL	Vent Line
VPP	Vent Pipe Penetration
ZPA	Zero Period Acceleration

LIST OF TABLES

<u>Number</u>	<u>Title</u>	<u>Page</u>
1-1.0-1	Hope Creek Containment Modification Summary	1-1.6
1-2.2-1	Primary Containment Operating Parameters	1-2.19
1-3.2-1	Event Combinations and Service Levels for Class MC Components and Internal Structures	1-3.11
1-3.2-2	Event Combinations and Service Levels for Class 2 and 3 Piping	1-3.13
1-4.0-1	Plant Unique Analysis/NUREG-0661 Load Sections Cross-Reference	1-4.2
1-4.1-1	Hydrodynamic Mass and Acceleration Drag Volumes for Two-Dimensional Structural Components (Length L For All Structures)	1-4.31
1-4.1-2	Plant Unique Parameters for LOCA Bubble Drag Load Development	1-4.35
1-4.1-3	DBA Condensation Oscillation Torus Shell Pressure Amplitudes	1-4.41
1-4.1-4	FSTF Response to Condensation Oscillation	1-4.43
1-4.1-5	Condensation Oscillation Onset and Duration	1-4.44
1-4.1-6	Downcomer Internal Pressure Loads for DBA Condensation Oscillation	1-4.51
1-4.1-7	Downcomer Differential Pressure Loads for DBA Condensation Oscillation	1-4.52
1-4.1-8	Downcomer Internal Pressure Loads For IBA Condensation Oscillation	1-4.53
1-4.1-9	Downcomer Differential Pressure Loads For IBA Condensation Oscillation	1.4.54
1-4.1-10	Condensation Oscillation Vent System Internal Pressures	1.4.55
1-4.1-11	Amplitudes at Various Frequencies for Condensation Oscillation Source Function for Loads on Submerged Structures	1-4.64

LIST OF TABLES
(Concluded)

<u>Number</u>	<u>Title</u>	<u>Page</u>
1-4.1-12	Chugging Onset and Duration	1-4.70
1-4.1-13	Post-Chug Rigid Wall Pressure Amplitudes on Torus Shell Bottom Dead Center	1-4.71
1-4.1-14	Amplitudes at Various Frequencies for Chugging Source Function for Loads on Submerged Structures	1-4.81
1-4.2-1	SRV Loss Case/Initial Conditions	1-4.92
1-4.2-2	Plant Unique Initial Conditions for Actuation Cases Used for SRVDL Clearing Transient Load Development	1-4.96
1-4.2-3	SRVDL Analysis Parameters	1-4.97
1-4.2-4	Comparison of Analysis and Monticello Test Results	1-4.101
1-4.3-1	SRV and LOCA Structural Loads	1-4.110
1-4.3-2	Event Timing Nomenclature	1-4.112
1-4.3-3	SRV Discharge Load Cases for Mark I Structural Analysis	1-4.113

LIST OF FIGURES

<u>Number</u>	<u>Title</u>	<u>Page</u>
1-2.1-1	Plan View of Containment	1-2.3
1-2.1-2	Elevation View of Containment	1-2.4
1-2.1-3	Suppression Chamber Section - Midcylinder Vent Line Bay	1-2.13
1-2.1-4	Suppression Chamber Section - Mitered Joint	1-2.14
1-2.1-5	Suppression Chamber Section - Midcylinder Non-Vent Bay	1-2.15
1-2.1-6	Developed View of Suppression Chamber Segment	1-2.16
1-2.1-7	Vent Header - Downcomer Intersection Stiffening Details	1-2.17
1-4.1-1	Downcomer Impact and Drag Pressure Transient	1-4.13
1-4.1-2	Application of Impact and Drag Pressure Transient to Downcomer	1-4.14
1-4.1-3	Pulse Shape for Impact and Drag on Cylindrical Structures	1-4.16
1-4.1-4	Pulse Shape for Impact and Drag on Flat Plate Structures	1-4.17
1-4.1-5	Froth Impingement Zone - Region I	1-4.22
1-4.1-6	Froth Impingement Zone - Region II	1-4.23
1-4.1-7	Condensation Oscillation Baseline Rigid Wall Pressure Amplitudes on Torus Shell Bottom Dead Center	1-4.45
1-4.1-8	Condensation Oscillation - Torus Vertical Cross-Section Pressure Distribution	1-4.46
1-4.1-9	Condensation Oscillation Downcomer Dynamic Load	1-4.56
1-4.1-10	Downcomer Pair Internal Pressure Loading for DBA CO	1-4.57

LIST OF FIGURES
(Continued)

<u>Number</u>	<u>Title</u>	<u>Page</u>
1-4.1-11	Downcomer Pair Differential Pressure Loading for DBA CO	1-4.58
1-4.1-12	Downcomer CO Dynamic Load Application	1-4.59
1-4.1-13	Downcomer Internal Pressure Loading for IBA CO	1-4.60
1-4.1-14	Typical Chugging Pressure Trace on the Torus Shell	1-4.66
1-4.1-15	Chugging - Torus Longitudinal Distribution for Asymmetric Pressure Amplitude	1-4.72
1-4.1-16	Chugging - Torus Vertical Cross-Section Pressure Distribution	1-4.73
1-4.1-17	Post-Chug Rigid Wall Pressure Amplitudes on Torus Shell Bottom Dead Center	1-4.74
1-4.1-18	Probability of Exceeding a Given Force Per Downcomer for Different Numbers of Downcomers	1-4.78
1-4.2-1	T-quencher and SRV Discharge Line	1-4.85
1-4.2-2	Elevation and Section Views of T-quencher Arm Hole Patterns	1-4.86
1-4.2-3	Comparison of Predicted and Measured Shell Pressure Time-Histories for Monticello Test 801	1-4.102
1-4.2-4	Modal Correction Factors for Analysis of SRV Discharge Torus Shell Loads	1-4.103
1-4.2-5	Plan View of T-quencher Arm Water Jet Sections	1-4.107
1-4.3-1	Loading Condition Combinations for the Vent Header, Main Vents, Downcomers, and Torus Shell During a DBA	1-4.114
1-4.3-2	Loading Condition Combinations for Submerged Structures During a DBA	1-4.115

LIST OF FIGURES
(Concluded)

<u>Number</u>	<u>Title</u>	<u>Page</u>
1-4.3-3	Loading Condition Combinations for Structures Above Suppression Pool During a DBA	1-4.116
1-4.3-4	Loading Condition Combinations for the Vent Header, Main Vents, Downcomers, Torus Shell, and Submerged Structures During an IBA	1-4.118
1-4.3-5	Loading Condition Combinations for the Vent Header, Main Vents, Downcomers, Torus Shell, and Submerged Structures During a SBA	1-4.120

INTRODUCTION

The primary containment for the Hope Creek Generating Station was designed, erected, pressure-tested, and N-stamped in accordance with the ASME Code, Section III, 1974 Edition with addenda up to and including Winter 1974. During the course of this effort, large-scale testing for the Mark III containment system and in-plant testing for Mark I primary containment systems were being performed in which new suppression chamber hydrodynamic loads were identified. The new loads are related to the postulated loss-of-coolant accident (LOCA) and safety relief valve (SRV) actuation.

The evaluation of the effects of these new loads were identified by the NRC as a generic open item for utilities with Mark I containments. To determine the magnitude, time characteristics, etc., of the dynamic loads in a timely manner and to identify courses of action needed to resolve any outstanding safety concerns, the utilities with Mark I containments formed the Mark I Owners Group. The Mark I Owners Group established a two-part program consisting of: (1) a short-term program (STP) which was completed in 1976, and (2) a long-term program

(LTP). The LTP was completed with the submittal of the "Mark I Containment Program Load Definition Report" (LDR) (Reference 1), the "Mark I Containment Program Structural Acceptance Criteria Plant Unique Analysis Application Guide" (PUAAG) (Reference 2), and supporting reports documenting experimental and analytical tasks of the long-term program. The NRC reviewed the LTP generic documents and issued acceptance criteria to be used during the implementation of the Mark I plant unique analyses. The NRC acceptance criteria are described in Appendix A of NUREG-0661 (Reference 3).

The objective of the LTP was to establish final design loads and load combinations and to verify that the existing or modified containment and related structures are capable of withstanding these loads with acceptable design margins. However, the original LTP completion schedule was not compatible with the construction schedule for Hope Creek. To comply with the objectives of the LTP and to meet the plant construction schedule, PSE&G committed to a containment evaluation program that provided design, analysis, and construction before the final loads and load combinations were determined by the Mark I Owners Group.

Accordingly, the design basis for the Hope Creek containment was revised in 1977 to include the newly defined suppression pool hydrodynamic loads. As the LTP loads had not yet been finalized, the characteristics of the hydrodynamic loads added to the containment design basis were established using available generic documents, with the objective of developing conservative design loads which would allow early plant construction with a high probability of bounding the final loads. These loadings and the resulting containment design are documented in the plant's Final Safety Analysis Report (FSAR) (Reference 4).

Examination of the containment geometry described in the Hope Creek FSAR reveals that the hydrodynamic loads added to the design basis resulted in a substantial containment design upgrade as compared to earlier Mark I containment designs. Examples of the design changes made include the use of a 1" thick torus shell, additional midbay ring beams and torus supports, use of a 9/16" thick vent header, additional vent system supports, downcomer bracing, and many others. As a result, the final LTP loads defined in NUREG-0661 have resulted in fewer, less

extensive containment modifications for Hope Creek. A summary of the containment modifications developed to address the NUREG-0661 requirements is provided in Table 1-1.0-1. The containment geometry is discussed in Section 1-2.1. The installation of these modifications and the associated engineering evaluations will be completed before fuel load.

The FSAR for Hope Creek up to and including Amendment 2 was submitted to the NRC for review by the Public Service Electric and Gas Company in October of 1983. A summary of ongoing efforts to address and resolve the NUREG-0661 requirements which affect the Hope Creek containment is included in Appendix 3b of the FSAR.

Some requirements of NUREG-0661, such as the installation of a suppression pool temperature monitoring system are addressed in Section 6.2.1.1.10 of Amendment 1 of the FSAR. The remaining requirements of NUREG-0661 are addressed in this PUAR. The assessment of other related issues, such as the low-low set logic design, drywell-wetwell vacuum breakers, and emergency procedures guidelines for 10 minute ADS, will be contained in separate submittals. References made

to the plant's FSAR in the PUAR include information contained in the initial submittal of the FSAR as well as Amendments 1 and 2 to the FSAR.

Accordingly, with the submittal of this PUAR, Public Service Electric and Gas Company believes that the containment evaluation program documented herein has addressed the requirements of NUREG-0661 for Hope Creek.

Table 1-1.0-1

HOPE CREEK CONTAINMENT MODIFICATION SUMMARY

ITEM	MODIFICATION DESCRIPTION (1)	
TORUS	COLUMN CONNECTIONS REINFORCED	
	RING BEAM COVER PLATES ADDED	
	MIDCYLINDER RING BEAM EXTENSIONS ADDED	
	RING BEAMS REINFORCED Laterally	
	COLUMN BASEPLATES REINFORCED	
VENT SYSTEM	DOWNCOMERS SHORTENED	
INTERNAL STRUCTURES	CATWALK	GRATING STRINGERS ADDED
		SUPPORTS REINFORCED
		GRATING REORIENTED
		HANDRAILS REPLACED
SRV PIPING	QUENCHER AND QUENCHER SUPPORTS ADDED	
TORUS ATTACHED PIPING	SUPPORTS ADDED	
	SUPPORTS REINFORCED	
	TORUS PENETRATIONS REINFORCED	
	INTERNAL RHR RETURN REROUTED AND ELBOWS ADDED	
SYSTEMS MODIFICATIONS	SRV LOW-LOW SET LOGIC ADDED	
	SUPPRESSION POOL TEMPERATURE MONITORING SYSTEM ADDED	

NOTE:

1. MODIFICATIONS TO BE INSTALLED BY FUEL LOAD.

BPC-01-300-1
Revision 0

The Mark I containment is a pressure suppression system which houses the Boiling Water Reactor (BWR) pressure vessel, the reactor coolant recirculation loops, and other branch connections of the Nuclear Steam Supply System. The containment system consists of a drywell, a pressure suppression chamber (wetwell or torus) approximately half-filled with water, and a vent system connecting the drywell to the suppression chamber. The toroidal shaped suppression chamber is located below and encircles the drywell. The drywell-to-wetwell main vents (vent lines, vent pipes) are connected to a vent header (ring header) contained within the airspace of the wetwell. Downcomers project from the vent header and terminate below the water surface of the suppression pool. The suppression chamber, vent system, and related internal structures are described in greater detail in Sections 1-2.1.1 thru 1-2.1.3 and in Volumes 2 and 3.

BWR's utilize safety relief valves attached to the main steam lines as a means of primary system over-pressure protection. The outlet of each valve is connected to discharge piping (SRV piping or SRVDL)

which is routed to the suppression pool. T-quencher discharge devices are attached to the end of each SRV discharge line. The SRV discharge lines are described in detail in Section 1-2.1.4 and in Volume 5.

Mark I containment systems utilize various process piping systems (TAP) attached to the suppression chamber. These piping systems include both large (LBP) and small bore (SBP) lines which perform both essential and non-essential containment functions. Small bore piping systems are attached directly to the suppression chamber or to large bore piping systems. The torus-attached piping systems are described in Section 1-2.1.5 and in Volume 6.

The following subsections provide a brief qualitative description of the various phenomena that could occur during a postulated LOCA and during SRV actuations. The LDR (Reference 1) provides a detailed description of the hydrodynamic loads which these phenomena could impose upon the suppression chamber and related structures. Section 1-4.0 presents the load definition procedures used to develop the plant unique hydrodynamic loads for Hope Creek.

Immediately following a postulated design basis accident (DBA) LOCA, the pressure and temperature of the drywell and vent system atmosphere rapidly increase. With the drywell pressure increase, the water initially present in the downcomers is accelerated into the suppression pool until the water is cleared from the downcomers. Following downcomer water clearing, the downcomer air, which is essentially at drywell pressure, is exposed to the relatively low pressure in the wetwell, producing a downward reaction force on the torus. The consequent bubble expansion causes the pool water to swell in the torus (pool swell), compressing the airspace above the pool. This airspace compression results in an upward reaction force on the torus. Eventually, the bubbles "break through" to the torus airspace, equalizing the pressures. An air-water froth mixture continues upward due to the momentum previously imparted to the water, causing impingement loads on elevated structures. The transient associated with this rapid drywell air venting to the suppression pool typically lasts for 3 to 5 seconds.

Following air carryover, there is a period of high steam flow through the vent system. The discharge of steam into the pool and its subsequent condensation causes pool pressure oscillations which are transmitted to submerged structures and the torus shell. This phenomenon is referred to as condensation oscillation (CO). As the reactor vessel depressurizes, the steam flowrate to the vent system decreases. Steam condensation during this period of reduced steam flow is characterized by up-and-down movement of the water-steam interface within the downcomer as the steam volumes are condensed and replaced by surrounding pool water. This phenomenon is referred to as chugging.

Postulated intermediate break accident (IBA) and small break accident (SBA) LOCA's produce drywell pressure transients which are sufficiently slow that the dynamic effects of vent clearing and pool swell are negligible. However, CO and chugging occur for an IBA and chugging occurs for a SBA.

1-1.2.2 SRV Discharge Phenomena

Hope Creek is equipped with 14 SRV's to control primary system pressure during transient conditions. The SRV's are mounted on the main steam lines inside the drywell, with the discharge piping routed down the main vents into the suppression pool. When a SRV is actuated steam is released from the primary system and discharges into the suppression pool where it is condensed.

Prior to the initial actuation of a SRV, the SRV piping contains air at atmospheric pressure and suppression pool water in the submerged portion of the piping. Following SRV actuation, steam enters the SRV piping and compresses the air within the line expelling the water slug into the suppression pool. During water clearing, the SRV piping undergoes a transient pressure loading.

Once the water has been cleared from the T-quencher discharge device, the compressed air enters the pool as high pressure bubbles. These bubbles expand, resulting in an outward acceleration of the surrounding pool water. The momentum of the accelerated water results in an overexpansion of the

bubbles, causing the bubble pressure to become negative relative to the ambient pressure of the surrounding pool. This negative bubble pressure slows and reverses the motion of the water, leading to a compression of the bubbles and a positive pressure relative to that of the pool. The bubbles continue to oscillate in this manner as they rise to the pool surface. The positive and negative pressures developed due to this phenomenon attenuate with distance and result in an oscillatory pressure loading on the "wetted" portion of the torus shell and submerged structures.

The structural and mechanical containment components addressed in the subsequent volumes of this report include the following.

o Containment Vessels

- The torus shell with associated penetrations, ring beams, and support attachments
- The torus supports
- The vent lines between the drywell and the vent header, including the SRV piping penetrations
- The local region of the drywell at the vent line penetrations
- The expansion bellows between the vent lines and the torus shell
- The vent header and attached downcomers
- The vent header supports
- The vacuum breaker penetrations at the vent line
- The downcomer bracing system and reinforcement plates

- o Internal Structures
 - The suppression chamber internal structures, including the monorail and catwalk and their supports
- o The safety-relief valve discharge piping, T-quenchers, and their supports
- o The internal and external torus-attached piping (TAP) systems and their various branch connections
 - The piping supports
 - The torus penetrations
 - The operability of valves
 - The operability of equipment

As discussed in Section 1-1.0, the requirements for suppression pool temperature monitoring are addressed in the plant's FSAR

The development of event sequences, basic assumptions, load definitions, analysis techniques, and all the other aspects of the Hope Creek plant unique analysis are specifically formulated to provide a conservative evaluation. This section describes, in qualitative terms, some of the conservative elements inherent in the Hope Creek plant unique analysis.

Event Sequences and Assumptions

Implicit in the analysis of a LOCA is the assumption that the event will occur, although the probability of such pipe breaks is low. No credit is taken for detection of leaks to prevent loss-of-coolant accidents. Furthermore, various sizes of pipe breaks are evaluated to consider various effects. The large, instantaneous pipe breaks are considered to evaluate the initial, rapidly occurring events such as vent system pressurization and pool swell. Smaller pipe breaks are analyzed to maximize prolonged effects such as CO and chugging.

The various LOCA's analyzed are assumed to occur coincident with plant conditions which maximize the parameter of interest. For example, the reactor is assumed to be at 102% of rated power; a single failure is assumed; and no credit is taken for normal auxiliary power. Operator action which can mitigate effects of a LOCA is assumed to be unavailable for a specified period. Other assumptions are also selected to maximize the particular parameter to be evaluated. This approach results in a conservative evaluation since the plant conditions are not likely to be in this worst case situation if a LOCA were to occur.

Test Results and Load Definitions

The load definitions utilized in the Hope Creek plant unique analysis (PUA) are based on conservative test results and analyses. For example, the LOCA steam condensation loads (CO and chugging) are based on tests in the Mark I Full-Scale Test Facility (FSTF). The FSTF is a full-size 1/16 segment of a Mark I torus. To ensure that conservative results would be obtained on a generic basis, the FSTF was specifically designed and constructed to promote rapid air and steam flow from

the drywell to the wetwell. While this maximizes hydrodynamic loads, it does not take into account the features of actual plants which would mitigate the LOCA effects. Actual Mark I drywells have piping and equipment which would absorb some of the energy released during a loss-of-coolant accident. There are other features of the FSTF which are not typical of actual plant configurations, yet contribute to more conservative load definitions. Pre-heating of the drywell to minimize condensation and heat losses is an example of this feature. Additionally, the load definitions developed from FSTF data apply the maximum observed load over the entire period during which the load may occur. This conservative treatment takes no credit for the load variation observed in the tests.

The LOCA pool swell loads were developed from similarly conservative tests at the Quarter-Scale Test Facility (QSTF). These tests were performed with the driving medium consisting of 100% noncondensables. This maximizes pool swell because this phenomenon would be driven by condensable steam if a LOCA were to occur in an actual plant. The QSTF tests also minimized the loss coefficient and maximized the drywell pressurization rate, thus

maximizing the pool swell loads. The drywell pressurization rate used in the tests was calculated using conservative analytical modeling and initial conditions. Structures above the pool are assumed to be rigid when analyzed for pool swell impact and drag loads. This assumption maximizes loads and is also used to evaluate loads on submerged structures.

The methodology used to develop SRV loads are based on conservative assumptions, modeling techniques, and full and subscale test data. Safety relief valve loads are calculated using a minimum or manufacturer-specified SRV opening time, a maximum steam flow rate, and a maximum steam line pressure. Appropriate assumptions are also applied to conservatively predict SRV load frequency ranges. The SRV loads on submerged structures are similarly determined with additional assumptions that maximize the pressure differential across the structure due to bubble pressure phasing. The conservatism in the SRV load definition approach has been demonstrated by in-plant tests performed at several other plants. All such tests have confirmed that actual plant responses are significantly less than predicted. The Hope Creek in-plant SRV tests are expected to confirm similar conservatisms.

Load Combinations

Conservative assumptions have also been made in developing the combinations of loading phenomena to be evaluated. Many combinations of loading phenomena are investigated although it is very unlikely for such combinations of phenomena to occur. For example, mechanistic analysis has shown that a SRV cannot actuate during the pool swell phase of a design basis loss-of-coolant accident. However, that combination of loading phenomena is evaluated. Both the pool swell and SRV load phenomena involve pressurized air bubbles in the pool and the structural response to these two different bubbles is assumed to be additive, either by absolute sum or by the square root of the sum of the squares (SRSS) method. However, this is a very conservative assumption since two oscillatory bubbles from independent events cannot physically combine to form one bubble at a pressure higher than the individual bubbles. This rationale is also valid for other hydrodynamic phenomena in the pool such as CO and chugging, which are also combined with SRV discharge effects.

When evaluating the structural response to combinations of loading phenomena, the peak responses due to the various loading phenomena are assumed to occur at the same time. While this is not an impossible occurrence, the probability that the actual responses will combine in that fashion is very remote. Furthermore, the initiating events themselves (e.g., LOCA or safe shutdown earthquake) are of extremely low probability.

Analysis Techniques

The methodology used for analyzing LOCA and SRV loads also contributes to conservatism. These loads are assumed to be smooth curves of regular or periodic shape. This simplifies load definitions and analyses, but maximizes predicted responses. Data from full scale tests show actual forcing functions to be much less "pure" or "perfect" than those assumed for analysis.

The analyses generally treat a nonlinear problem as a linear, elastic problem with the load "tuned" to the structural frequencies which produce maximum response. The nonlinearities which exist in both the pool and structural dynamics would preclude the

attainment of the elastic transient and steady-state responses that are predicted mathematically.

Inherent in the structural analyses are additional conservatisms. Damping is assumed to be low to maximize response, but in reality, damping is likely to be much higher. Conservative reductions in material thicknesses are made during containment stress calculations to account for corrosion. Allowable stress levels are low compared to the expected material capabilities. Conservative boundary conditions are also used in the analyses.

Conclusion

The loads, methods, and results described above and elsewhere in this report demonstrate that the margins of safety which actually existed for the original design loads have not only been restored, but have, in some cases, been increased. The advancements in understanding the hydrodynamic phenomena and in the structural analyses and modeling techniques have substantially increased since the original design and analysis were completed. This increased understanding and analysis capability is applied to the original loads

as well as to the newly defined loads. Thus, not only have the original safety margins been restored, but even greater margins now exist than in the original design.

1-2.0

PLANT UNIQUE CHARACTERISTICS

This section describes the general plant unique geometric and operating parameters applicable to the evaluation of the primary containment system. Specific details are provided in subsequent volumes, where the detailed analyses of individual components are described.

The Hope Creek primary containment system is a General Electric Company Mark I design with a drywell and toroidal suppression chamber. The major components and basic dimensions of the containment are shown in Figures 1-2.1-1 and 1-2.1-2.

This report section provides a general description of the suppression chamber, vent system, internal structures, SRV piping, and torus-attached piping. These containment components are described in greater detail in Volumes 2 through 6.

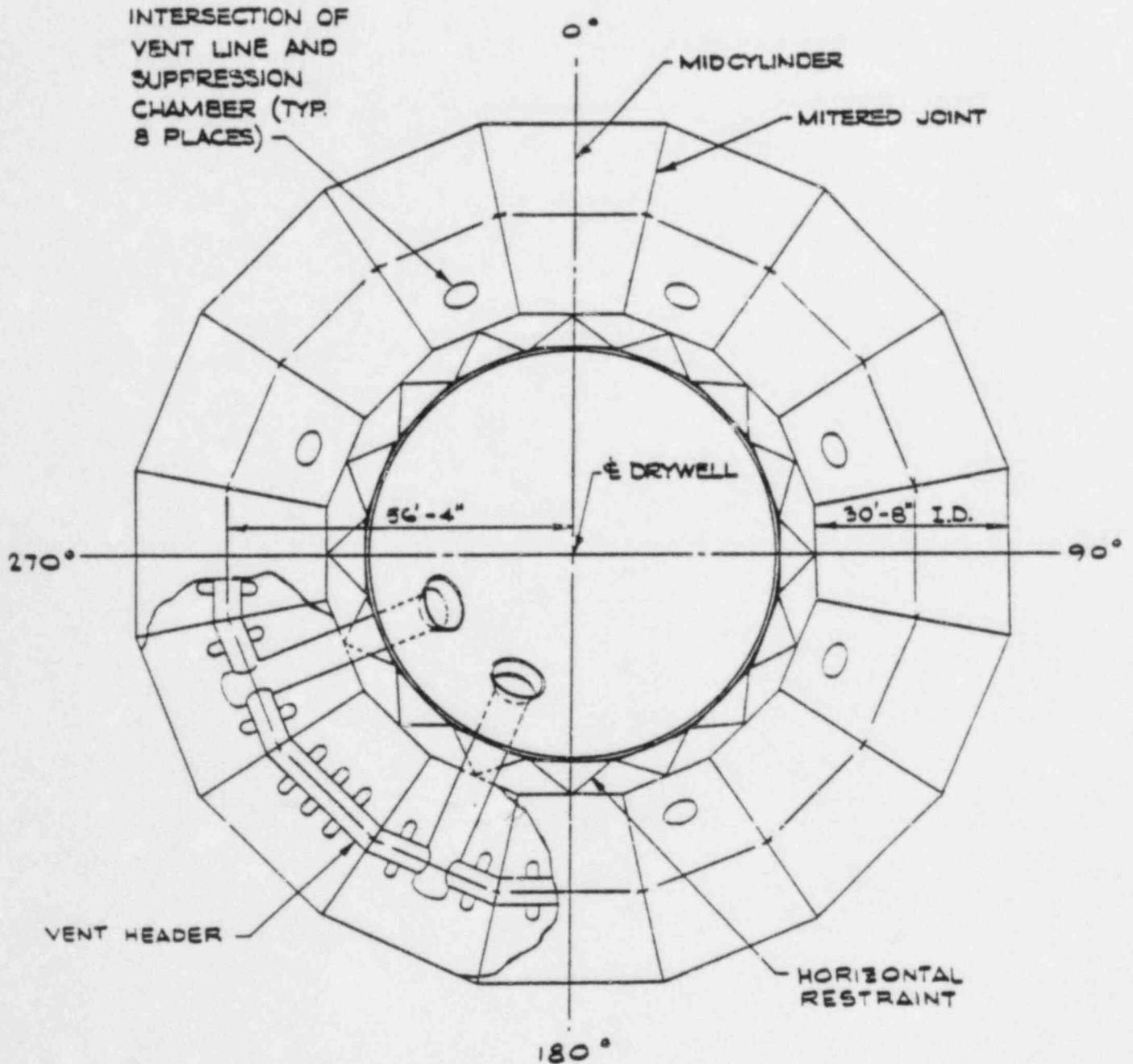


Figure 1-2.1-1

PLAN VIEW OF CONTAINMENT

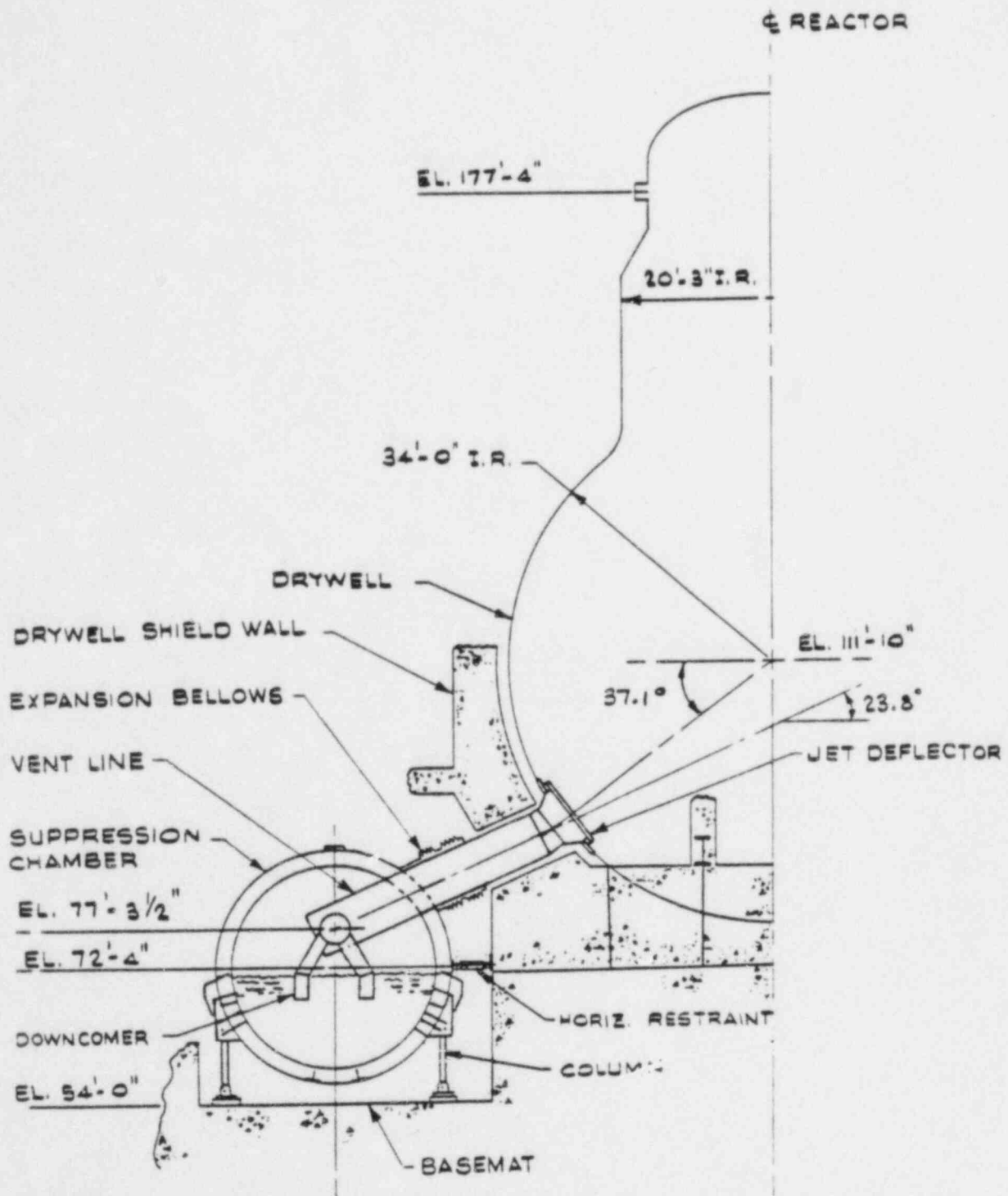


Figure 1-2.1-2
ELEVATION VIEW OF CONTAINMENT

The suppression chamber is in the general form of a torus and is constructed of 16 mitered cylindrical shell segments as shown in Figure 1-2.1-1. The mitered cylinders which make up the torus have an inside diameter of 30'-8", with a shell plate thickness of 1". The radius from the centerline of the drywell to the center of the torus at a section taken midway between the mitered joints is 56'-4".

The suppression chamber shell is reinforced at each mitered joint and at the midpoint of each mitered cylinder by T-shaped ring beams. The centerline of the ring beam at the mitered joint is offset 3-1/2" in a plane parallel to the plane of the mitered joint. The flange and cover plates of the mitered joint ring beams are rolled to a constant inside radius. The mitered joint ring beam web depth varies around the circumference of the suppression chamber. The midcylinder ring beams are of constant depth. The components of the suppression chamber are shown in Figures 1-2.1-3 through 1-2.1-5.

The drywell is connected to the suppression chamber by eight vent lines. The vent lines are connected to a common header within the suppression chamber. Eighty downcomers are connected to the vent header which terminate below the normal water level of the suppression pool. A bellows assembly at each vent line suppression chamber penetration permits differential expansion between the drywell and the suppression chamber to occur. The general arrangement of the vent system is shown in Figures 1-2.1-3 through 1-2.1-7.

The vent lines have a 6'-2" inside diameter with a nominal 9/16" wall thickness. The upper ends of the vent lines include a locally thickened conical transition segment at the penetration to the drywell. Inside the suppression chamber, the nominal thickness of the vent line is increased to 1-1/2", and is further increased to 2" near the vent header junction. The end of the cylindrical vent line in the suppression chamber is capped with a 3" thick plate, which is penetrated by a 24" diameter drywell/wetwell vacuum breaker support pipe. There

are 24" GPE vacuum breakers located on each of the eight vent lines, as shown in Figure 1-2.1-3.

The vent header inside the suppression chamber has a 4'-3" inside diameter, and a 9/16" nominal wall thickness. The downcomers have a 2'-0" outside diameter and a 3/8" nominal wall thickness. A longitudinal bracing system stiffens the downcomer intersections in a direction parallel to the vent header. Additional stiffening is provided in the plane of the downcomers by crotch plates between the downcomers and by outer gusset plates as shown in Figure 1-2.1-7.

1-2.1.3 Internal Structures

The location of the catwalk relative to other major components within the suppression chamber is shown in Figures 1-2.1-3 through 1-2.1-5. The catwalk is located parallel to the longitudinal centerline of each suppression chamber mitered cylinder. The catwalk is supported by hangers at the mitered joint ring beam and at two locations between each mitered joint.

The location of the monorail relative to the other major components within the suppression chamber is shown in Figures 1-2.1-3 through 1-2.1-5. The monorail forms a complete circle around the inside of the suppression chamber. The monorail supports consist of plates and angles providing vertical and horizontal support.

1-2.1.4 SRV Discharge Piping

The SRV piping inside the drywell and the suppression chamber consists of fourteen 10 inch diameter Schedule 80 discharge lines. These discharge lines enter the suppression chamber from the interior of the vent line through a reinforced penetration in the vent line as shown in Figure 1-2.1-3. From the vent line, the piping runs horizontally to the suppression chamber mitered joint, parallel to the vent header. The piping then turns and runs diagonally to a point below the vent header directly above bottom dead center of the mitered joint ring beam, and then runs vertically down into the suppression pool.

Standard Mark I T-quenchers, developed by General Electric, are located at the mitered joints, with the quencher arms located in the plane of the vertical centerline of the suppression chamber as shown in Figure 1-2.1-6. Each T-quencher is supported by a quencher support pipe which is attached to three adjacent ring girders.

The SRV piping in the drywell is supported by hangers, struts, and snubbers connected to the back-up steel structures. Supports for the SRV piping are provided by a frame type support assembly inside the vent line, and by struts attached to the mitered joint ring beam and vent header inside the suppression chamber.

The large bore TAP systems consist of 4" and larger nominal diameter piping, which penetrate or are directly attached to the suppression chamber. Large bore TAP lines range in size from 4" to 24" nominal diameter and have varying schedules.

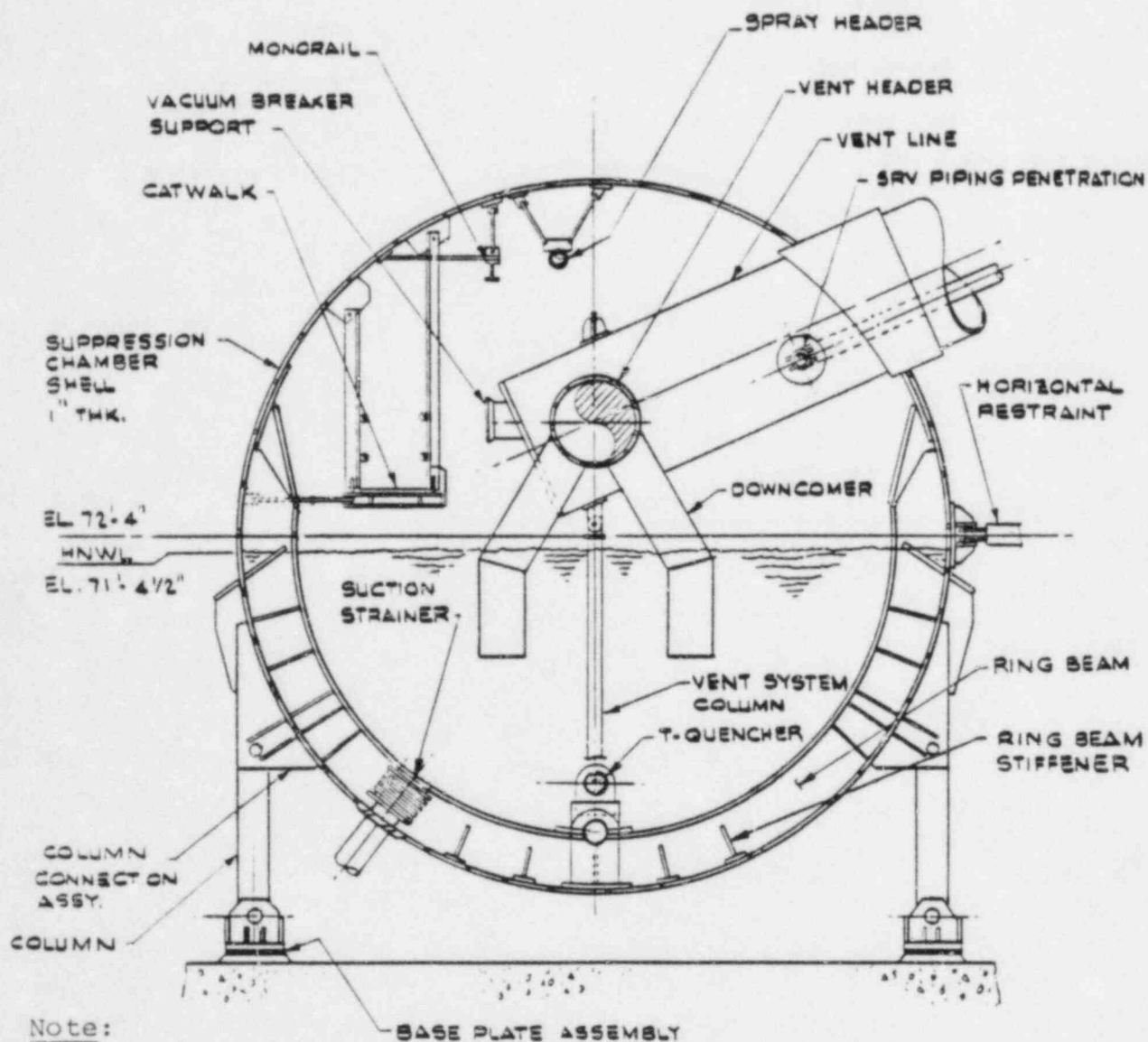
Large bore TAP may be grouped into two general categories: (1) torus external piping, and (2) torus internal piping. Examples of systems with only torus external piping are the residual heat removal (RHR) pump suction lines and the emergency core cooling system (ECCS) suction lines. Typical systems having both torus external and internal piping are the high pressure coolant injection (HPCI) turbine exhaust line and the residual heat removal (RHR) discharge lines. Typical internal large bore TAP systems are shown in Figures 1-2.1-3 through 1-2.1-5.

The small bore TAP for Hope Creek consists of piping with a nominal diameter of less than 4", which is attached to the suppression chamber or to the large bore torus attached piping.

The small bore piping (SBP) lines may be grouped into the following system types:

- (1) Cantilevered Drains and Vents
- (2) Torus Attached SBP lines
- (3) SBP lines attached to large bore TAP lines

The TAP systems penetrate the suppression chamber at many locations. The principal components of the penetrations are the nozzles, the insert plates, and the nozzle reinforcements. The nozzle extends from the outer circumferential pipe weld through the insert plate to the inner circumferential pipe weld or flange. The insert plate provides local reinforcement of the suppression chamber shell adjacent to the penetration.



Note:

1. Downcomer stiffener plates not shown for clarity.

Figure 1-2.1-3

SUPPRESSION CHAMBER SECTION - MIDCYLINDER VENT LINE BAY

BPC-01-300-1
Revision 0

1-2.13

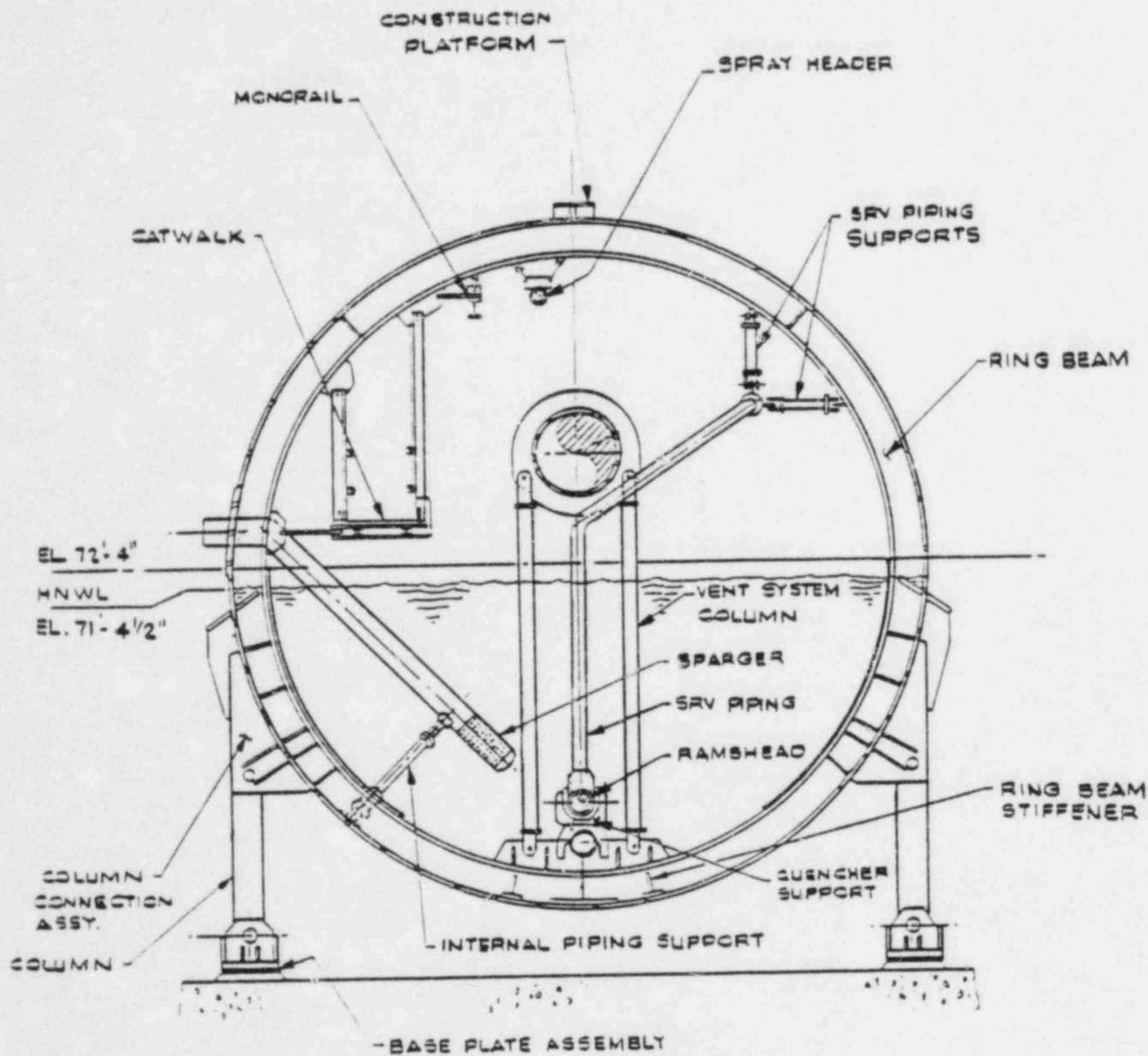
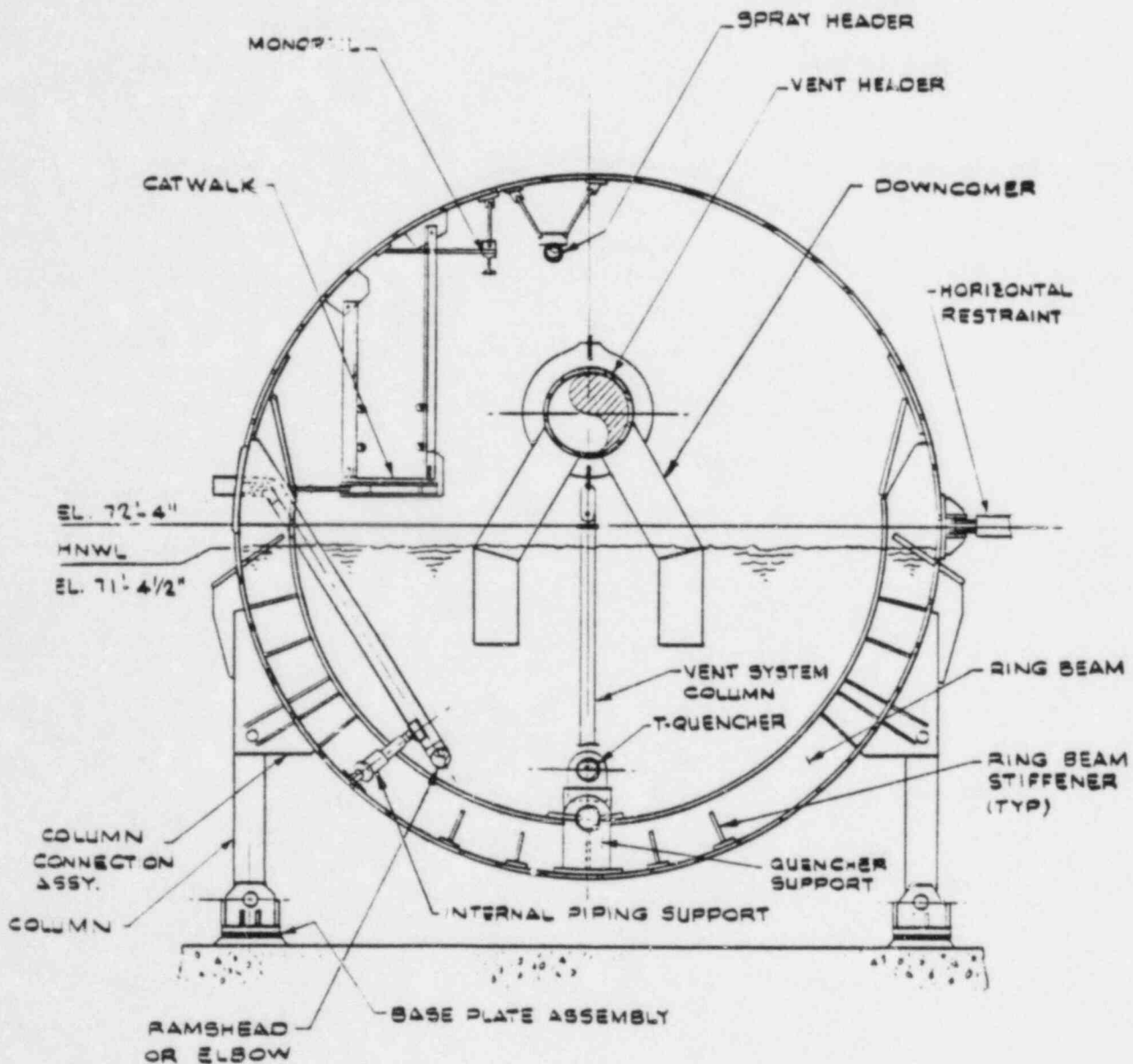


Figure 1-2.1-4

SUPPRESSION CHAMBER SECTION - MITERED JOINT

BPC-01-300-1
Revision 0

1-2.14



Note:

1. Downcomer stiffener plates not shown for clarity.

Figure 1-2.1.5

SUPPRESSION CHAMBER SECTION - MIDCYLINDER NON-VENT BAY

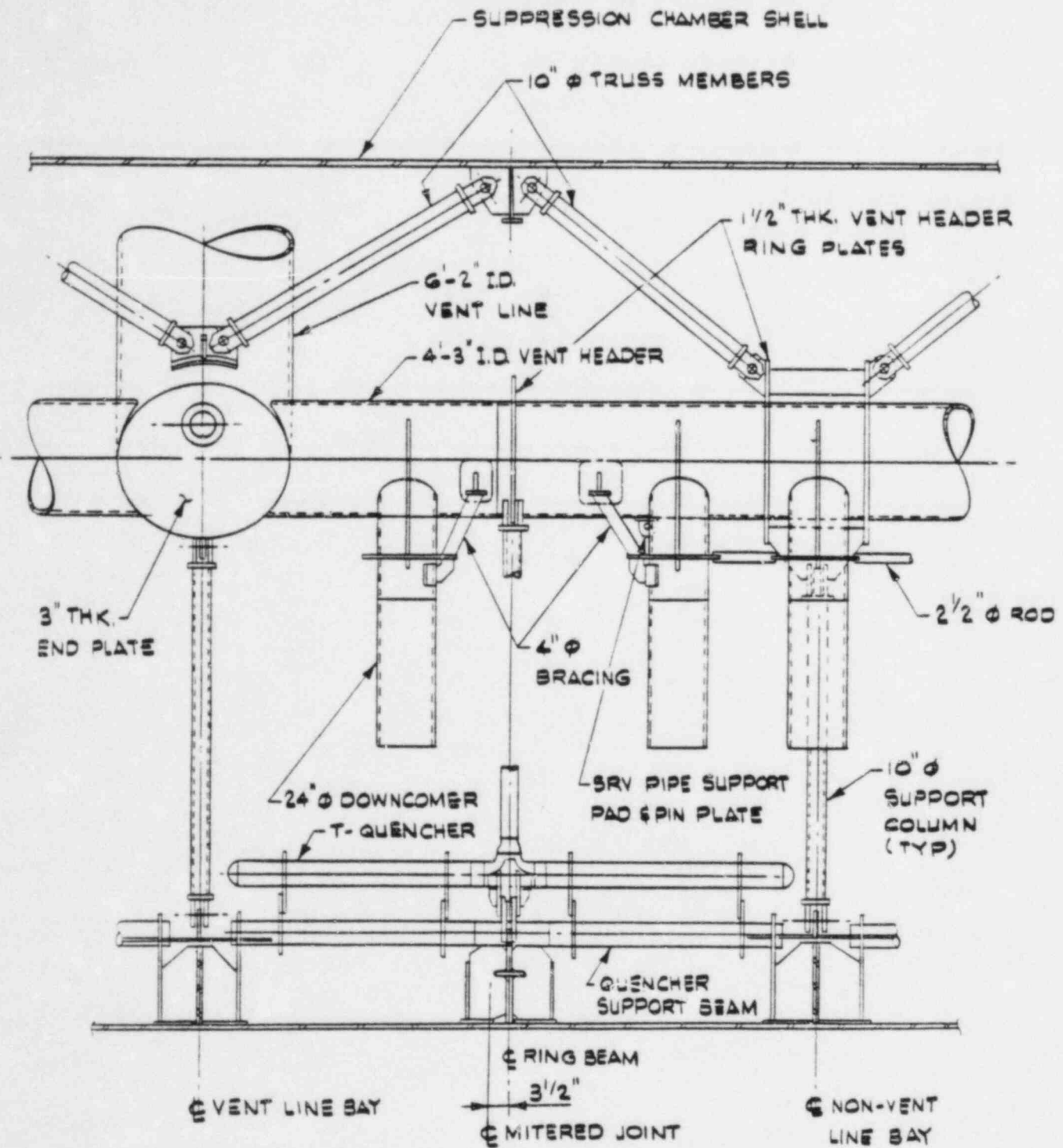


Figure 1-2.1-6

DEVELOPED VIEW OF SUPPRESSION CHAMBER SEGMENT

BPC-01-300-1
Revision 0

1-2.16

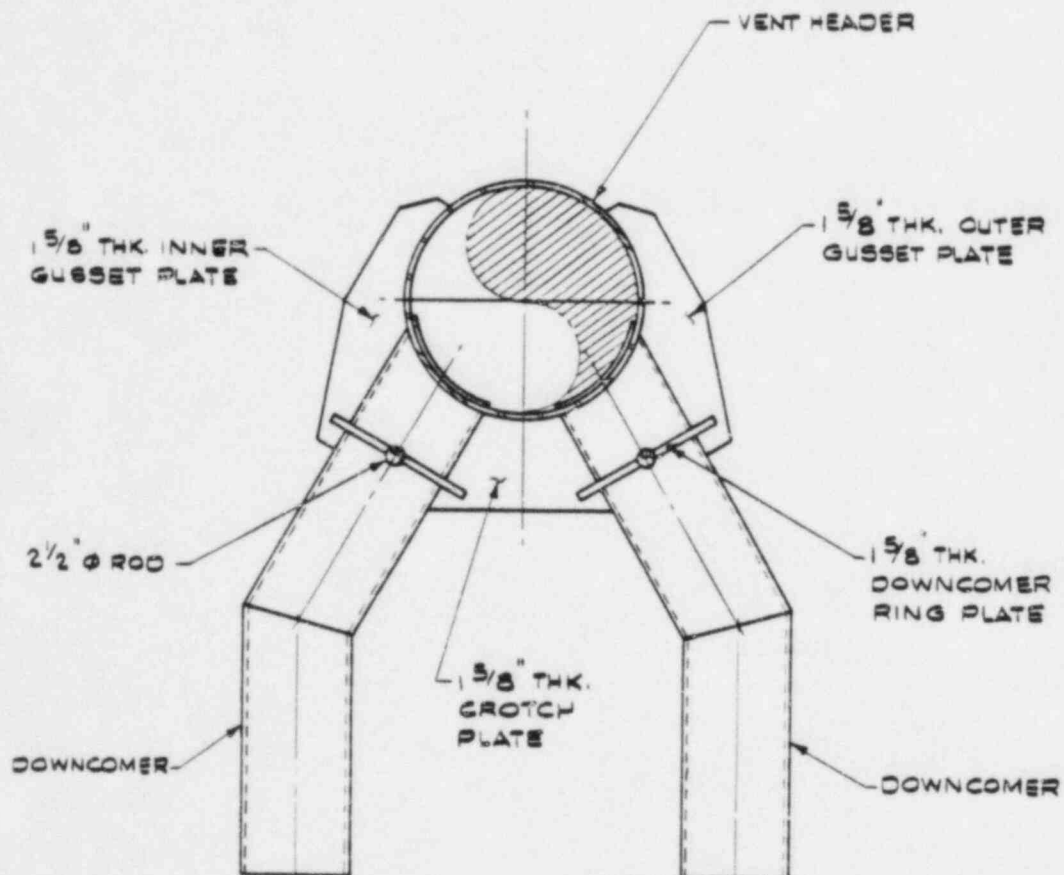


Figure 1-2.1-7

VENT HEADER - DOWNCOMER INTERSECTION
STIFFENING DETAILS

BPC-01-300-1
 Revision 0

Plant operating parameters are used to determine many of the hydrodynamic loads utilized in the Hope Creek plant unique analysis. Table 1-2.2-1 is a summary of the primary containment operating parameters used for the development of these hydrodynamic loads.

Table 1-2.2-1

PRIMARY CONTAINMENT OPERATING PARAMETERS

COMPONENTS	CONDITION/ITEM	VALUE
DRYWELL	FREE AIR VOLUME (1)	169,000 cu ft +0% -10%
	NORMAL OPERATING PRESSURE	HIGH 1.5 psig LOW -0.5 psig
	NORMAL OPERATING TEMPERATURE	NOMINAL BULK 135°F MAX BULK 150°F MIN BULK 120°F
	NORMAL OPERATING RELATIVE HUMIDITY RANGE	HIGH 100% LOW 10%
	PRESSURE SCRAM INITIATION SETPOINT	2 psig \pm 0.2 psig
	DESIGN INTERNAL PRESSURE	62 psig
	DESIGN EXTERNAL PRESSURE MINUS INTERNAL PRESSURE	-3 psid
	DESIGN TEMPERATURE	340°F
SUPPRESSION CHAMBER	POOL VOLUME	MAX (HIGH WATER LEVEL) 122,000 ft ³ MIN (LOW WATER LEVEL) 118,000 ft ³
	FREE AIR VOLUME (2)	MIN (HIGH WATER LEVEL) 133,500 ft ³ MAX (LOW WATER LEVEL) 137,000 ft ³
	LOCA VENT SYSTEM DOWNCOMER SUBMERGENCE (DISTANCE OF DOWNCOMER DISCHARGE PLANE BELOW WATER LEVEL)	MIN (LOW WATER LEVEL) 3.00 ft MAX (HIGH WATER LEVEL) 3.33 ft
	WATER LEVEL DISTANCE TO TORUS CENTERLINE	MAX (LOW WATER LEVEL) 1.292 ft MIN (HIGH WATER LEVEL) 0.958 ft
	SUPPRESSION POOL SURFACE EXPOSED TO SUPPRESSION CHAMBER AIRSPACE	MIN 10,680 ft ² MAX 10,710 ft ²
	NORMAL OPERATING PRESSURE RANGE	HIGH 1.5 psig LOW -0.5 psig

Table 1-2.2-1

PRIMARY CONTAINMENT OPERATING PARAMETERS

(Concluded)

COMPONENTS	CONDITION/ITEM	VALUE
SUPPRESSION CHAMBER	TEMPERATURE RANGE OF SUPPRESSION POOL DURING NORMAL OPERATION	HIGH 95°F (3) LOW 60°F
	NORMAL OPERATING TEMPERATURE RANGE OF SUPPRESSION CHAMBER FREE AIR VOLUME	HIGH 100°F LOW (3) 60°F
	NORMAL OPERATING RELATIVE HUMIDITY RANGE	HIGH 100% LOW (3) 50%
	DESIGN INTERNAL PRESSURE	62 psig
	EXTERNAL PRESSURE MINUS INTERNAL PRESSURE	-3 psid
	DESIGN TEMPERATURE	340°F
	NORMAL OPERATING PRESSURE DIFFERENTIAL DRYWELL-TO-WETWELL	ZERO
DOWNCOMER	ID AT DISCHARGE	1.9375 ft.
	OD AT DISCHARGE	2 ft
	TOTAL NUMBER OF DOWNCOMERS	80
CONTAINMENT	LONG-TERM POST-LOCA CONTAINMENT LEAK RATE	MAX 0.5%/DAY
	DRYWELL-TO-WETWELL LEAKAGE SOURCE BYPASSING SUPPRESSION POOL WATER	MAX 0.2 ft ² (ESTIMATED)
	SERVICE WATER TEMPERATURE LIMITS	MAX NORMAL 95°F
		MIN NORMAL 65°F

SAFETY RELIEF VALVE (4)	SET POINT (psig)	CAPACITY AT 103% OF SET POINT (lbm/hr)
4	1108	884,000
5	1120	893,000
5 (ADS)	1130	901,000

NOTES:

1. INCLUDES FREE AIR VOLUME OF THE LOCA VENT SYSTEM.
2. DOES NOT INCLUDE FREE AIR VOLUME OF THE LOCA VENT SYSTEM.
3. NOT CONTROLLED.
4. ALL FIVE VALVES IN 1130 PSIG SETPOINT GROUP HAVE ADS FUNCTION.

This section describes the acceptance criteria used in the Hope Creek plant unique analysis for hydrodynamic loads development and structural evaluations.

The acceptance criteria used in the PUA are a result of the NRC review of the long-term program LDR, the PUAAG, and the supporting analytical and experimental programs conducted by the Mark I Owners Group. These criteria are documented in NUREG-0661 for both hydrodynamic load definitions and structural applications. Sections 1 and 2 of NUREG-0661 provide an introduction and background information; Section 3 presents a detailed discussion of the hydrodynamic load evaluation; Section 4 presents the structural and mechanical analyses and acceptance criteria, and Appendix A presents the hydrodynamic loads acceptance criteria.

Appendix A of NUREG-0661 resulted from the NRC review of the load definition procedures for suppression pool hydrodynamic loads contained in the LDR. The NRC review was limited to those events or event combinations involving suppression pool hydrodynamic loads. Unless specified otherwise, all loading conditions or structural analysis techniques used in the PUA, but not addressed in NUREG-0661, are in accordance with the Hope Creek FSAR.

Wherever feasible, the conservative hydrodynamic acceptance criteria of NUREG-0661 were incorporated directly into the detailed plant unique load determinations and associated structural analyses. Where this simple, direct approach resulted in unrealistic hydrodynamic loads, more detailed plant unique analyses were performed. Many of these analyses have indicated that a specific interpretation of the generic rules was justified. These specific applications of the generic hydrodynamic acceptance criteria are identified in the following sections and are discussed in greater detail in Section 1-4.0.

The hydrodynamic loads criteria are based on the NRC review and resulting revisions to experimentally-formulated hydrodynamic loads. Pool swell loads derived from plant unique quarter-scale two-dimensional tests are used to obtain net torus uploads, downloads, and local pressure distributions. Vent system impact and drag loads resulting from pool swell effects are also based on experimental results, using analytical techniques where appropriate.

Condensation oscillation and chugging loads were derived from FSTF results. Downcomer loads are based on test data, using comparisons of plant unique and FSTF dynamic load factors.

The acceleration drag volumes used in determining loads on submerged structures are calculated based upon the values in published technical literature rather than on the procedure which might be inferred from NUREG-0661, where the structure is idealized as a cylindrical section for both velocity and acceleration drag (see Section 1-4.1-5).

Condensation oscillation and post-chug torus shell and submerged structure loads are defined in terms of 50 harmonics. Random phasing of the loading harmonics is assumed, based on FSTF data and subsequent analysis (see Section 1-4.1.7.1).

NUREG-0661 states that the fluid-structure interaction (FSI) effect on CO and chugging loads on submerged structures can be accounted for by adding the shell boundary accelerations to the local fluid acceleration. For Hope Creek, the FSI effects for a given structure are included by adding the pool fluid acceleration at the location of the structure rather than the shell boundary acceleration (see Section 1-4.1.7.3).

The analysis techniques for SRV discharge loads were developed to generically define T-quencher air clearing loads on the torus. However, a number of Mark I licensees have indicated that the generic load definition procedures are overly conservative for their plant design, particularly when the procedures are coupled with conservative structural analysis techniques. To allow for these special cases, the NRC has specified requirements whereby in-plant tests could be used to derive the plant specific structural response to the SRV air clearing loads on the torus and submerged structures.

Because of the various phenomena associated with the air clearing phase of SRV discharge, some form of analysis procedure is necessary to extrapolate from test conditions to the design cases. Therefore, the NRC requirements are predicated on formulating a coupled load-structure analysis technique which is calibrated to the plant specific conditions for the simplest form of discharge (i.e., single valve, first actuation) and then applied to the design basis event conditions.

The SRV torus shell loads are evaluated using the alternate approach of NUREG-0661, which allows the use of in-plant SRV tests to calibrate a coupled load-structure analytical model. This method utilizes shell pressure waveforms more characteristic of those observed in tests. A series of in-plant SRV tests will be performed for Hope Creek after fuel load to confirm that the computed loadings and predicted structural responses for SRV discharges are conservative (see Section 1-4.2.3).

For SRV bubble-induced drag loads on submerged structures, a bubble pressure multiplier which bounds the maximum peak positive bubble pressure and the maximum bubble pressure differential across the quencher observed during the Monticello in-plant SRV discharge tests is used (see Section 1-4.2.4).

As part of the PUA, each licensee is required to either demonstrate that previously submitted pool temperature response analyses are adequate or provide plant specific pool temperature response analyses to assure that SRV discharge transients will not exceed specified pool temperature limits. A suppression pool temperature monitoring system is also required to ensure that the suppression pool bulk temperature remains within the allowable limits set forth in the plant technical specifications. Section 6.2.1.1.10 of the Hope Creek FSAR discusses specific implementation of these considerations.

Several loads are classified as secondary loads because of their inherent low magnitudes. These loads include seismic slosh pressure loads, post-pool swell wave loads, asymmetric pool swell pressure loads on the torus as a whole, sonic and compression wave loads, and downcomer air clearing loads. In accordance with Appendix A of NUREG-0661, these secondary loads are considered to be negligible compared to other loads in the PUA and are not evaluated.

Section 4.0 of NUREG-0661 presents the NRC evaluation of the generic structural and mechanical acceptance criteria and of the general analysis techniques proposed by the Mark I Owners Group for use in the plant unique analyses. Because the Mark I plants were designed and constructed at different times, there are variations in the codes and standards to which they were constructed and subsequently licensed. For this assessment of the containment, the criteria described in this subsection were developed to provide a consistent and uniform basis for acceptability for all Mark I plants. In this evaluation, references to "original design criteria" mean those specific criteria in the Hope Creek FSAR.

1-3.2.1 Classification of Components

The structures described in Section 1-1.3 were categorized according to their functions to assign the appropriate service limits. The general components of a Mark I containment system have been classified in accordance with Section III of the ASME Boiler and Pressure Vessel Code, as specified in NUREG-0661.

1-3.2.2 Service Level Assignments

The criteria used in the plant unique analysis to evaluate the acceptability of the existing containment design or to provide the basis for plant modifications follow Section III of the ASME Boiler and Pressure Vessel Code through the Summer 1977 Addenda.

Service Limits

The service limits are defined in terms of the Winter 1976 Addenda of the ASME Code, which introduced Levels A, B, C, and D. The selection of specific service limits for each load combination is dependent on the functional requirements of the component analyzed and the nature of the applied load. Tables 1-3.2-1 and 1-3.2-2 provide the assignments of service levels for each load combination. Reference 2 describes details regarding service level assignments and other aspects of Tables 1-3.2-1 and 1-3.2-2.

Table 1-3.2-1

EVENT COMBINATIONS AND SERVICE LEVELS FOR CLASS MC
COMPONENTS AND INTERNAL STRUCTURES

EVENT COMBINATIONS			SRV	SRV + EQ		SBA IBA		SBA + EQ IBA + EQ				SBA+SRV IBA+SRV				SBA + SRV + EQ IBA + SRV + EQ				DBA		DBA + EQ				DBA+SRV		S + EQ + SRV			
							CO, CH			CO, CH			CO, CH			CO, CH		PS (1)	CO, CH	PS	CO, CH	PS	CO, CH	PS	CO, CH	PS	CO, CH				
TYPE OF EARTHQUAKE				0	S			0	S	0	S			0	S	0	S			0	S	0	S				S	0	S		
COMBINATION NUMBER				1	2	3	4	5	6	7	8	9	10	11	12	13	14	15	16	17	18	19	20	21	22	23	24	25	26	27	
LOADS	NORMAL (2)	N	X	X	X	X	X	X	X	X	X	X	X	X	X	X	X	X	X	X	X	X	X	X	X	X	X	X	X		
	EARTHQUAKE	EQ		X	X			X	X	X	X			X	X	X	X			X	X	X	Y			X	X	X	X		
	SRV DISCHARGE	SRV	X	X	X							X	X	X	X	X	X							X	X(7)	X	X	X(7)	X(7)		
	LOCA THERMAL	T _A				X	X	X	X	X	X	X	X	X	X	X	X	X	X	X	X	X	X	X	X	X	X	X	X		
	LOCA REACTIONS	R _A				X	X	X	X	X	X	X	X	X	X	X	X	X	X	X	X	X	X	X	X	X	X	X	X		
	LOCA QUASI-STATIC PRESSURE	P _A				X	X	X	X	X	X	X	X	X	X	X	X	X	X	X	X	X	X	X	X	X	X	X	X		
	LOCA POOL SWELL	P _{PS}																X		X	X			X		X	X				
	LOCA CONDENSATION OSCILLATION	P _{CO}					X			X	X		X			X	X		X				X	X		X			X	X	
LOCA CHUGGING	P _{CH}					X			X	X		X			X	X		X			X	X		X			X	X			
STRUCTURAL ELEMENT			ROW																												
EXTERNAL CLASS MC	TORUS, EXTERNAL VENT PIPE, BELLGWS, DRYWELL (AT VENT), ATTACHMENT WELDS, TORUS SUPPORTS, SEISMIC RESTRAINTS	1	A	B	C	A	A	B	C	B	C	A	A	B	C	B	C	A	B	C	A	B	C	C	C	C	C	C	C	C	
INTERNAL VENT PIPE	GENERAL AND ATTACHMENT WELDS	2	A	B	C	A	A	B	C	B	C	A	A	B	C	B	C	A	B	C	A	B	C	C	C	C	C	C	C	C	
	AT PENETRATIONS (e.g., HEADER)	3	A	B	C	A	A	B	C	B	C	A	A	B	C	B	C	A	B	C	A	B	C	C	C	C	C	C	C	C	
VENT HEADER	GENERAL AND ATTACHMENT WELDS	4	A	B	C	A	A	B	C	B	C	A	A	B	C	B	C	A	B	C	A	B	C	C	C	C	C	C	C	C	
	AT PENETRATIONS (e.g., DOWNCOMERS)	5	A	B	C	A	A	B	C	B	C	A	A	B	C	B	C	A	B	C	A	B	C	C	C	C	C	C	C	C	
DOWNCOMERS	GENERAL AND ATTACHMENT WELDS	5	A	B	C	A	A	B	C	B	C	A	A	B	C	B	C	A	B	C	A	B	C	C	C	C	C	C	C	C	
INTERNAL SUPPORTS			7	A	B	C	A	A	B	C	B	C	A	A	B	C	B	C	A	A	B	C	B	C	C	C	C	C	C	C	C
INTERNAL STRUCTURES	GENERAL	8	A	B	C	A	A	C	D	C	D	C	C	D	E	D	E	E	E	E	E	E	E	E	E	E	E	E	E	E	
	VENT DEFLECTOR	9	A	B	C	A	A	C	D	C	D	C	C	D	D	D	D	D	D	D	D	D	D	D	D	D	D	D	D	D	

NOTES TO TABLE 1-3.2-1

1. REFERENCE 3 STATES "WHERE THE DRYWELL-TO-WETWELL PRESSURE DIFFERENTIAL IS NORMALLY UTILIZED AS A LOAD MITIGATOR, AN ADDITIONAL EVALUATION SHALL BE PERFORMED WITHOUT SRV LOADINGS BUT ASSUMING LOSS OF THE PRESSURE DIFFERENTIAL." IN THE ADDITIONAL EVALUATION LEVEL D SERVICE LIMITS SHALL APPLY FOR ALL STRUCTURAL ELEMENTS EXCEPT ROW 8 INTERNAL STRUCTURES, WHICH NEED NOT BE EVALUATED.
2. NORMAL LOADS (N) CONSIST OF THE COMBINATION OF DEAD LOADS, LIVE LOADS, COLUMN PRESET LOADS, THERMAL EFFECTS DURING OPERATION, AND PIPE REACTIONS DURING OPERATION.
3. EVALUATION OF PRIMARY-PLUS-SECONDARY STRESS INTENSITY RANGE (NE-3221.4) AND OF FATIGUE (NE-3221.5) IS NOT REQUIRED.
4. WHEN CONSIDERING THE LIMITS ON LOCAL MEMBRANE STRESS INTENSITY (NE-3221.2) AND PRIMARY-MEMBRANE-PLUS-PRIMARY-BENDING STRESS (NE-3221.3), THE S_{mc} VALUE MAY BE REPLACED BY $1.3 S_{mc}$.

(NOTE: THE MODIFICATION TO THE LIMITS DOES NOT AFFECT THE NORMAL LIMITS ON PRIMARY-PLUS-SECONDARY STRESS INTENSITY RANGE (NE-3221.4 OR NE-3228.3) NOR THE NORMAL LIMITS ON FATIGUE EVALUATION (NE-3221.5(e) OR APPENDIX II-1500). THE MODIFICATION IS THAT THE LIMITS ON LOCAL MEMBRANE STRESS INTENSITY (NE-3221.2) AND ON PRIMARY-MEMBRANE-PLUS-PRIMARY BENDING STRESS INTENSITY (NE-3221.3) HAVE BEEN MODIFIED BY USING $1.3 S_{mc}$ IN PLACE OF THE NORMAL S_{mc} .

THIS MODIFICATION IS A CONSERVATIVE APPROXIMATION TO RESULTS FROM LIMIT ANALYSIS TESTING AS REPORTED IN REFERENCE 2 AND IS CONSISTENT WITH THE REQUIREMENTS OF NE-3228.2.
5. SERVICE LEVEL LIMITS SPECIFIED APPLY TO THE OVERALL STRUCTURAL RESPONSE OF THE VENT SYSTEM. AN ADDITIONAL EVALUATION WILL BE PERFORMED TO DEMONSTRATE THAT SHELL STRESSES DUE TO THE LOCAL POOL SWELL IMPINGEMENT PRESSURES DO NOT EXCEED SERVICE LEVEL C LIMITS.
6. FOR THE SUPPRESSION CHAMBER SHELL, THE S_{mc} VALUE MAY BE REPLACED BY $1.0 S_{mc}$ TIMES THE DYNAMIC LOAD FACTOR DERIVED FROM THE TORUS STRUCTURAL MODEL. AS AN ALTERNATIVE, THE 1.0 MULTIPLIER MAY BE REPLACED BY THE PLANT UNIQUE RATIO OF THE SUPPRESSION CHAMBER DYNAMIC FAILURE PRESSURE TO THE STATIC FAILURE PRESSURE.
7. SRV ACTUATION IS ASSUMED TO OCCUR COINCIDENT WITH THE POOL SWELL EVENT. ALTHOUGH SRV ACTUATION CAN OCCUR LATER IN THE DBA, THE RESULTING AIR LOADING ON THE SUPPRESSION CHAMBER SHELL IS NEGLIGIBLE SINCE THE AIR AND WATER INITIALLY IN THE LINE WILL BE CLEARED AS THE DRYWELL-TO-WETWELL ΔP INCREASES DURING THE DBA TRANSIENT.

Table 1-3.2-2

EVENT COMBINATIONS AND SERVICE LEVELS
FOR CLASS 2 AND 3 PIPING

EVENT COMBINATIONS			SRV	SRV + EQ		SBA IBA		SBA + EQ IBA + EQ				SBA+SRV IBA+SRV		SBA + SRV + EQ IBA + SRV + EQ				DBA		DBA + EQ				DBA+SRV		DBA + EQ + SRV				
						CO, CH		CO, CH				CO, CH		CO, CH				PS (1)	CO, CH	PS				PS	CO, CH	PS				
TYPE OF EARTHQUAKE				0	S			0	S	0	S			0	S	0	S			0	S	0	S			0	S	0	S	
COMBINATION NUMBER				1	2	3	4	5	6	7	8	9	10	11	12	13	14	15	16	17	18	19	20	21	22	23	24	25	26	27
LOADS	NORMAL (2)	N	X	X	X	X	X	X	X	X	X	X	X	X	X	X	X	X	X	X	X	X	X	X	X	X	X	X	X	
	EARTHQUAKE	EQ		X	X			X	X	X	X			X	X	X	X			X	X	X	X			X	X	X	X	
	SRV DISCHARGE	SRV	X	X	X							X	X	X	X	X	X							X	X(6)	X	X	X(6)	X(6)	
	THERMAL	T _A	X	X	X	X	X	X	X	X	X	X	X	X	X	X	X	X	X	X	X	X	X	X	X	X	X	X	X	
	PIPE PRESSURE	P _A	X	X	X	X	X	X	X	X	X	X	X	X	X	X	X	X	X	X	X	X	X	X	X	X	X	X	X	
	LOCA POOL SWELL	P _{PS}																	X		X	X			X		X	X		
	LOCA CONDENSATION OSCILLATION	P _{CO}					X			X	X		X			X	X		X				X					X		
LOCA CHUGGING	P _{CH}					X			X	X		X			X	X		X			X	X		X			X	X		
STRUCTURAL ELEMENT			ROW																											
ESSENTIAL PIPING SYSTEMS	WITH IBA/DBA	10	B	B (3)	B (3)	B (4)	B (4)	B (4)	B (4)	B (4)	B (4)	B (4)	B (4)	B (4)	B (4)	B (4)	B (4)	B (4)	B (4)	B (4)	B (4)	B (4)	B (4)	B (4)	B (4)	B (4)	B (4)	B (4)	B (4)	
	WITH SBA	11				B (3)	B (3)	B (4)	B (4)	B (4)	B (4)	B (3)	B (3)	B (4)	B (4)	B (4)	B (4)	-	-	-	-	-	-	-	-	-	-	-	-	
NONESENTIAL PIPING SYSTEMS	WITH IBA/DBA	12	B	C (5)	D (5)	D (5)	D (5)	D (5)	D (5)	D (5)	D (5)	D (5)	D (5)	D (5)	D (5)	D (5)	D (5)	D (5)	D (5)	D (5)	D (5)	D (5)	D (5)	D (5)	D (5)	D (5)	D (5)	D (5)	D (5)	
	WITH SBA	13				C (5)	C (5)	D (5)	D (5)	D (5)	D (5)	D (5)	D (5)	D (5)	D (5)	D (5)	D (5)	-	-	-	-	-	-	-	-	-	-	-	-	

NOTES TO TABLE 1-3.2-2

1. REFERENCE 3 STATES "WHERE A DRYWELL-TO-WETWELL PRESSURE DIFFERENTIAL IS NORMALLY UTILIZED AS A LOAD MITIGATOR, AN ADDITIONAL EVALUATION SHALL BE PERFORMED WITHOUT SRV LOADINGS BUT ASSUMING THE LOSS OF THE PRESSURE DIFFERENTIAL." SERVICE LEVEL D LIMITS SHALL APPLY FOR ALL STRUCTURAL ELEMENTS OF THE PIPING SYSTEM FOR THIS EVALUATION. THE ANALYSIS NEED ONLY BE ACCOMPLISHED TO THE EXTENT THAT INTEGRITY OF THE FIRST PRESSURE BOUNDARY ISOLATION VALUE IS DEMONSTRATED.
2. NORMAL LOADS (N) CONSIST OF DEAD LOADS (D).
3. AS AN ALTERNATIVE, THE $1.2 S_h$ LIMIT IN EQUATION 9 OF NC-3652.2 MAY BE REPLACED BY $1.8 S_h$, PROVIDED THAT ALL OTHER LIMITS ARE SATISFIED. FATIGUE REQUIREMENTS ARE APPLICABLE TO ALL COLUMNS, WITH THE EXCEPTION OF 16, 18, 19, 22, 24 AND 25.
4. FOOTNOTE 3 APPLIES EXCEPT THAT INSTEAD OF USING $1.8 S_h$ IN EQUATION 9 OF NC-3652.2, $2.4 S_h$ IS USED.
5. EQUATION 10 OF NC OR ND-3659 WILL BE SATISFIED, EXCEPT THE FATIGUE REQUIREMENTS ARE NOT APPLICABLE TO COLUMNS 16, 18, 19, 22, 24 AND 25 SINCE POOL SWELL LOADINGS OCCUR ONLY ONCE. IN ADDITION, IF OPERABILITY OF AN ACTIVE COMPONENT IS REQUIRED TO ENSURE CONTAINMENT INTEGRITY, OPERABILITY OF THAT COMPONENT MUST BE DEMONSTRATED.
6. SRV ACTUATION IS ASSUMED TO OCCUR COINCIDENT WITH THE POOL SWELL EVENT. ALTHOUGH SRV ACTUATION CAN OCCUR LATER IN THE DBA, THE RESULTING AIR LOADING ON THE SUPPRESSION CHAMBER SHELL IS NEGLIGIBLE SINCE THE AIR AND WATER INITIALLY IN THE LINE WILL BE CLEARED AS THE DRYWELL-TO-WETWELL ΔP INCREASES DURING THE DBA TRANSIENT.

The general structural analysis techniques proposed by the Mark I Owners Group are utilized in the Hope Creek plant unique analysis with sufficient detail to account for all significant structural response modes. These methods are consistent with those used to develop the loading functions defined in the load definition report. For those loads considered in the original design but not redefined by the LDR, either the results of the original analysis are used or a new analysis is performed, based on the methods employed in the original plant design.

The damping values used in the analysis of dynamic loading events are those specified in Regulatory Guide 1.61, "Damping Values for Seismic Design of Nuclear Power Plants" (Reference 5), which is in accordance with NUREG-0661.

The structural responses resulting from two dynamic phenomena are combined by either the absolute sum or the SRSS method. Responses due to dynamic loads for containment structures are combined using the absolute sum method except as noted. Response due to dynamic loads for piping systems are combined

using the SRSS method. The time phasing of the responses for two dynamic loadings is such that the combined state of the stress results in the maximum stress intensity.

HYDRODYNAMIC LOADS METHODOLOGY AND EVENT SEQUENCE
SUMMARY

This section presents the load definition procedures used to develop the Hope Creek hydrodynamic loads. The section is organized in accordance with NUREG-0661, Section 3. Table 1-4.0-1 provides a cross-reference between the PUAR sections and the sections of NUREG-0661 Appendix A, where each load or event is addressed.

Table 1-4.0-1

PLANT UNIQUE ANALYSIS/NUREG-0661 LOAD SECTIONS
CROSS-REFERENCE

LOAD/EVENT	PUAR SECTION	NUREG-0661 APPENDIX A SECTION
CONTAINMENT PRESSURE AND TEMPERATURE RESPONSE	1-4.1.1	2.0
VENT SYSTEM DISCHARGE LOADS	1-4.1.2	2.2
POOL SWELL LOADS ON TORUS SHELL	1-4.1.3	2.3 & 2.4
POOL SWELL LOADS ON ELEVATED STRUCTURES	1-4.1.4	2.6 - 2.10
POOL SWELL LOADS ON SUBMERGED STRUCTURES	1-4.1.5 & 1-4.1.6	2.14.1 & 2.14.2
CONDENSATION OSCILLATION LOADS ON TORUS SHELL	1-4.1.7	2.11.1
CONDENSATION OSCILLATION LOADS ON DOWNCOMERS AND VENT SYSTEM	1-4.1.7	2.11.2
CONDENSATION OSCILLATION LOADS ON SUBMERGED STRUCTURES	1-4.1.7	2.14.5
CHUGGING LOADS ON TORUS SHELL	1-4.1.8	2.12.1
CHUGGING LOADS ON DOWNCOMERS	1-4.1.8	2.12.2
CHUGGING LOADS ON SUBMERGED STRUCTURES	1-4.1.8	2.14.6
SRV ACTUATION CASES	1-4.2.1	2.13.7
SRV DISCHARGE LINE CLEARING LOADS	1-4.2.2	2.13.2 & 2.13.1
SRV LOADS ON TORUS SHELL	1-4.2.3	2.13.3
SRV LOADS ON SUBMERGED STRUCTURES	1-4.2.4	2.14.3 & 2.14.4
DESIGN BASIS ACCIDENT	1-4.3.1	3.2.1
INTERMEDIATE BREAK ACCIDENT	1-4.3.2	3.2.1
SMALL BREAK ACCIDENT	1-4.3.3	3.2.1

This subsection describes the procedures used to define the Hope Creek LOCA-related hydrodynamic loads. The sources of structural loads generated during a LOCA are primarily a result of the following conditions.

- Pressures and temperatures within the drywell, vent system, and wetwell
- Fluid flow through the vent system
- Initial LOCA bubble formation in the pool and the resulting displacement of water resulting in pool swell
- Steam flow into the suppression pool (CO and chugging).

For postulated pipe breaks inside the drywell, three LOCA categories are considered. These three categories, selected on the basis of break size, are referred to as a design basis accident (DBA), an intermediate break accident (IBA), and a small break accident (SBA).

The DBA for a Mark I containment is defined as the instantaneous guillotine rupture of the largest pipe in the primary system (recirculation suction line). This LOCA leads to a specific combination of dynamic, quasi-static, and static loads. However, the DBA does not represent the limiting case for all loads and structural responses. Consequently, an IBA and a SBA are also evaluated. The IBA is defined as a 0.1 ft^2 instantaneous liquid line break in the primary system, and the SBA is defined as a 0.01 ft^2 instantaneous steam line break in the primary system.

1-4.1.1

Containment Pressure and Temperature Response

The drywell and suppression chamber transient pressure and temperature responses are calculated using the "General Electric Company Pressure Suppression Containment Analytical Model" (Reference 6). This analytical model calculates the thermodynamic response of the drywell, vent system, and suppression chamber volumes to mass and energy released from the primary system following a postulated loss-of-coolant accident.

The containment pressure and temperature analyses are performed in accordance with Appendix A of NUREG-0661 and are documented in Reference 7.

1-4.1.2 Vent System Discharge Loads

Of the three postulated LOCA categories, the DBA causes the most rapid pressurization of the containment system, the largest vent system mass flow rate, and therefore, the most severe vent system thrust loads. The pressurization of the containment for the IBA and SBA is much less rapid than for the design basis accident. Thus, the resulting vent system thrust loads for the SBA and IBA are bounded by the DBA thrust loads. Consequently, vent system thrust loads are only evaluated for the design basis accident.

Reaction loads occur on the vent system (main vent, vent header, and downcomers) following a LOCA due to pressure imbalances between the vent system and the surrounding torus airspace, and due to forces resulting from changes in linear momentum.

The LDR thrust equations consider the forces due to pressure distributions and momentum to define horizontal and vertical thrust forces. These equations are included in the analytical procedures applied to the main vents, vent header, and downcomer portions of the vent system.

Because main vents and downcomers are located symmetrically about the center of the vent system, the horizontal vent system thrust loads equilibrate each other, resulting in a zero unbalanced horizontal vent system thrust load.

The bases, analytical procedures, and assumptions used to calculate thrust loads are described in the load definition report. The Hope Creek plant unique DBA thrust loads for the main vent, the vent header, and downcomers were developed using a zero initial drywell-to-wetwell pressure differential. The thrust loads used in this PUA are documented in Reference 7.

PUAR Volume 3 presents the analysis of the vent system for discharge loads. The vent system discharge loads are developed in accordance with Appendix A of NUREG-0661.

During the postulated LOCA, the air initially in the drywell and vent system is expelled into the suppression pool, producing a downward reaction force on the torus followed by an upward reaction force. These vertical loads create a dynamic imbalance of forces on the torus, which acts in addition to the weight of the water contained in the torus. This dynamic force history lasts for only a few seconds.

The bases, assumptions, and justifications for the pool swell loads on the torus shell due to the DBA are described in the load definition report. The pool swell loads on the torus shell are based on a series of Hope Creek unique tests conducted using the OSTF (Reference 8). The pool swell loads on the torus shell used in the PUA are based on the information contained in Reference 8, with the addition of the upload and download margins specified in Appendix A of NUREG-0661.

From the plant unique average submerged pressure and the torus air pressure-time histories, the local average submerged pressure transients at different locations on the shell can be calculated using the

LDR methodology and the criteria given in
NUREG-0661.

The effects of pool swell torus shell loads on containment structures are discussed in PUAR Volume 2.

This subsection describes the load definition procedures used to define the hydrodynamic loads on the vent system and other elevated structures inside the torus above normal water level. These load components include:

- Pool Swell Impact and Drag Loads
- Froth Impingement Loads, Region I
- Froth Impingement Loads, Region II
- Pool Fallback Loads
- Froth Fallback Loads

The analysis for the effects of pool swell loads on elevated structures are discussed in PUAR Volumes 3 through 6.

1-4.1.4.1 Impact and Drag Loads on the Vent System

In the event of a postulated design basis LOCA, the pool surface rises during the pool swell phase and impacts structures in its path. The resulting loading condition of primary interest is the impact on the vent system. The impact phenomenon consists of two events: (1) the impact of the pool on the structure, and (2) the drag on the structure as the pool flows past it following impact. The load definition includes both the impact and drag portions of the loading transient.

The vent system components which are potentially impacted during pool swell include the vent lines, the vent header, and the downcomers. The vent header will experience pool swell impact and drag loads since Hope Creek does not require a vent header deflector due to the use of a thicker vent header. The vent system pool swell impact and drag loads are developed from plant unique quarter-scale tests (Reference 8).

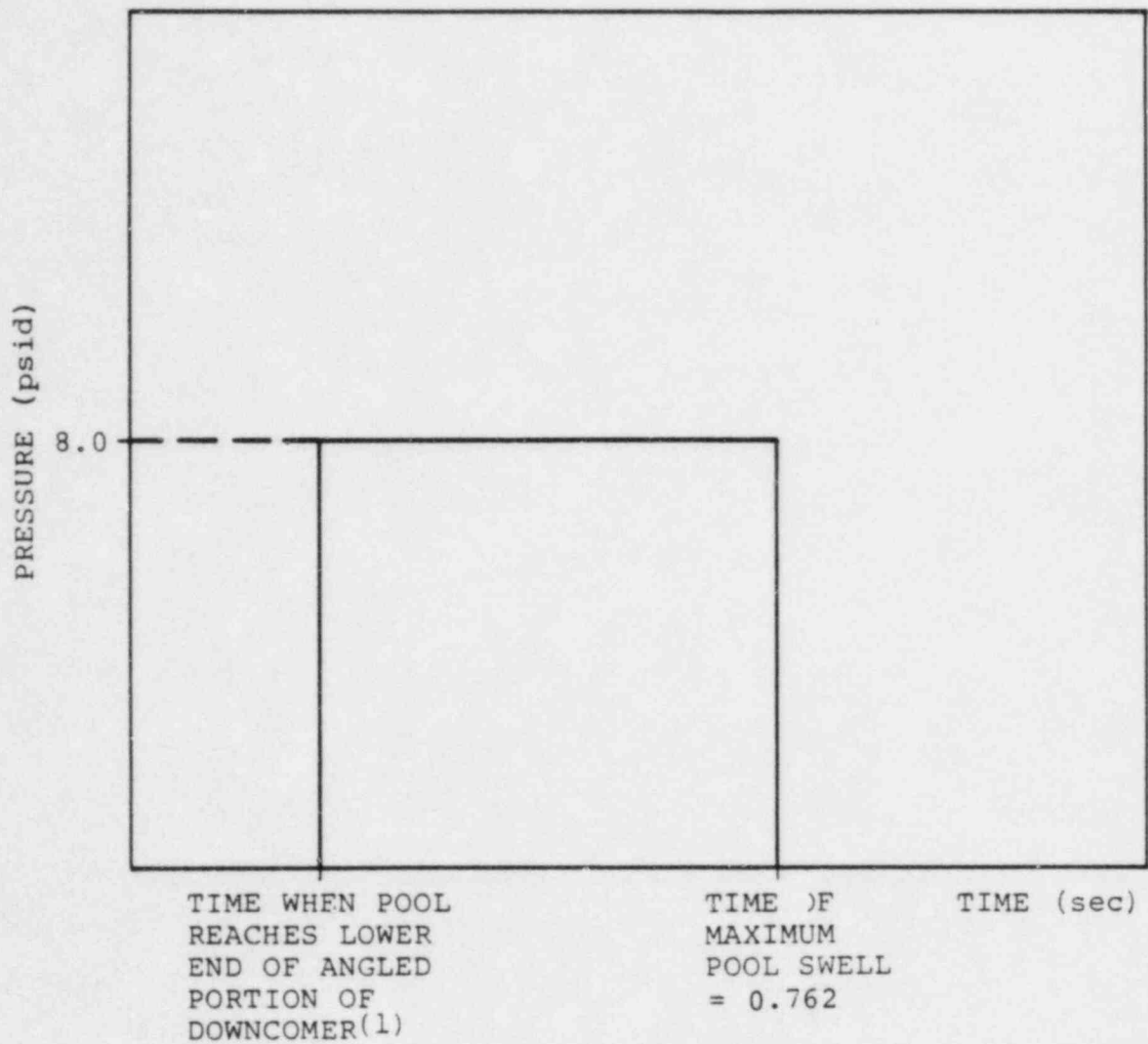
A generic pressure transient is specified for the downcomers and is assumed to apply uniformly over the bottom 50° of the angled portion of the

downcomer. The load transient and distribution are shown in Figures 1-4.1-1 and 1-4.1-2.

The vent header loads are developed on a plant unique basis. The LDR provides the bases, assumptions, and justifications for vent header impact loads. Reference 7 presents the full-scale vent header loads used for Hope Creek. These loads are based on a zero initial drywell-to-wetwell pressure differential and include the load definition requirements specified in Appendix A of NUREG-0661.

Pool swell impact and drag loads on the main vent line are calculated using the procedure specified in Appendix A of NUREG-0661.

The analysis of vent system for pool swell impact and drag loads is discussed in PUAR Volume 3.



NOTE:

1. THE TIME OF INITIAL IMPACT IS DEPENDENT ON THE DOWNCOMER LOCATION.

Figure 1-4.1-1

DOWNCOMER IMPACT AND DRAG PRESSURE TRANSIENT

BPC-01-300-1
Revision 0

1-4.13

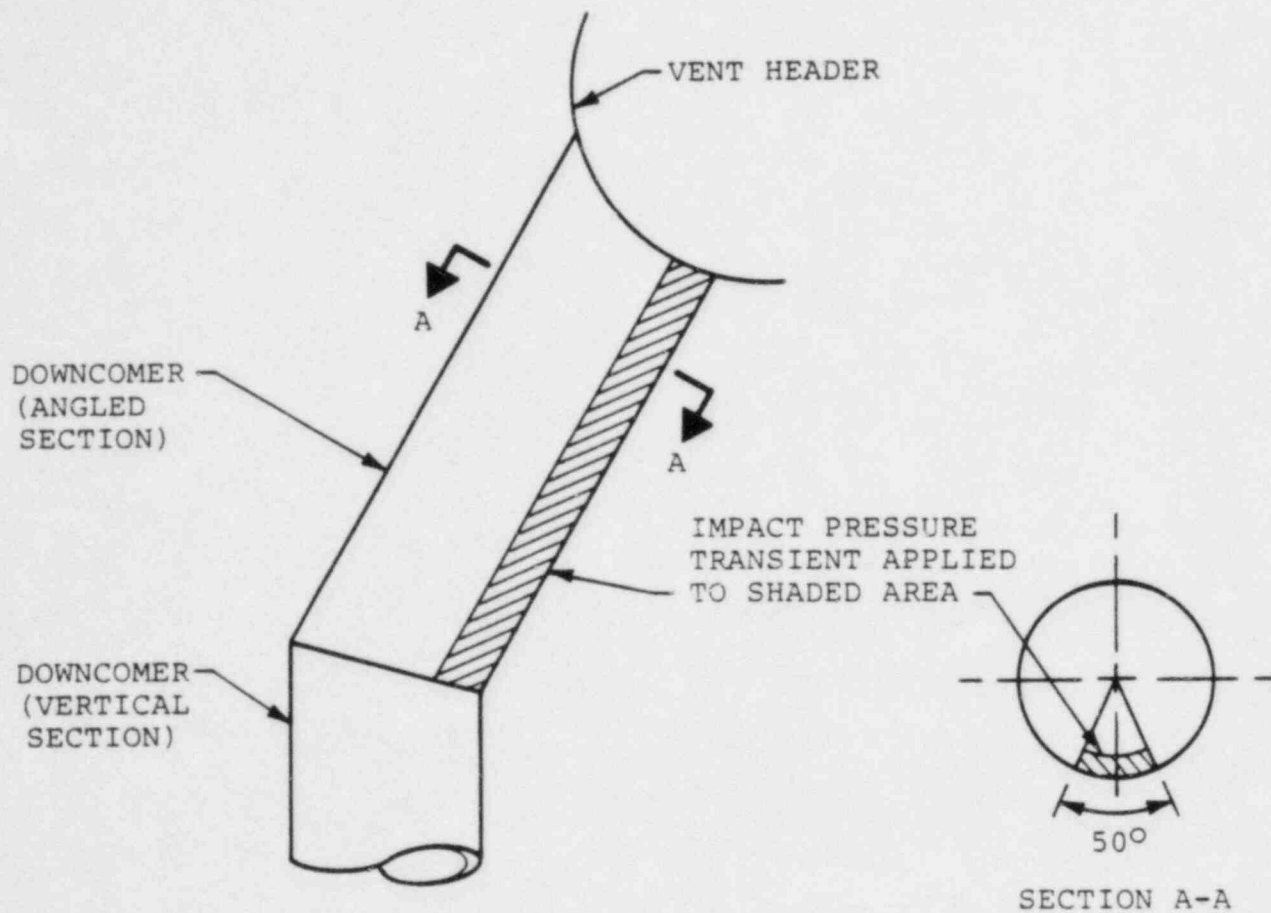


Figure 1-4.1-2

APPLICATION OF IMPACT AND DRAG PRESSURE
TRANSIENT TO DOWNCOMER

BPC-01-300-1
Revision 0

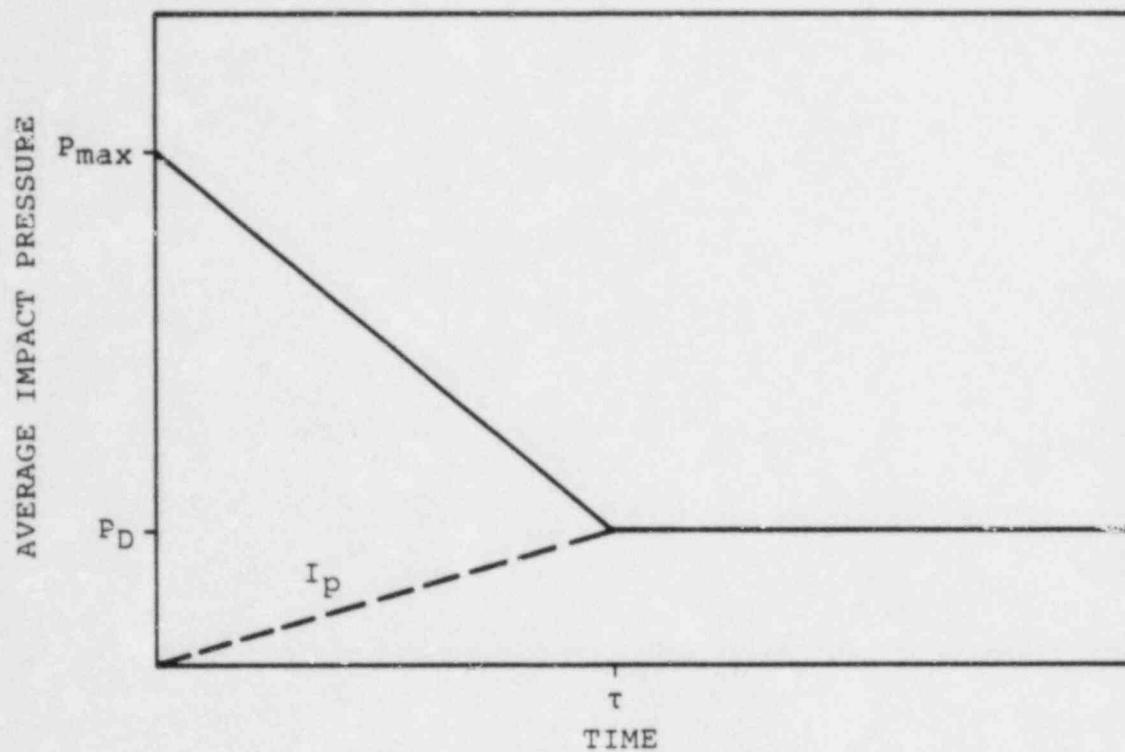
1-4.14

1-4.1.4.2 Impact and Drag Loads on Other Structures

As the pool surface rises due to the bubbles forming at the downcomer exits, it may impact structures located in the wetwell airspace. In the present context, "other structures" are defined as all structures located above the initial pool surface, exclusive of the vent system.

The LDR presents the bases, assumptions, and methodology used in determining the pool swell impact and drag loads on structures located above the pool surface. These load specifications correspond to impact on "rigid" structures. When performing structural dynamic analysis, the "rigid body" impact loads are applied. The mass of the impacted structure is adjusted by adding the hydrodynamic mass of impact, except for gratings. The value of hydrodynamic mass is obtained using the methods described in the LDR.

The development and application of impact and drag loads are in accordance with Appendix A of NUREG-0661. Typical impact and drag load transients are shown in Figures 1-4.1-3 and 1-4.1-4. The analysis of elevated structures for impact and drag loads is discussed in PUAR Volumes 3 through 6.



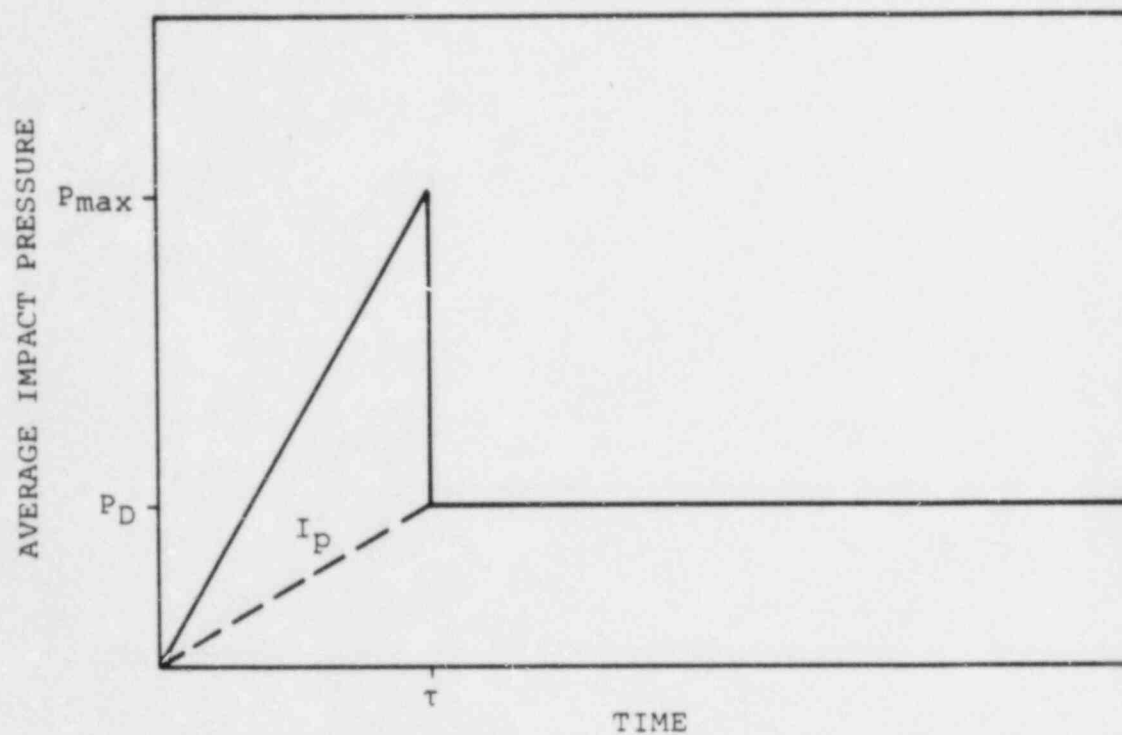
WHERE

I_p = IMPULSE OF IMPACT PER UNIT AREA

τ = PULSE DURATION

Figure 1-4.1-3

PULSE SHAPE FOR IMPACT AND DRAG ON CYLINDRICAL STRUCTURES



WHERE

I_p = IMPULSE OF IMPACT PER UNIT AREA

τ = PULSE DURATION

Figure 1-4.1-4

PULSE SHAPE FOR IMPACT AND DRAG ON FLAT PLATE STRUCTURES

BPC-01-300-1

Revision 0

1-4.17

1-4.1.4.3 Pool Swell Froth Impingement Loads

During the final stages of the pool swell phase of a DBA LOCA, the rising pool breaks up into a two-phase froth mixture of air and water. This froth rises above the pool surface and may impinge on structures within the torus airspace. Subsequently, as the froth falls back, it creates froth fallback loads. Froth may be generated by two mechanisms as described below.

Region I Froth

As the rising pool strikes the bottom of the vent header, a froth spray which travels upward and to both sides of the vent header is formed. This is defined as the Region I froth impingement zone (Figure 1-4.1-5).

Region II Froth

A portion of the water above the expanding air bubble becomes detached from the bulk pool and travels vertically upward. This water is influenced only by its own inertia and gravity. The "bubble breakthrough" creates a froth which rises into the

airspace beyond the maximum bulk pool swell height. This is defined as the Region II froth impingement zone (Figure 1-4.1-6).

The LDR methods are used to define the froth impingement loads for Region I. For the Region I froth formation, the LDR method assumes the froth density to be 20% of full water density for structures with maximum cross-section dimensions of less than 1', and a proportionally lower density for structures greater than 1'. The load is applied as a step function for a duration of 80 milliseconds in the direction most critical to the structure within the region of load application.

The froth density of Region II is assumed to be 100% of water density for structures or sections of structures with a maximum cross-sectional dimension less than or equal to 1', 25% of water density for structures greater than 1', and 10% of water density for structures located within the projected region directly above the vent header. The load is applied as a rectangular pulse with a duration of 100 milliseconds in the direction most critical to the structure within the region of load application.

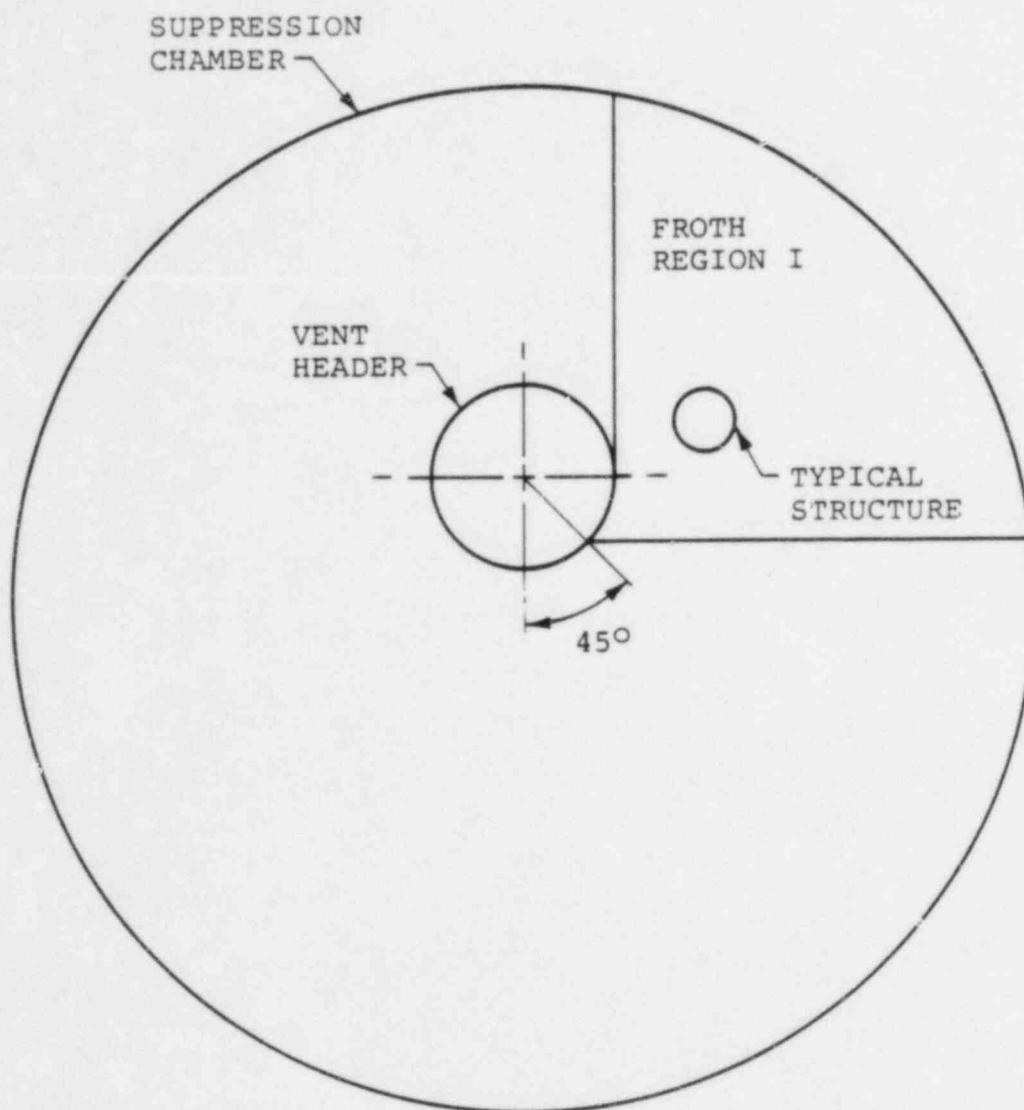
For some structures, the procedures described above result in unrealistically conservative loads. In these situations, the alternate procedure outlined in Appendix A of NUREG-0661 is used. This procedure consists of calculating Region I froth loads from high-speed QSTF movies. In this case, the froth source velocity, mean jet angle, and froth density in Region I are derived from a detailed analysis of the QSTF plant specific high-speed films.

With either methodology for Region I, the vertical component of the source velocity is decelerated to the elevation of the target structure to obtain the froth impingement velocity. The load is applied in the direction most critical to the structure within the sector obtained from QSTF movies. The QSTF movies are also used to determine whether a structure is impinged by Region I froth. Uncertainty limits for each parameter are applied to assure a conservative load specification.

The froth fallback pressure is based on the conservative assumption that all of the froth fallback momentum is transferred to the structure. The froth velocity is calculated by allowing the froth to fall freely from the height of the upper torus shell

directly above the subject structure. The froth fallback pressure is applied uniformly to the upper projected area of the structure being analyzed in the direction most critical to the behavior of the structure. The froth fallback is specified to start when the froth impingement load ends and lasts for 1.0 second. The range of direction of application is downward ± 45 degrees from the vertical.

The pool swell froth impingement and froth fallback loads used in the PUA are in accordance with Appendix A of NUREG-0661. The effects of these loadings on elevated structures are discussed in PUAR Volumes 3 through 6.

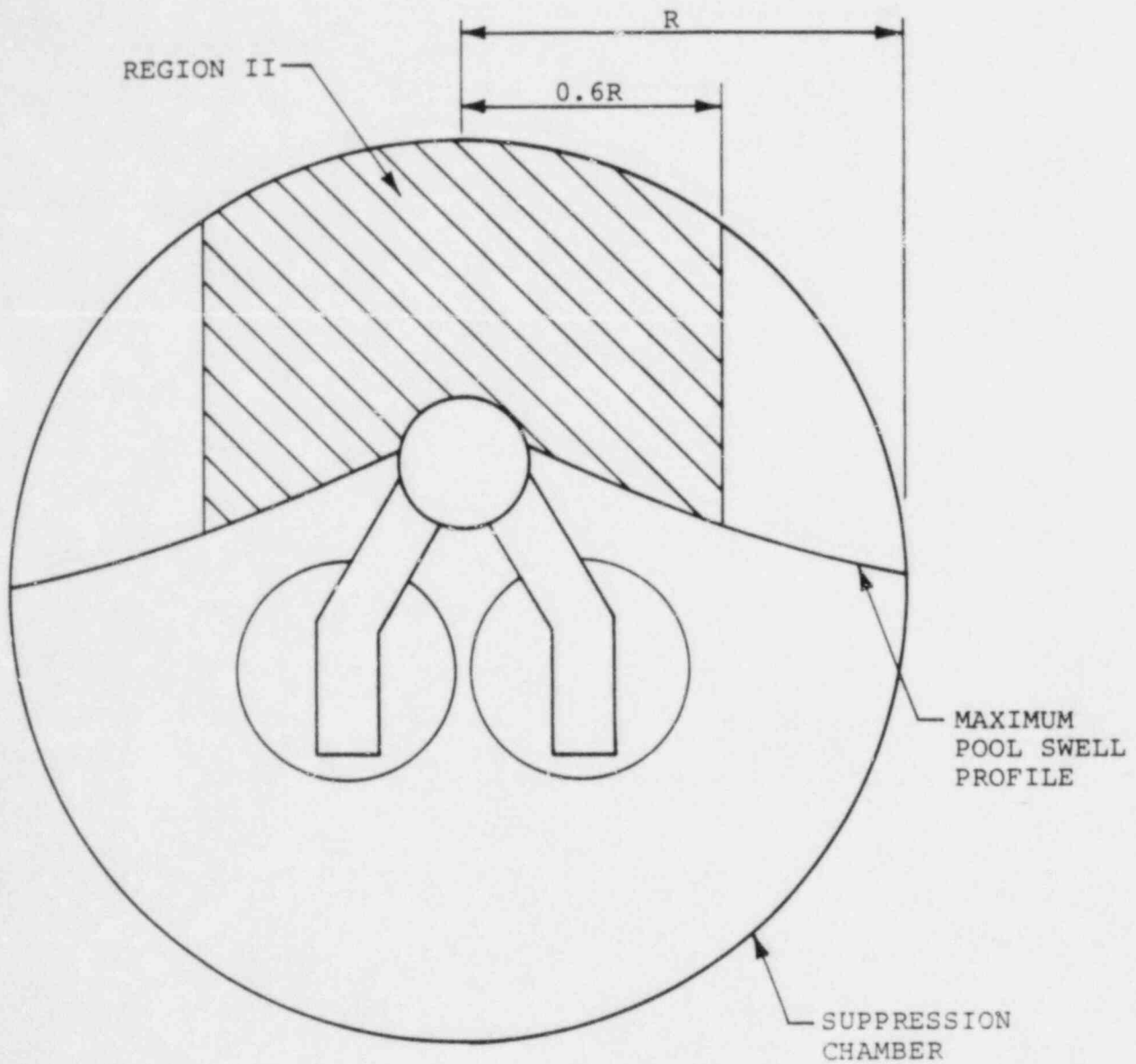


NOTE:

1. REGION IS SYMMETRICAL ON BOTH SIDES OF VENT HEADER.

Figure 1-4.1-5

FROTH IMPINCEMENT ZONE - REGION I



NOTE:

1. REGION IS SYMMETRICAL ON BOTH SIDES OF VENT HEADER.

Figure 1-4.1-6

FROTH IMPINGEMENT ZONE - REGION II

1-4.1.4.4 Pool Fallback Loads

This subsection describes pool fallback loads which apply to structures within the torus that are below the upper surface of the pool at its maximum height and above the downcomer exit level. After the pool surface has reached maximum height as a result of pool swell, it falls back under the influence of gravity and creates drag loads on structures inside the torus shell. The structures affected are between the maximum bulk pool swell height and the downcomer exit level, or immersed in an air bubble extending beneath the downcomer exit level.

For structures immersed in the pool, the drag force during fallback (as described in the LDR) is the sum of standard drag (proportional to the velocity squared) and acceleration drag (proportional to the acceleration). For structures which are beneath the upper surface of the pool but within the air bubble, there is an initial load associated with resubmergence of the structure by either an irregular impact with the bubble-pool interface or a process similar to froth fallback. This initial load is bounded by the standard drag because conservative assumptions are made in calculating the standard drag.

The load calculation procedure, as described in the LDR, requires determination of the maximum pool swell height above the height of the top surface of the structure. Freefall of the bulk fluid from this height is assumed to occur, producing both standard drag and acceleration drag. The total drag is calculated to be the sum of the two.

The LDR procedure results in a conservative calculation of the velocity since it is unlikely that any appreciable amount of pool fluid will be in freefall through this entire distance. The maximum pool swell height is determined from the OSTF plant unique tests (Reference 8).

The procedures outlined in Appendix A of NUREG-0661 are used to account for interference effects associated with both standard and acceleration drag forces.

Structures which may be enveloped by the LOCA bubble are evaluated for potential fallback loads as a result of bubble collapse to ensure that such loads are not larger than the LOCA bubble drag loads (Section 1-4.1.6).

The fallback load is applied uniformly over the upper projected surface of the structure in the direction most critical to the behavior of the structure. The range of ± 45 degrees from the vertical is applied to both the radial and longitudinal planes of the torus.

The procedures used to determine pool fallback loads in the PUA are in accordance with Appendix A of NUREG-0661. The effects of this loading on elevated structures are discussed in PUAR Volumes 3 through 6.

As the drywell pressurizes during a postulated DBA LOCA, the water slug initially standing in the submerged portion of the downcomer vents is accelerated downward into the suppression pool. As the water slug enters the pool, it forms a jet which loads structures which are intercepted by the discharge. Forces due to the pool acceleration and velocity induced by the advancing jet front are also included in the analysis.

The LOCA water jet loads affect structures which are enclosed by the jet boundaries and last from the time that the jet first reaches the structure until the last particle of the water slug passes the structure. Pool motion can create loads on structures which are within the region of motion for the duration of the water jet. The assumptions included in the methodology are presented in the load definition report.

The calculation procedure used to obtain LOCA jet loads is based on experimental data obtained from tests performed at the Quarter-Scale Test Facility

(Reference 8), and on the analytical model described in Reference 1.

As the jet travels through the pool, the particles at the rear of the water slug, which were discharged from the downcomer at higher velocities, catch up with particles at the front of the water slug, which were discharged at lower velocities. When this "overtaking" occurs, both particles are assumed to continue on at the higher velocity. As the rear particles catch up to the particles in front, the jet becomes shorter and wider. When the last fluid particle leaving the downcomer catches up to the front of the jet, the jet dissipates.

Forces due to pool motion induced by the advancing jet are calculated for structures that are within four downcomer diameters below the downcomer exit elevation. The flow field, standard drag, and acceleration drag are calculated using the equations in the LDR.

Structures that are within four downcomer diameters below the downcomer exit elevation will sustain a loading, first from the flow field induced by the jet, then from the jet itself if it is within the

cross-section of the jet. Forces resulting from the flow field are due to standard drag and acceleration drag. The force from the jet is due to standard drag only, since particles within the jet travel at a constant discharge velocity (i.e., there is no acceleration).

The standard drag force on the submerged structure is computed based on the normal component of velocity intercepting the structure, the projected area of the structure intercepted by the normal component of velocity, and the jet or flow field area.

For LOCA water jet loads, downcomers are modeled as jet sources for submerged structures based on the location of the structure.

Structures are divided into several sections, following the procedure given in the LDR and the criteria given in NUREG-0661. For each section, the location, acceleration drag volume, drag coefficient, and orientation are input into the LOCA jet model.

The LOCA water jet loads on circular, cross-sectional structures due to standard and acceleration drag are developed in accordance with Appendix A of NUREG-0661. For structures with sharp corners, these drag loads are calculated considering forces on an equivalent cylinder of diameter $D_{eq} = 2^{1/2} L_{max}$, where L_{max} is the maximum transverse dimension. For acceleration drag, this technique results in unrealistic loads on some structures such as I-beams due to the significant increase in the acceleration drag volume. In these cases, the acceleration drag volumes in Table 1-4.1-1 are used in the acceleration drag load calculation. A literature search concluded that these acceleration drag volumes are appropriate in this application. References 9 and 10 show that the values in this table are applicable for the cases evaluated in this analysis.

The effect of LOCA water jet loads on submerged structures are discussed in PUAR Volumes 2, 3, 5 and 6.

Table 1-4.1-1

HYDRODYNAMIC MASS AND ACCELERATION DRAG VOLUMES
FOR TWO-DIMENSIONAL STRUCTURAL COMPONENTS
 (LENGTH L FOR ALL STRUCTURES)


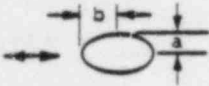
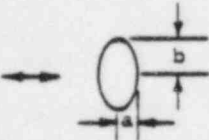
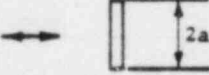
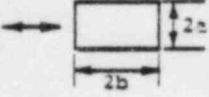
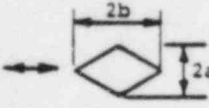
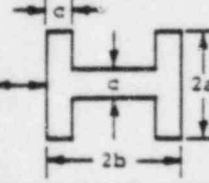
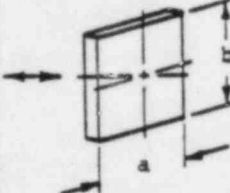
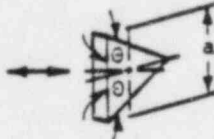
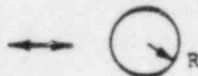
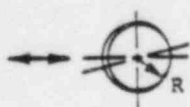
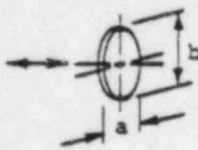
BODY	SECTION THROUGH BODY AND UNIFORM FLOW DIRECTION	HYDRODYNAMIC MASS	ACCELERATION DRAG VOLUME V_A
CIRCLE		$\rho \pi R^2 L$	$2\pi R^2 L$
ELLIPSE		$\rho \pi a^2 L$	$\pi a(a+b)L$
ELLIPSE		$\rho \pi b^2 L$	$\pi b(a+b)L$
PLATE		$\rho \pi a^2 L$	$\pi a^2 L$
RECTANGLE		$\frac{a/b}{10 \quad 1.14 \quad \rho \pi a^2 L}$ $\frac{a/b}{5 \quad 1.21 \quad \rho \pi a^2 L}$ $\frac{a/b}{2 \quad 1.36 \quad \rho \pi a^2 L}$ $\frac{a/b}{1 \quad 1.51 \quad \rho \pi a^2 L}$ $\frac{a/b}{1/2 \quad 1.70 \quad \rho \pi a^2 L}$ $\frac{a/b}{1/5 \quad 1.98 \quad \rho \pi a^2 L}$ $\frac{a/b}{1/10 \quad 2.23 \quad \rho \pi a^2 L}$	$aL(4b+a)$ $aL(4b+1.14\pi a)$ $aL(4b+1.21\pi a)$ $aL(4b+1.36\pi a)$ $aL(4b+1.51\pi a)$ $aL(4b+1.70\pi a)$ $aL(4b+1.98\pi a)$ $aL(4b+2.23\pi a)$
DIAMOND		$\frac{a/b}{2 \quad 0.85 \quad \rho \pi a^2 L}$ $\frac{a/b}{1 \quad 0.76 \quad \rho \pi a^2 L}$ $\frac{a/b}{1/2 \quad 0.67 \quad \rho \pi a^2 L}$ $\frac{a/b}{1/5 \quad 0.61 \quad \rho \pi a^2 L}$	$aL(2b+0.85\pi a)$ $aL(2b+0.76\pi a)$ $aL(2b+0.67\pi a)$ $aL(2b+0.61\pi a)$
I-BEAM		$\frac{a}{c} = 2.6 \quad \frac{c}{a} = 3.6$ $2.11 \rho \pi a^2 L$	$(2.11\pi a^2 + 2c(2a+b-c))L$

Table 1-4.1-1

HYDRODYNAMIC MASS AND ACCELERATION DRAG VOLUMES
FOR TWO-DIMENSIONAL STRUCTURAL COMPONENTS

(LENGTH L FOR ALL STRUCTURES)

(Concluded)

BODY	BODY AND FLOW DIRECTION	HYDRODYNAMIC MASS	ACCELERATION DRAG VOLUME V_A
RECTANGULAR PLATE		$\frac{b/a}{\begin{array}{l} 1 \quad 0.478 \quad \rho \pi a^2 b/4 \\ 1.5 \quad 0.680 \quad \rho \pi a^2 b/4 \\ 2 \quad 0.840 \quad \rho \pi a^2 b/4 \\ 2.5 \quad 0.953 \quad \rho \pi a^2 b/4 \\ 3 \quad \rho \pi a^2 b/4 \\ \infty \quad \rho \pi a^2 b/4 \end{array}}$	$\begin{array}{l} 0.478 \pi a^2 b/4 \\ 0.680 \pi a^2 b/4 \\ 0.840 \pi a^2 b/4 \\ 0.953 \pi a^2 b/4 \\ \pi a^2 b/4 \\ \pi a^2 b/4 \end{array}$
TRIANGULAR PLATE		$\frac{\rho a^3 (\tan \theta)^{1/2}}{3\pi}$	$\frac{a^3 (\tan \theta)^{1/2}}{3\pi}$
SPHERE		$\rho 2\pi R^3/3$	$2\pi R^3/3$
CIRCULAR DISK		$\rho 8R^3/3$	$8R^3/3$
ELLIPTICAL DISK		$\frac{b/a}{\begin{array}{l} \infty \quad 1.0 \quad \rho \pi b a^2/6 \\ 3 \quad 0.9 \quad \rho \pi b a^2/6 \\ 2 \quad 0.826 \quad \rho \pi b a^2/6 \\ 1.5 \quad 0.748 \quad \rho \pi b a^2/6 \\ 1.0 \quad 0.637 \quad \rho \pi b a^2/6 \end{array}}$	$\begin{array}{l} 1.0 \quad \pi b a^2/6 \\ 0.9 \quad \pi b a^2/6 \\ 0.826 \pi b a^2/6 \\ 0.748 \pi b a^2/6 \\ 0.637 \pi b a^2/6 \end{array}$

During the initial phase of the DBA, pressurized drywell air is purged into the suppression pool through the submerged downcomers. After the vent clearing phase of a DBA, a single bubble is formed around each downcomer. During the bubble growth period, unsteady fluid motion is created within the suppression pool. During this period, submerged structures will be subjected to transient hydrodynamic loads.

The bases of the flow model and load evaluation for the definition of LOCA bubble-induced loads on submerged structures are presented in Section 4.3.8 of the LDR.

After contact between bubbles of adjacent downcomers, the pool swell flow field above the downcomer exit elevation is derived from QSTF plant unique tests (Reference 8). After bubble contact, the load will only act vertically. This pool swell drag load is computed using the method described in Section 1-4.1.4.2.

The parameters which affect load determination are torus geometry, downcomer locations, and thermodynamic properties. Table 1-4.1-2 presents values for these plant specific parameters. The DBA plant unique transient drywell pressure-time history (Reference 8) is also used for load determination.

The torus is modeled as a rectangular cell with dimensions given in Table 1-4.1-2. The structures are divided into sections and the loads on each section are calculated following the procedure given in the LDR and the criteria given in NUREG-0661.

The procedure used for calculating drag loads on structures with circular and sharp-cornered cross-sections is in accordance with Appendix A of NUREG-3661. For some structures with sharp corners such as I-beams, the acceleration drag volumes are calculated using the information in Table 1-4.1-1.

The effects of LOCA bubble loads on submerged structures are discussed in PUAR Volumes 2, 3, 5, and 6.

Table 1-4.1-2

PLANT UNIQUE PARAMETERS
FOR LOCA BUBBLE DRAG LOAD DEVELOPMENT

PARAMETER		VALUE
NUMBER OF DOWNCOMERS		8-10
WATER DEPTH IN TORUS (ft)		14.37
CELL	WIDTH (ft)	30.6
	LENGTH (ft)	33.63 to 44.84
VERTICAL DISTANCE FROM DOWNCOMER EXIT TO TORUS CENTERLINE (ft)		4.29
DOWNCOMER	INSIDE RADIUS (ft)	0.969
	SUBMERGENCE (ft)	3.333
UNDISTURBED PRESSURE AT BUBBLE CENTER ELEVATION BEFORE THE BUBBLE APPEARS (psia)		16.564
INITIAL DRYWELL	PRESSURE BEFORE LOCA (psia)	15.2
	TEMPERATURE BEFORE LOCA (°F)	135
OVERALL VENT PIPE FRICTION FACTOR (f _l /d)		4.35
INITIAL LOCA BUBBLE WALL VELOCITY (ft/sec)		12.93

This subsection describes the CO loads acting on the various containment structures and piping systems.

Following the poci swell phase of a postulated LOCA, there is a period during which condensation oscillations occur at the downcomer exit. Condensation oscillations are associated with the pulsating movement of the steam-water interface, caused by variations in the condensation rate at the downcomer exit. These condensation oscillations cause periodic pressure oscillations on the torus shell, submerged structures, and inside the vent system. The loads specified for CO are based on the FSTF tests (References 11, 12, and 13). The LDR and NUREG-0661 discuss the bases, assumptions, and methodology for computation of the CO loads.

1-4.1.7.1 CO Loads on Torus Shell

Loads on the submerged portion of the torus shell during the CO phenomenon consist of pressure oscillations superimposed on the prevailing local static pressures.

The CO load on the torus shell is a rigid wall load specified in terms of the pressure at the torus bottom dead center. It is used in conjunction with a flexible wall coupled fluid-structure torus model. The LDR load definition for CO consists of 50 harmonic loadings with amplitudes which vary with frequency. Three alternate rigid wall pressure amplitude variations in the range of 4 to 16 hertz are specified in the load definition report. A fourth alternate load case is also considered, based on the results of Test M12 from the supplemental test series conducted at the FSTF (References 12 and 13). Table 1-4.1-3 and Figure 1-4.1-7 give the rigid wall pressure amplitude variation with frequency. The alternate frequency spectrum which produces the maximum total response is used for analysis.

The effects of all harmonics are summed to obtain the total response of the structure. Random phasing of the loading harmonics is assumed, based on experimental observations and subsequent analysis.

The implementation of the random phasing approach for the structural evaluation is accomplished by multiplying the absolute sum of the responses of all 50 harmonics by a scale factor. This scale factor is calculated using cumulative distribution function (CDF) curves of the responses at 14 locations on the FSTF torus shell. Each of the CDF curves is generated using 200 sets of random phase angles. Using this approach, a scale factor of 0.65 is developed which results in a nonexceedance probability (NEP) of 84% at a confidence level of 90% (Table 1-4.1-4). This scale factor is applied to the absolute sum of the responses of all 50 harmonics for all Hope Creek torus shell locations evaluated.

Table 1-4.1-4 compares measured and calculated FSTF response to CO loads. The calculated FSTF response in this table is determined using CO Load Alternates 1, 2, and 3 and the random phasing approach described above. The calculated response is greater

than the measured response in all cases, demonstrating the conservatism of this approach. Although not shown in Table 1-4.1-4, CO Load Alternate 4 adds approximately 20% to the calculated shell response. Thus, using Alternate 4 in the Hope Creek analysis results in additional conservatism to the comparison shown in Table 1-4.1-4 since the calculated response for Alternates 1, 2, and 3 already bounds the measured response for Alternate 4 or test M12.

Table 1-4.1-5 specifies the onset times and durations for condensation oscillation. Test results indicate that for the postulated IBA, CO loads are bounded by chugging loads. Test results also indicate that for the postulated SBA, CO loads are not significant; therefore, none is specified.

The longitudinal CO pressure distribution along the torus centerline is uniform. The cross-sectional variation of the torus wall pressure varies linearly with elevation, from zero at the water surface to the maximum at the torus bottom (Figure 1-4.1-8).

Since torus dimensions and the number of downcomers vary, the magnitude of the CO load differs for each Mark I plant. A multiplication factor is developed

to account for the effect of the pool-to-vent area ratio. This factor is 0.87 for Hope Creek, developed using the method described in the LDR. The Hope Creek plant unique CO load is determined by multiplying the amplitude of the baseline rigid wall load (Table 1-4.1-3) by this factor.

The effects of CO torus shell loads on the suppression chamber are discussed in PUAR Volume 2.

Table 1-4.1-3

DBA CONDENSATION OSCILLATION TORUS
SHELL PRESSURE AMPLITUDES

FREQUENCY INTERVALS (Hz)	MAXIMUM PRESSURE AMPLITUDE (psi)			
	ALTERNATE 1	ALTERNATE 2	ALTERNATE 3	ALTERNATE 4
0-1	0.29	0.29	0.29	0.25
1-2	0.25	0.25	0.25	0.28
2-3	0.32	0.32	0.32	0.33
3-4	0.48	0.48	0.48	0.56
4-5	1.86	1.20	0.24	2.71
5-6	1.05	2.73	0.48	1.17
6-7	0.49	0.42	0.99	0.97
7-8	0.59	0.38	0.30	0.47
8-9	0.59	0.38	0.30	0.34
9-10	0.59	0.38	0.30	0.47
10-11	0.34	0.79	0.18	0.49
11-12	0.15	0.45	0.12	0.38
12-13	0.17	0.12	0.11	0.20
13-14	0.12	0.08	0.08	0.10
14-15	0.06	0.07	0.03	0.11
15-16	0.10	0.10	0.02	0.08
16-17	0.04	0.04	0.04	0.04
17-18	0.04	0.04	0.04	0.05
18-19	0.04	0.04	0.04	0.03
19-20	0.27	0.27	0.27	0.34
20-21	0.20	0.20	0.20	0.23
21-22	0.30	0.30	0.30	0.49
22-23	0.34	0.34	0.34	0.37
23-24	0.33	0.33	0.33	0.31
24-25	0.16	0.16	0.16	0.22

Table 1-4.1-3

DBA CONDENSATION OSCILLATION TORUS
SHELL PRESSURE AMPLITUDES
 (Concluded)

FREQUENCY INTERVALS (Hz)	MAXIMUM PRESSURE AMPLITUDE (psi)			
	ALTERNATE 1	ALTERNATE 2	ALTERNATE 3	ALTERNATE 4
25-26	0.25	0.25	0.25	0.50
26-27	0.58	0.58	0.58	0.31
27-28	0.13	0.13	0.13	0.39
28-29	0.19	0.19	0.19	0.27
29-30	0.14	0.14	0.14	0.09
30-31	0.08	0.08	0.08	0.08
31-32	0.03	0.03	0.03	0.07
32-33	0.03	0.03	0.03	0.05
33-34	0.03	0.03	0.03	0.04
34-35	0.05	0.05	0.05	0.04
35-36	0.03	0.08	0.08	0.07
36-37	0.10	0.10	0.10	0.11
37-38	0.07	0.07	0.07	0.06
38-39	0.06	0.06	0.06	0.05
39-40	0.09	0.09	0.09	0.03
40-41	0.33	0.33	0.33	0.08
41-42	0.33	0.33	0.33	0.19
42-43	0.33	0.33	0.33	0.19
43-44	0.33	0.33	0.33	0.13
44-45	0.33	0.33	0.33	0.18
45-46	0.33	0.33	0.33	0.30
46-47	0.33	0.33	0.33	0.18
47-48	0.33	0.33	0.33	0.19
48-49	0.33	0.33	0.33	0.17
49-50	0.33	0.33	0.33	0.21

Table 1-4.1-4

FSTF RESPONSE TO CONDENSATION OSCILLATION

RESPONSE QUANTITY	CALCULATED FSTF RESPONSE AT 84% NEP(1)	MAXIMUM MEASURED FSTF RESPONSE		
		M8	M11B	M12
BOTTOM DEAD CENTER AXIAL STRESS (ksi)	3.0	2.3	1.6	2.7
BOTTOM DEAD CENTER HOOP STRESS (ksi)	3.7	2.6	1.4	2.9
BOTTOM DEAD CENTER DISPLACEMENT (in)	0.17	0.11	0.08	0.14
INSIDE COLUMN FORCE (kips)	184	93	68	109
OUTSIDE COLUMN FORCE (kips)	208	110	81	141

NOTE:

1. USING CO LOAD ALTERNATES 1, 2, AND 3.

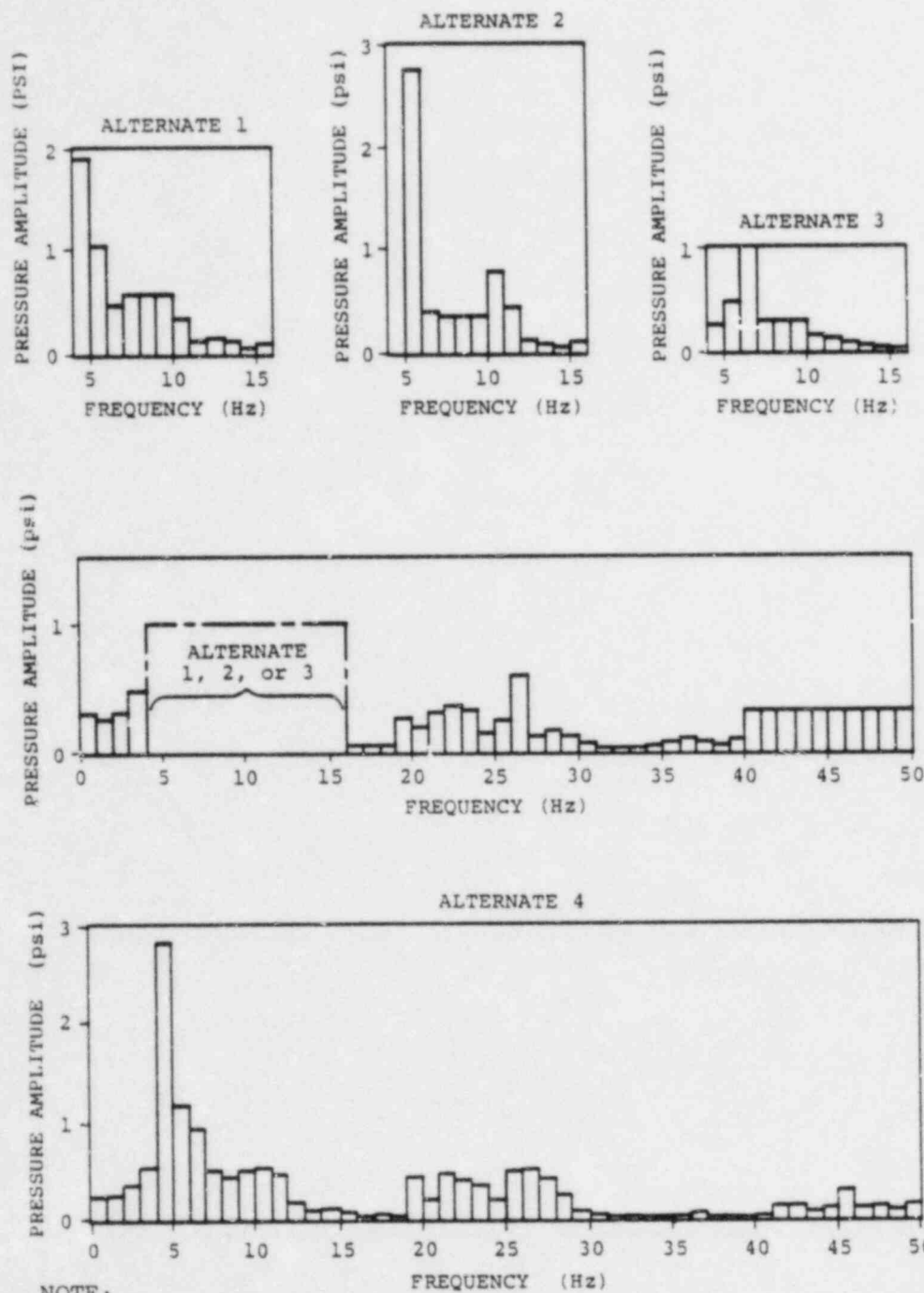
Table 1-4.1-5

CONDENSATION OSCILLATION ONSET AND DURATION

BREAK SIZE	ONSET TIME AFTER BREAK	DURATION AFTER ONSET
DBA	5 SECONDS	30 SECONDS
IBA	5 SECONDS ⁽¹⁾	300 SECONDS ⁽¹⁾
SBA	NOT APPLICABLE	NOT APPLICABLE

NOTE:

1. FOR THE IBA, CHUGGING LOADS AS DEFINED IN SECTION 1-4.1.8.2 ARE USED.

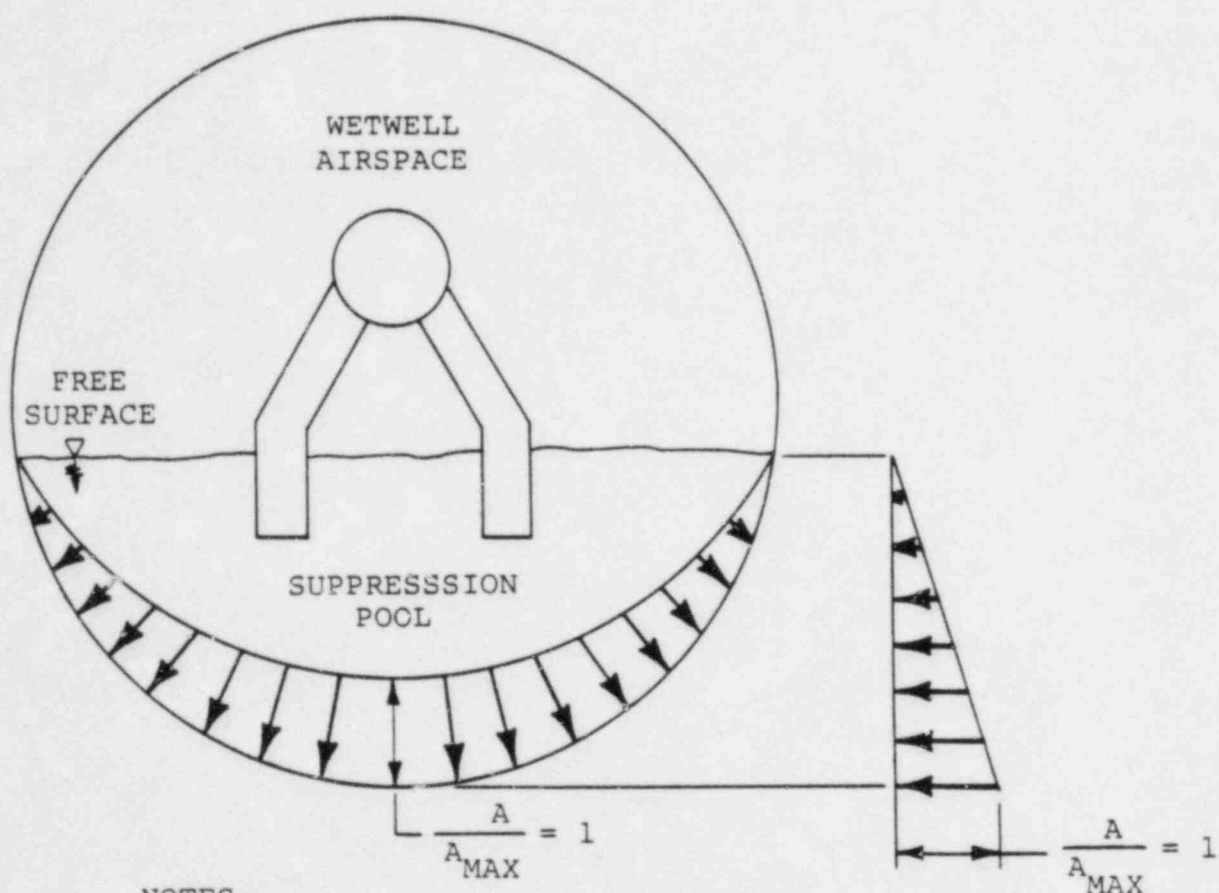


NOTE:

1. ALL AMPLITUDES REPRESENT ONE-HALF OF THE PEAK-TO-PEAK AMPLITUDE.

Figure 1-4.1- 7

CONDENSATION OSCILLATION BASELINE RIGID WALL PRESSURE
AMPLITUDES ON TORUS SHELL BOTTOM DEAD CENTER



NOTES:

1. A = LOCAL PRESSURE OSCILLATION AMPLITUDE.
2. A_{MAX} = MAXIMUM PRESSURE OSCILLATION AMPLITUDE
(AT TORUS BOTTOM DEAD CENTER).

Figure 1-4.1- 8

CONDENSATION OSCILLATION -
TORUS VERTICAL CROSS-SECTION PRESSURE DISTRIBUTION

1-4.1.7.2 CO Loads on Downcomers and Vent System

Downcomer Dynamic Loads

The downcomers experience loading during the CO phase of a postulated LOCA. The procedure for defining the dynamic portion of this loading for both a DBA and an IBA is presented in this section. Condensation oscillation loads do not occur for the SBA. The bases, assumptions, and loading definition details are presented in the LDR.

The downcomer dynamic load involves two components:

- (1) an internal pressure load of equal magnitude in each downcomer in a pair, and
- (2) a differential pressure load between downcomers in a pair.

Both the internal pressure load and the differential pressure load have three frequency bands over which they are applied. Figure 1-4.1-9 shows a typical downcomer and a schematic of downcomer loading conditions during the CO phase of a LOCA.

Table 1-4.1-6 lists the downcomer internal pressure loads for DBA CO. Figure 1-4.1-10 shows the internal pressure load and the three frequency bands over which it is applied. The dominant downcomer frequency is determined from a harmonic analysis, where the dominant downcomer frequency is shown to occur in the frequency range of the second CO downcomer load harmonic (see Volume 3). The first and third CO downcomer load harmonics are therefore applied at frequencies equal to 0.5 and 1.5 times the value of the dominant downcomer frequency.

Table 1-4.1-7 defines the downcomer differential pressure loads for DBA CO. Application of the dominant harmonic differential pressures is the same as for the internal pressure application previously discussed. Figure 1-4.1-11 shows the differential pressure amplitudes and frequency ranges.

Figure 1-4.1-12 shows how the downcomer CO dynamic loads are applied to the different downcomer pairs on the Hope Creek vent system. The total response of the downcomer-vent header intersection to the CO dynamic load is the sum of the responses from the internal and differential pressure components.

Table 1-4.1-8 provides the downcomer internal pressure loads for IBA CO. Figure 1-4.1-13 shows these downcomer internal pressure load values and the range of application. Table 1-4.1-9 gives the downcomer differential pressure loads for IBA CO. The procedure used to evaluate the IBA CO downcomer loads is the same as that used for the DBA CO downcomer loads. The load cases for the IBA loads are also the same as for the DBA loads; therefore, Figure 1-4.1-12 is used.

Vent System Loads

Loads on the vent system during the CO phenomenon result from harmonic pressure oscillations superimposed on the prevailing local static pressures in the vent system.

Condensation oscillation loads are specified for all three major components of the vent system: (1) the main vents, (2) the vent header, and (3) the downcomers (Table 1-4.1-10). As determined from FSTF data, these loads are generic and thus directly applicable to all Mark I plants.

In addition to the oscillating pressure described above, a uniform static pressure is applied to the main vents, vent header, and the downcomers to account for the nominal submergence of the downcomers.

The effects of CO loads on the vent system are evaluated in PUAR Volume 3.

Table 1-4.1-6

DOWNCOMER INTERNAL PRESSURE LOADS
FOR DBA CONDENSATION OSCILLATION

FREQUENCY	PRESSURE (psi)	APPLIED FREQUENCY RANGE (Hz)
DOMINANT	3.6	4-8
SECOND HARMONIC	1.3	8-16
THIRD HARMONIC	0.6	12-24

Table 1-4.1-7

DOWNCOMER DIFFERENTIAL PRESSURE LOADS FOR DBA
CONDENSATION OSCILLATION

FREQUENCY	PRESSURE (psi)	APPLIED FREQUENCY RANGE (Hz)
DOMINANT	2.85	4-8
SECOND HARMONIC	2.6	8-16
THIRD HARMONIC	1.2	12-24

Table 1-4.1-8

DOWNCOMER INTERNAL PRESSURE LOADS FOR IBA
CONDENSATION OSCILLATION

FREQUENCY	PRESSURE (psi)	APPLIED FREQUENCY RANGE (Hz)
DOMINANT	1.1	6-10
SECOND HARMONIC	0.8	12-20
THIRD HARMONIC	0.2	18-30

Table 1-4.1-9

DOWNCOMER DIFFERENTIAL PRESSURE LOADS FOR IBA
CONDENSATION OSCILLATION

FREQUENCY	PRESSURE (psi)	APPLIED FREQUENCY RANGE (Hz)
DOMINANT	0.2	6-10
SECOND HARMONIC	0.2	12-20
THIRD HARMONIC	0.2	18-30

Table 1-4.1-10

CONDENSATION OSCILLATION
VENT SYSTEM INTERNAL PRESSURES

COMPONENTS		DBA	IBA
MAIN VENT AND VENT HEADER	AMPLITUDE	± 2.5 psi	± 2.5 psi
	FREQUENCY RANGE	AT FREQUENCY OF MAXIMUM RESPONSE IN 4-8 Hz RANGE	AT FREQUENCY OF MAXIMUM RESPONSE IN 6-10 Hz RANGE
	FORCING FUNCTION	SINUSOIDAL	SINUSOIDAL
	SPATIAL DISTRIBUTION	UNIFORM	UNIFORM
DOWNCOMERS	AMPLITUDE	± 5.5 psi	± 2.1 psi
	FREQUENCY RANGE	AT FREQUENCY OF MAXIMUM RESPONSE IN 4-8 Hz RANGE	AT FREQUENCY OF MAXIMUM RESPONSE IN 6-10 Hz RANGE
	FORCING FUNCTION	SINUSOIDAL	SINUSOIDAL
	SPATIAL DISTRIBUTION	UNIFORM	UNIFORM

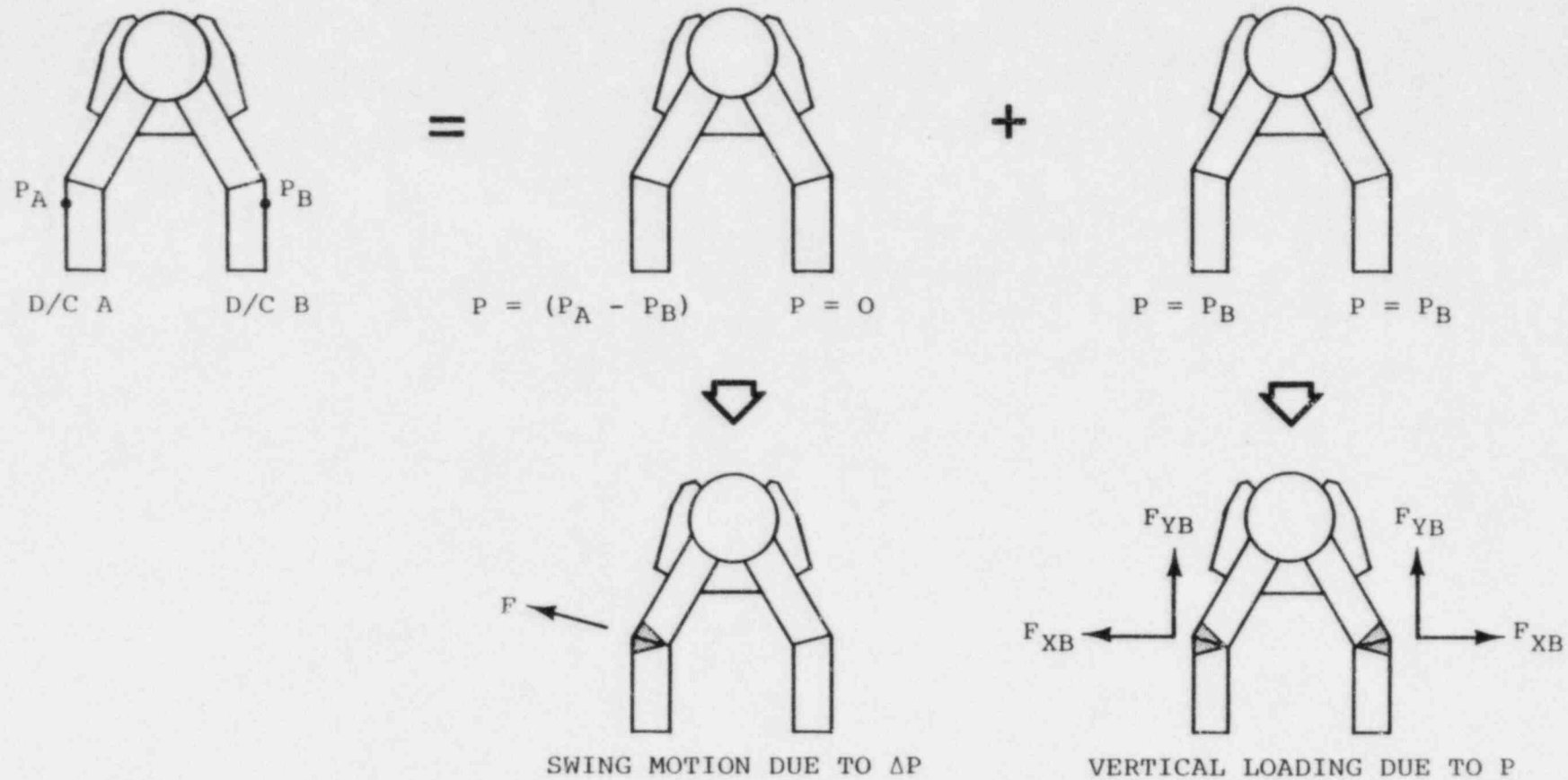
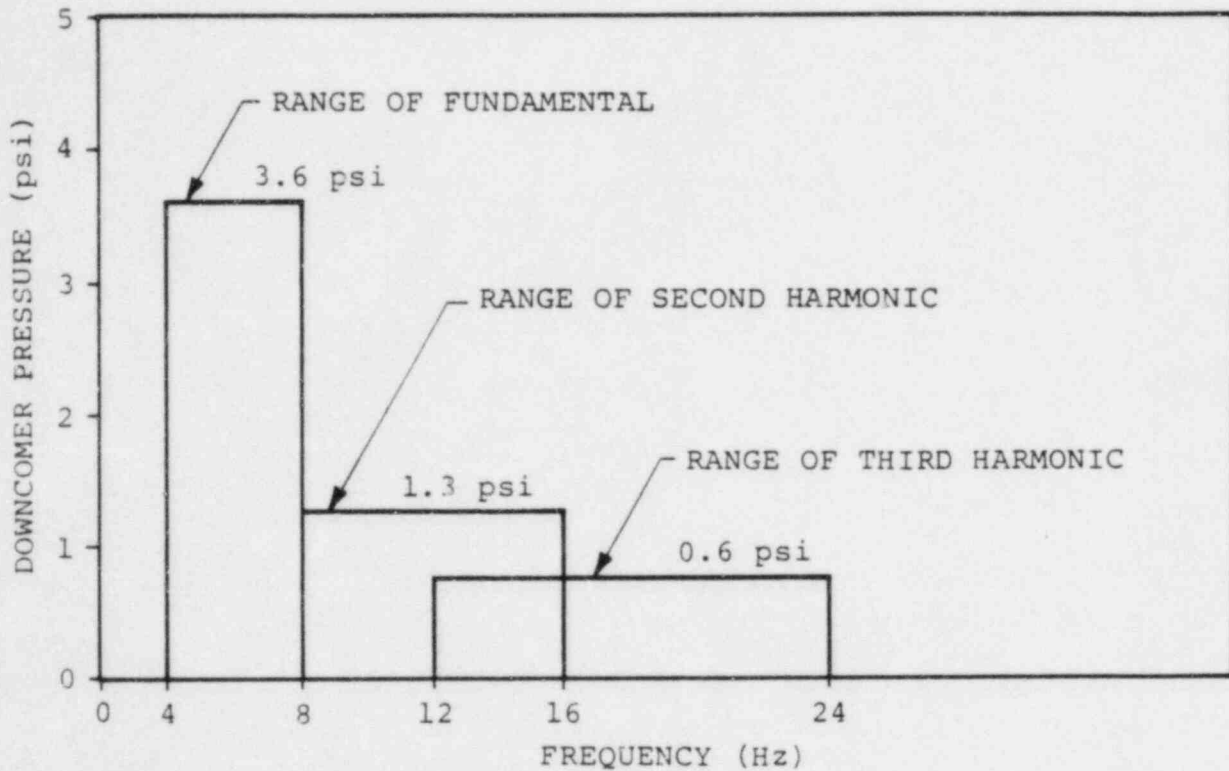


Figure 1-4.1-9

CONDENSATION OSCILLATION DOWNCOMER DYNAMIC LOAD

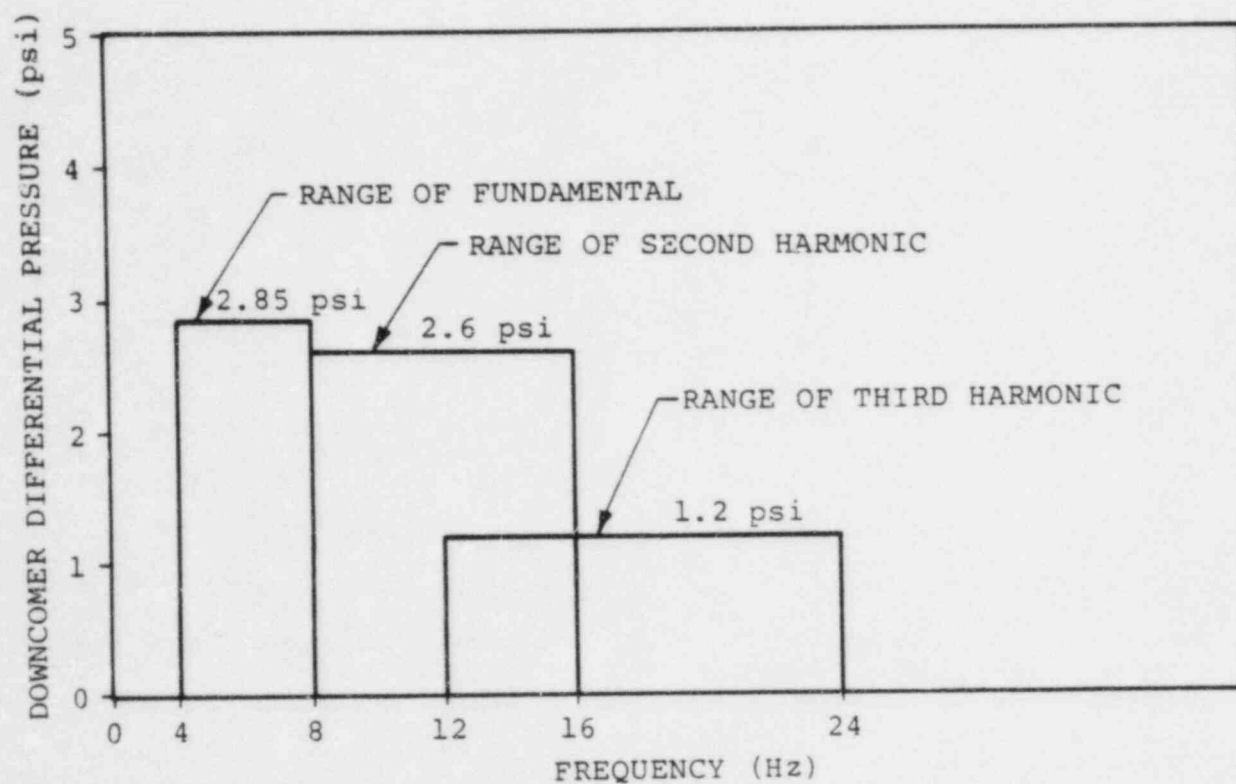


NOTE:

1. THE AMPLITUDES SHOWN ARE HALF-RANGE (ONE-HALF OF THE PEAK-TO-PEAK VALUE) .

Figure 1-4.1-10

DOWNCOMER PAIR INTERNAL PRESSURE LOADING FOR DBA CO

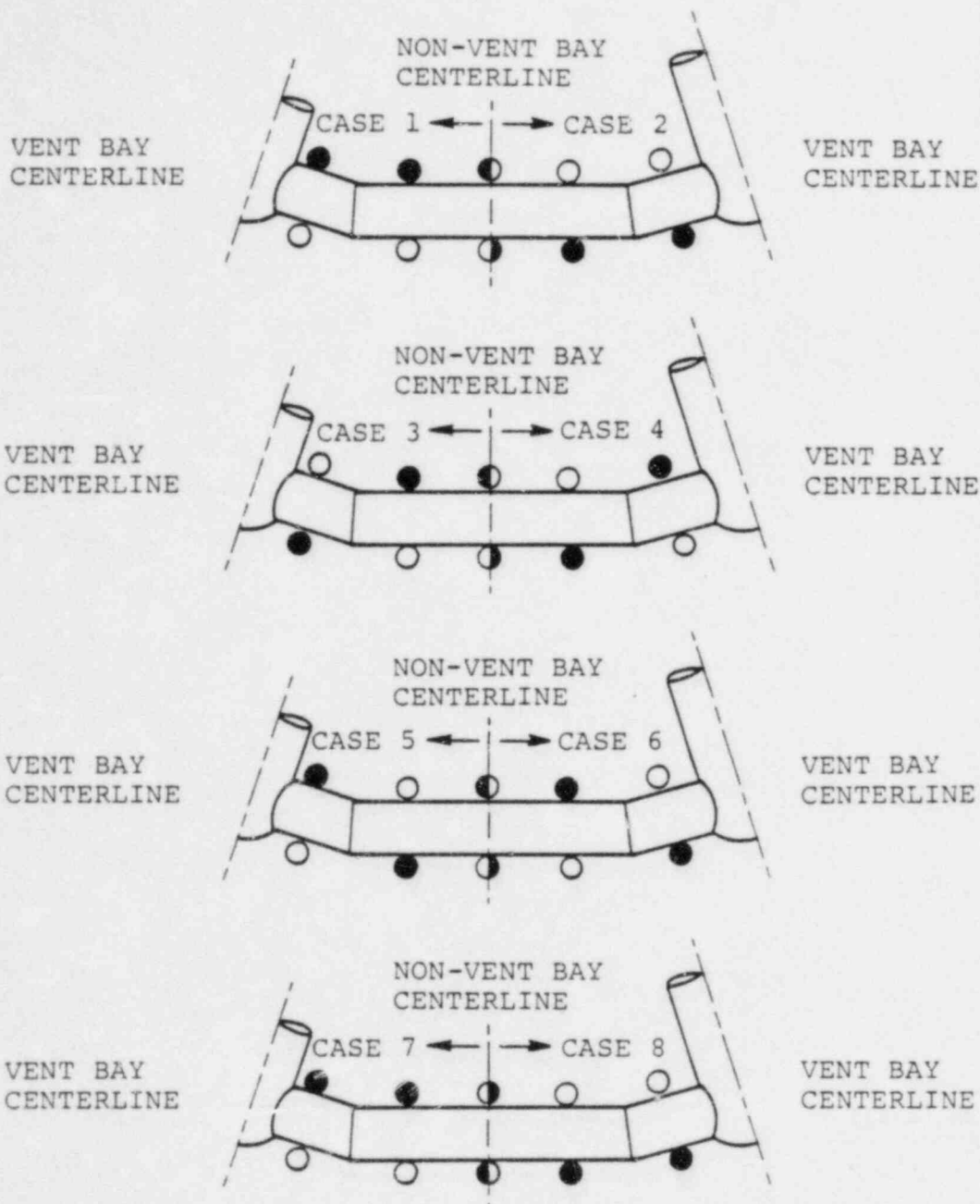


NOTE:

1. THE AMPLITUDES SHOWN ARE HALF-RANGE (ONE-HALF OF THE PEAK-TO-PEAK VALUE).

Figure 1-4.1- 11

DOWNCOMER PAIR DIFFERENTIAL PRESSURE LOADING FOR DEA CO

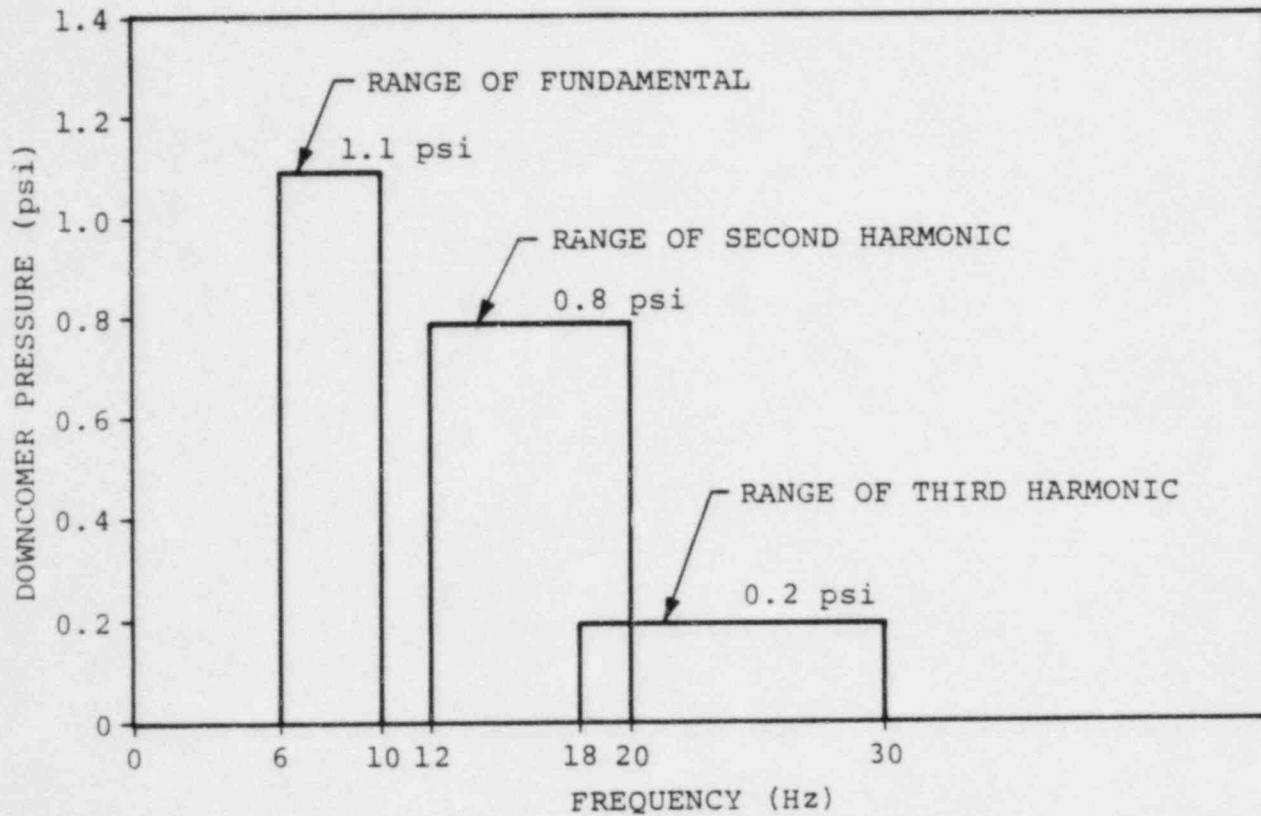


NOTES:

1. • D/C WITH INITIAL DIFFERENTIAL PRESSURE LOAD.
2. ALL D/C's HAVE INTERNAL PRESSURE LOAD IN PHASE WITH DIFFERENTIAL PRESSURE LOAD.
3. ANALYZED ALL EIGHT CASES-USED MAXIMUM RESPONSE FOR DESIGN.

Figure 1-4.1-12

DOWNCOMER CO DYNAMIC LOAD APPLICATION



NOTE:

1. THE AMPLITUDES SHOWN ARE HALF-RANGE (ONE-HALF OF THE PEAK-TO-PEAK VALUE).

Figure 1-4.1-13

DOWNCOMER INTERNAL PRESSURE LOADING FOR IBA CO

1-4.1.7.3 CO Loads on Submerged Structures

The CO phase of a postulated LOCA induces bulk pool motion, creating drag loads on structures submerged in the pool. The basis of the analytical model used to determine CO loads on submerged structures is presented in the LDR.

Condensation oscillations result in pressure sources located at the downcomer exits. The average source strengths are determined from wall load measurements. By using potential flow theory and the method of images to account for the effects of solid walls and the free surface, the velocity and acceleration flow fields within the torus are established. For each structure, the loads are computed using both the average source strength applied at all downcomers and the maximum source strength applied at the nearest downcomer.

The FSI effects are included when the local fluid acceleration is less than twice the torus boundary acceleration. Suppression pool fluid accelerations are computed within the torus using frequency-decomposed radial shell accelerations obtained from the torus analysis described in PUAR Volume 2. The

FSI effects for a given structure are computed using the pool fluid accelerations at the location of the structure.

The CO drag forces on submerged structures can be separated into two components: (1) standard drag, and (2) acceleration drag. The sum of these two effects gives the total drag load on a submerged structure. The calculations for CO loads on submerged structures use the same procedure used for calculating LOCA bubble-induced drag loads on submerged structures. Acceleration drag volumes for some structures with sharp corners (e.g., I-beams) are calculated using equations from Table 1-4.1-1 instead of volumes derived by circumscribed cylinders, as noted in Section 1-4.1.5.

Presented in Table 1-4.1-11 are the source amplitudes used for CO loads on submerged structures, which are in accordance with NUREG-0661. The source forcing function has the form of a sinusoidal wave characterized by the appropriate amplitude and frequency taken from Table 1-4.1-11. The LDR defines the total drag force as the summation of the resulting responses from all 50 harmonics. As

described in Section 1-4.1.7.1, the summation is performed to achieve a NEP of 84%.

The effects of CO loads on submerged structures are assessed in PUAR Volumes 2, 3, 5, and 6.

Table 1-4.1-11

AMPLITUDES AT VARIOUS FREQUENCIES
FOR CONDENSATION OSCILLATION SOURCE FUNCTION
FOR LOADS ON SUBMERGED STRUCTURES

FREQUENCY (Hz)	AMPLITUDE (ft ³ /sec ²)	FREQUENCY (Hz)	AMPLITUDE (ft ³ /sec ²)
0-1	28.38	26-27	56.75
1-2	24.46	27-28	12.72
2-3	31.31	28-29	18.59
3-4	46.97	29-30	13.70
4-5	182.00	30-31	7.83
5-6	267.13	31-34	2.94
6-7	96.87	34-35	4.89
7-10	57.73	35-36	7.83
10-11	77.30	36-37	9.79
11-12	44.03	37-38	6.85
12-13	16.63	38-39	5.87
13-14	11.74	39-40	8.81
14-15	6.85	40-41	32.29
15-16	9.79	41-42	32.29
16-19	3.91	42-43	32.29
19-20	26.42	43-44	32.29
20-21	19.57	44-45	32.29
21-22	29.36	45-46	32.29
22-23	33.27	46-47	32.29
23-24	32.29	47-48	32.29
24-25	15.66	48-49	32.29
25-26	24.46	49-50	32.29

This subsection describes the chugging loads on the various containment structures and piping systems.

Chugging occurs during a postulated LOCA when the steam flow through the vent system falls below the rate necessary to maintain steady condensation at the downcomer exits. The corresponding flowrates for chugging are less than those of the CO phenomenon. During chugging, steam bubbles form at the downcomer exits, oscillate as they grow to a critical size (approximately downcomer diameter), and begin to collapse independently in time. The resulting load on the torus shell due to a chug cycle consists of a low frequency oscillation (pre-chug) which corresponds to the oscillating bubbles at the downcomer exit as they grow, followed by a higher frequency "ring-out" of the torus shell-pool water system (post-chug) in response to the collapsing bubbles (Figure 1-4.1-14).

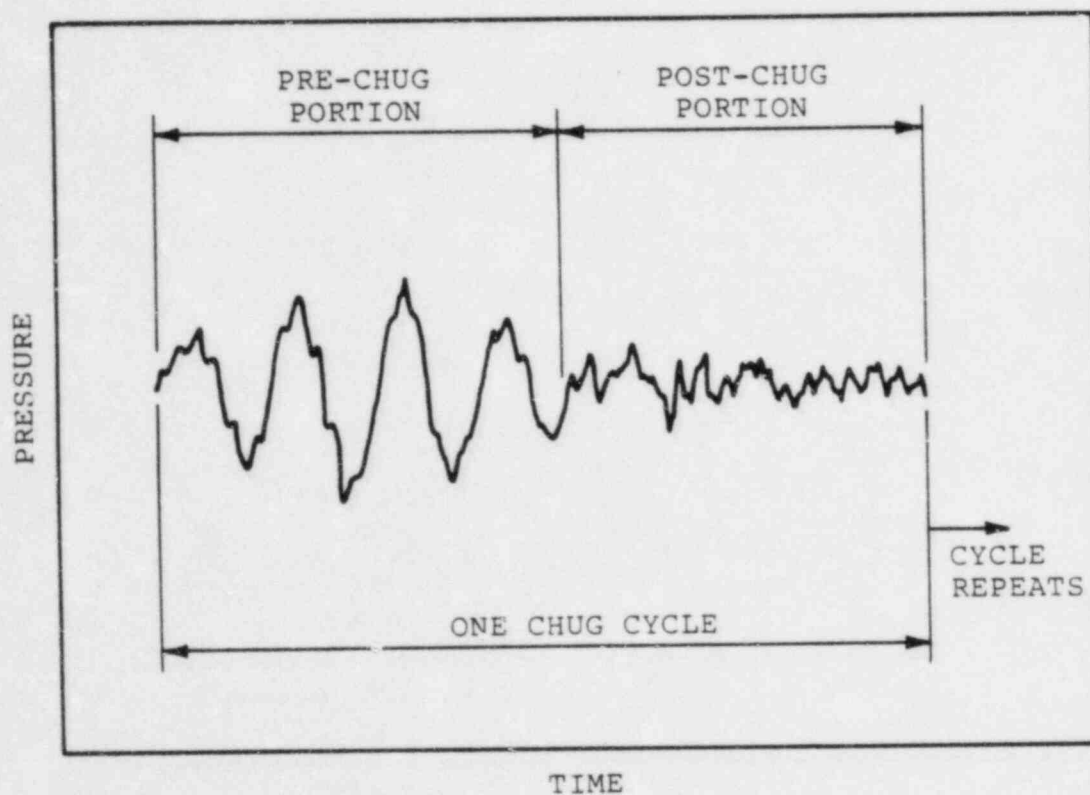


Figure 1-4.1-14

TYPICAL CHUGGING PRESSURE TRACE ON THE TORUS SHELL

BPC-01-300-1
Revision 0

1-4.66

nutech
ENGINEERS

1-4.1.8.1 Chugging Loads on Torus Shell

During the chugging phase of a postulated LOCA, the chugging loads on the torus shell occur as a series of chug cycles. The chugging load cycles are divided into pre-chug and post-chug portions. The bases for pre-chug and post-chug rigid wall load definitions are presented in the load definition report.

For the pre-chug portion of the chug cycle, both symmetric and asymmetric loading conditions are used to conservatively account for any randomness in the chugging phenomenon. The asymmetric loading is based on both low and high amplitude chugging data conservatively distributed around the torus in order to maximize the asymmetric loading.

In order to bound the post-chug portion of the chug cycle, symmetric loads are used. Asymmetric loads are not specified since any azimuthal response would be governed by the asymmetric pre-chug low frequency load specification.

Presented in Table 1-4.1-12 are the chugging onset times and durations for the DBA, IBA, and SBA, which are in accordance with the LDR. Hope Creek utilizes turbine driven feedwater pumps, and the IBA scenario for this configuration is described in Section 2.2 of the LDR. For the SBA, the automatic depressurization system (ADS) is assumed to initiate 300 seconds after the break and the reactor is assumed to be depressurized 200 seconds after ADS initiation, when chugging ends. For the IBA, the reactor is assumed to be depressurized 600 seconds after ADS initiation, when chugging ends.

a. Pre-Chug Load

The symmetric pre-chug torus shell pressure load is specified as ± 2 psi, applied uniformly along the torus longitudinal axis. Figure 1-4.1-15 shows the longitudinal distribution of the asymmetric pre-chug pressure load, which varies from ± 0.4 to ± 2.0 psi. The pre-chug cross-sectional distribution for both symmetric and asymmetric cases is the same as for CO (Figure 1-4.1-16). The pre-chug loads are applied at the structural frequency in the range of 6.9 to 9.5 hertz. Table 1-4.1-12

shows the pre-chug load is conservatively assumed to be a steady state harmonic load applied throughout the chugging durations shown in Table 1-4.1-12.

b. Post-Chug Load

Table 1-4.1-13 and Figure 1-4.1-17 define the amplitude versus frequency variation for the post-chug torus shell pressure load. The load is applied uniformly along the torus longitudinal axis. The cross-sectional variation is the same for CO and pre-chug loads (Figure 1-4.1-16). The steady-state responses from the application of the pressure amplitudes at each frequency given in Figure 1-4.1-17 are summed. The summation is performed to achieve a NEP of 84% as described in Section 1-4.1.7.1 for the CO load. The post-chug load is conservatively assumed to be a steady state harmonic load applied throughout the chugging durations shown in Table 1-4.1-12.

The effects of chugging loads on the torus shell are evaluated in PUAR Volume 2.

Table 1-4.1-12

CHUGGING ONSET AND DURATION

BREAK SIZE	ONSET TIME AFTER BREAK	DURATION AFTER ONSET
DBA	35 SECONDS	30 SECONDS
IBA	305 SECONDS	200 SECONDS
SBA	300 SECONDS	900 SECONDS

Table 1-4.1-13

POST-CHUG RIGID WALL PRESSURE AMPLITUDES
ON TORUS SHELL BOTTOM DEAD CENTER

FREQUENCY RANGE (1) (Hz)	PRESSURE (psi)	FREQUENCY RANGE (1) (Hz)	PRESSURE (psi)
0-1	0.04	25-26	0.04
1-2	0.04	26-27	0.28
2-3	0.05	27-28	0.18
3-4	0.05	28-29	0.12
4-5	0.06	29-30	0.09
5-6	0.05	30-31	0.03
6-7	0.10	31-32	0.02
7-8	0.10	32-33	0.02
8-9	0.10	33-34	0.02
9-10	0.10	34-35	0.02
10-11	0.06	35-36	0.03
11-12	0.05	36-37	0.05
12-13	0.03	37-38	0.03
13-14	0.03	38-39	0.04
14-15	0.02	39-40	0.04
15-16	0.02	40-41	0.15
16-17	0.01	41-42	0.15
17-18	0.01	42-43	0.15
18-19	0.01	43-44	0.15
19-20	0.04	44-45	0.15
20-21	0.03	45-46	0.15
21-22	0.05	46-47	0.15
22-23	0.05	47-48	0.15
23-24	0.05	48-49	0.15
24-25	0.04	49-50	0.15

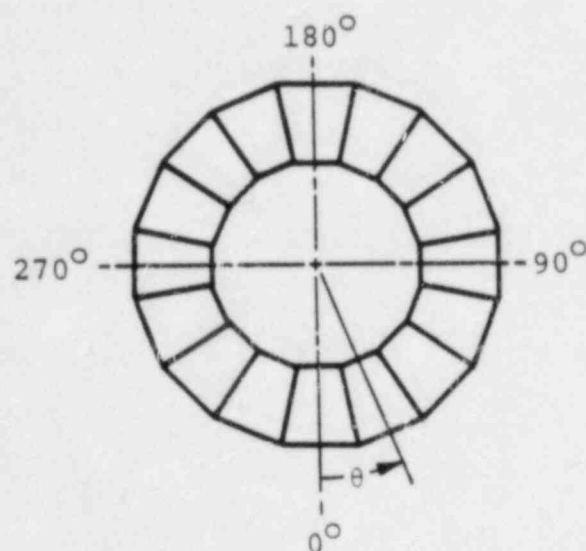
NOTE:

1. HALF-RANGE (= ONE-HALF PEAK-TO-PEAK AMPLITUDE).

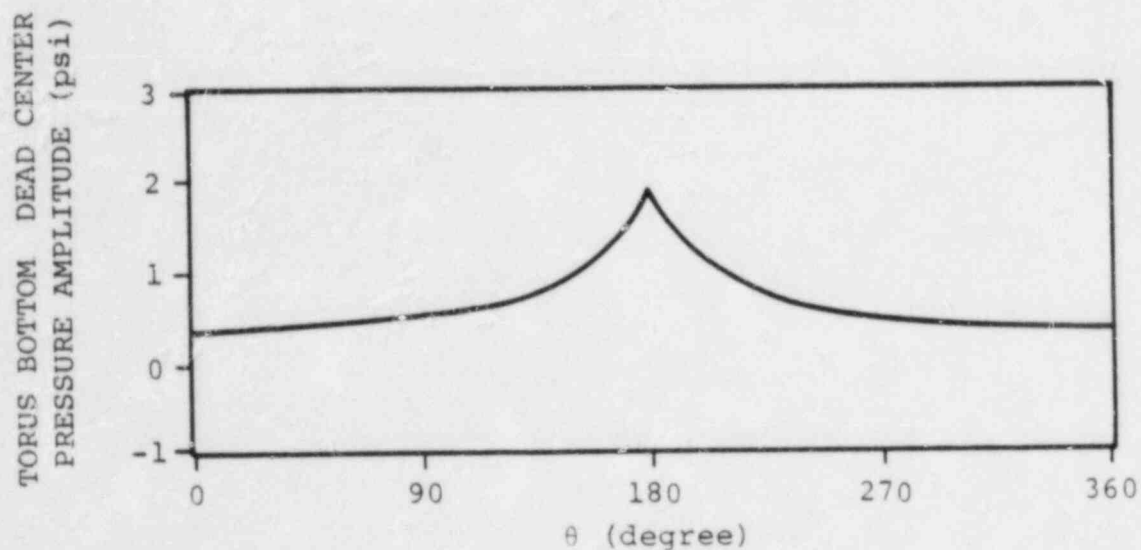
BPC-01-300-1

Revision 0

1-4.71



PLAN VIEW OF TORUS



NOTES:

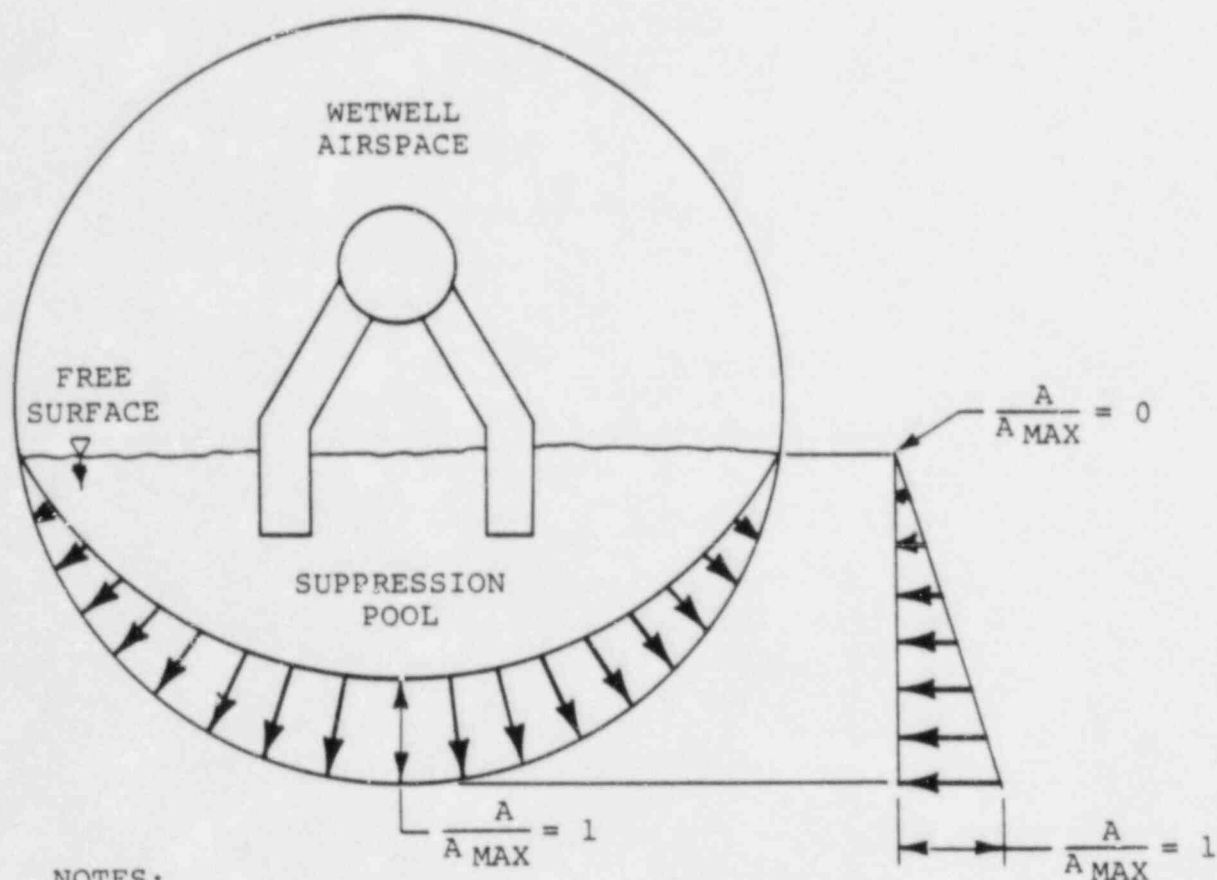
1. THE AMPLITUDE SHOWN HERE REPRESENTS ONE-HALF OF THE PEAK-TO-PEAK AMPLITUDE.
2. HIGHEST VALUE IN BAY APPLIED OVER THE ENTIRE BAY.

Figure 1-4.1- 15

CHUGGING - TORUS LONGITUDINAL
DISTRIBUTION FOR ASYMMETRIC PRESSURE AMPLITUDE

BPC-01-300-1
Revision 0

1-4.72



NOTES:

1. A = LOCAL PRESSURES OSCILLATION AMPLITUDE.
2. A_{MAX} = MAXIMUM PRESSURE OSCILLATION AMPLITUDE (AT TORUS BOTTOM DEAD CENTER).

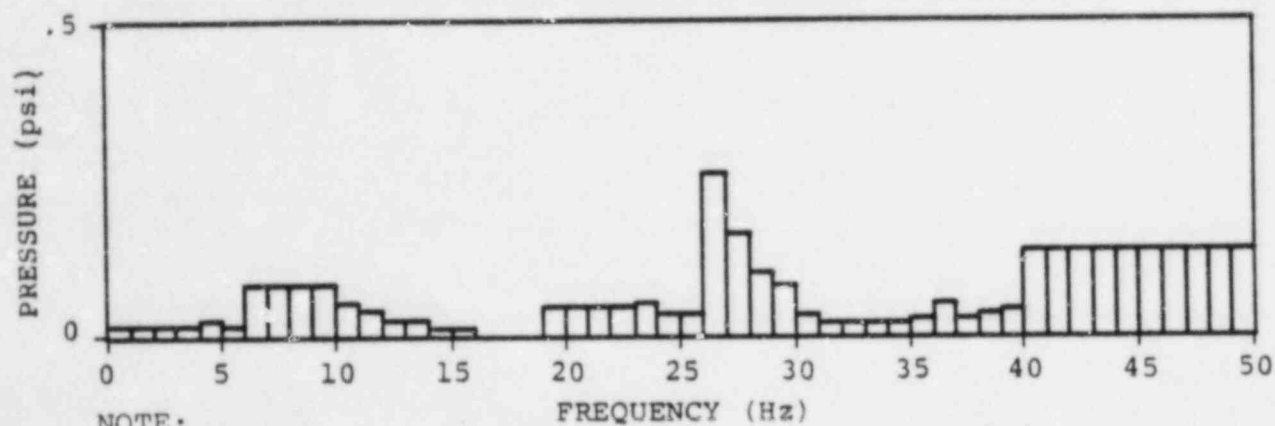
Figure 1-4.1-16

CHUGGING - TORUS VERTICAL CROSS-SECTION
PRESSURE DISTRIBUTION

BPC-01-300-1
Revision 0

1-4.73

nutech
ENGINEERS



NOTE:

1. THE AMPLITUDE SHOWN HERE REPRESENTS ONE-HALF OF THE PEAK-TO-PEAK AMPLITUDE.

Figure 1-4.1- 17
POST-CHUG RIGID WALL PRESSURE AMPLITUDES
ON TORUS SHELL BOTTOM DEAD CENTER

BPC-01-300-1
 Revision 0

1-4.74

1-4.1.8.2 Chugging Downcomer Lateral Loads

During the chugging phase of a postulated LOCA, bubbles which form at the downcomer exits collapse suddenly and intermittently to produce lateral loads on the downcomers. This section presents the procedure used for defining the dynamic portion of this loading.

The basis for the chugging lateral load definition is the data obtained from the instrumented downcomers of the FSTF. The load definition was developed for, and is directly applicable to, downcomer pairs which are untied. Based on FSTF observations, this load definition is also applicable to tied downcomers.

The FSTF downcomer lateral loads are defined as resultant static-equivalent loads (RSEL) which, when applied statically to the end of the downcomer, reproduce the maximum measured bending response near the downcomer-vent header (DC/VH) junction.

The loads associated with chugging obtained from the FSTF data are scaled to determine plant specific loads for Hope Creek. The maximum downcomer load

magnitude, histograms of load reversals, and the maximum vent system loading produced by synchronous chugging of the downcomers are determined from the FSTF loads.

NUREG-0661 states that the force per downcomer should be based on a probability of exceedance of 10^{-4} per LOCA for multiple downcomers during chugging. This requirement relates to the potential for a number of downcomers experiencing a lateral load in the same direction at the same time. The correlation between load magnitude and probability level was derived from a statistical analysis of FSTF data. A probability of exceedance of 10^{-4} per LOCA bounds all the load cases up to about 120 downcomers during chugging at the same time in a given plant. Hope Creek has 80 downcomers; therefore, a probability of exceedance of 10^{-4} per LOCA is conservative and is used for the multiple downcomer chugging load cases (Figure 1-4.1-18).

For fatigue evaluation of the downcomers, the required stress reversals at the downcomer-vent header junction are obtained from the FSTF RSEL reversal histograms. The plant unique junction stress reversals are obtained by scaling the FSTF

RSEL reversals by the ratio of the chugging duration specified for Hope Creek to that of the full-scale test facility. Table 1-4.1-12 specifies chugging durations for the DBA, IBA, and small break accident.

The effects of chugging downcomer lateral loads on the vent system are evaluated in PUAR Volume 3.

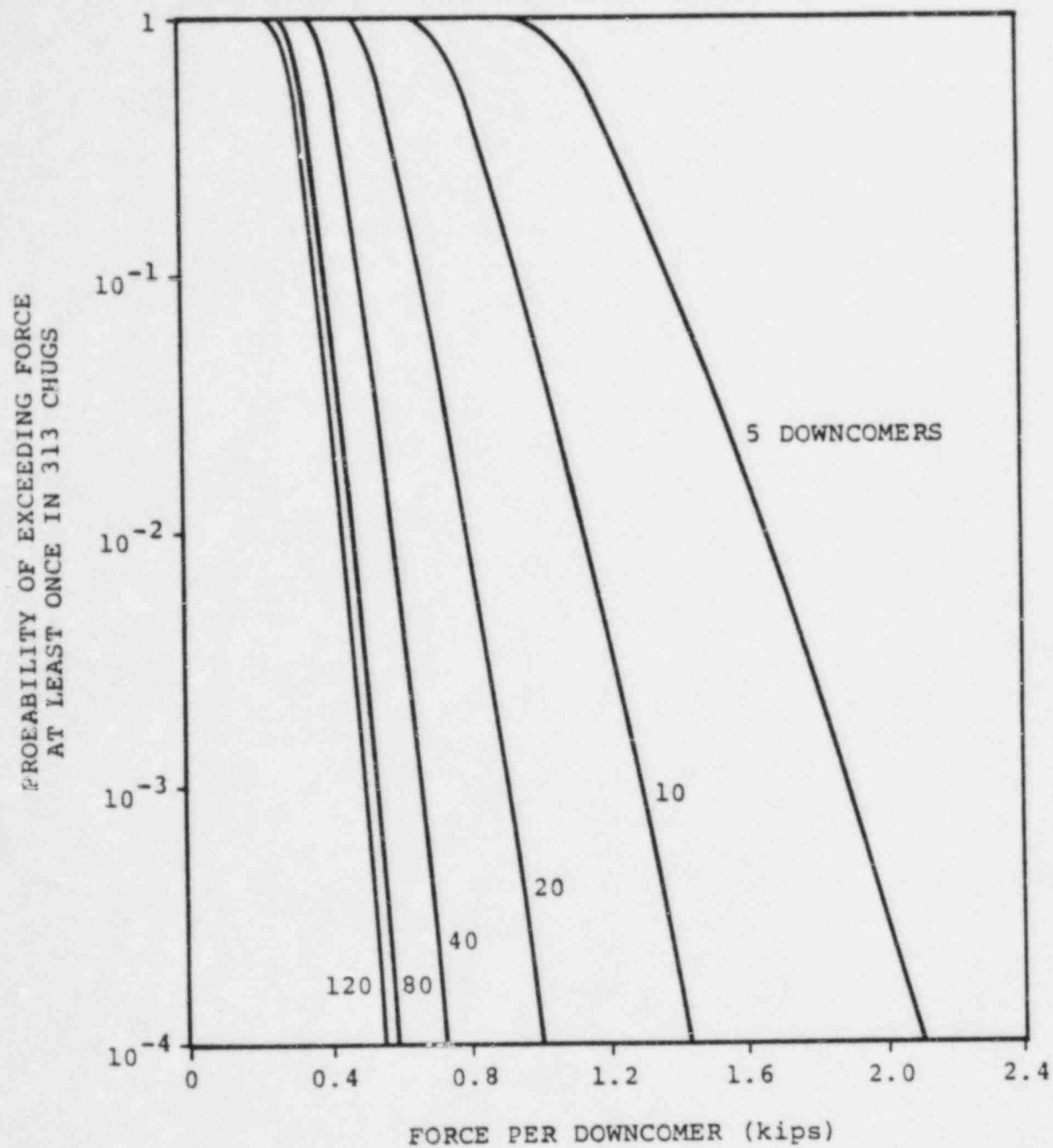


Figure 1-4.1- 18

PROBABILITY OF EXCEEDING A GIVEN FORCE PER DOWNCOMER
FOR DIFFERENT NUMBERS OF DOWNCOMERS

1-4.1.8.3 Chugging Loads on Submerged Structures

Chugging at the downcomer exits induces bulk pool motion, and therefore creates drag loads on structures submerged in the pool. The submerged structure load definition method for chugging follows that used to predict drag forces caused by condensation oscillations (see Section 1-4.1.7.3), except that the source strength for chugging is proportional to the wall load measurement corresponding to the chugging regime.

The LDR presents the bases and assumptions of the analytical model used for the chugging load definition. Table 1-4.1-14 presents the source amplitudes for pre-chug and post-chug regimes.

The load development procedure for chugging loads on submerged structures is the same as presented in Section 1-4.1.7.3 for CO loads and is in accordance with NUREG-0661. The responses from the 50 harmonics are summed as described in Section 1-4.1.7.1. Acceleration drag volumes for structures with sharp corners (e.g., I-beams) are calculated using equations from Table 1-4.1-1. Fluid-structure

interaction effects are included as described in
Section 1-4.1.7.3.

The effects of chugging loads on submerged
structures are evaluated in PUAR Volumes 2, 3, 5,
and 6.

Table 1-4.1-14

AMPLITUDES AT VARIOUS FREQUENCIES FOR CHUGGING
SOURCE FUNCTION FOR LOADS ON SUBMERGED STRUCTURES

CHUGGING	FREQUENCY (Hz)	AMPLITUDE (ft ³ /sec ²)
PRE	6.9 - 9.5	195.70
POST	0-2	11.98
	2-3	10.36
	3-4	9.87
	4-5	17.40
	5-6	17.00
	6-10	18.88
	10-11	87.90
	11-12	76.18
	12-13	41.01
	13-14	35.89
	14-15	6.82
	15-16	6.20
	16-17	3.14
	17-18	4.18
	18-19	2.94
	19-20	16.82
	20-21	17.53
	21-22	30.67

Table 1-4.1-14

AMPLITUDES AT VARIOUS FREQUENCIES FOR CHUGGING
SOURCE FUNCTION FOR LOADS ON SUBMERGED STRUCTURES
(Concluded)

CHUGGING	FREQUENCY (Hz)	AMPLITUDE (ft ³ /sec ²)
POST	22-24	92.39
	24-25	134.50
	25-26	313.84
	26-27	377.83
	27-28	251.89
	28-29	163.32
	29-30	116.66
	30-31	43.14
	31-32	21.57
	32-33	37.91
	33-34	50.54
	34-35	42.54
	35-36	61.87
	36-37	41.95
	37-38	20.97
	38-39	24.47
	39-40	29.37
	40-50	224.90

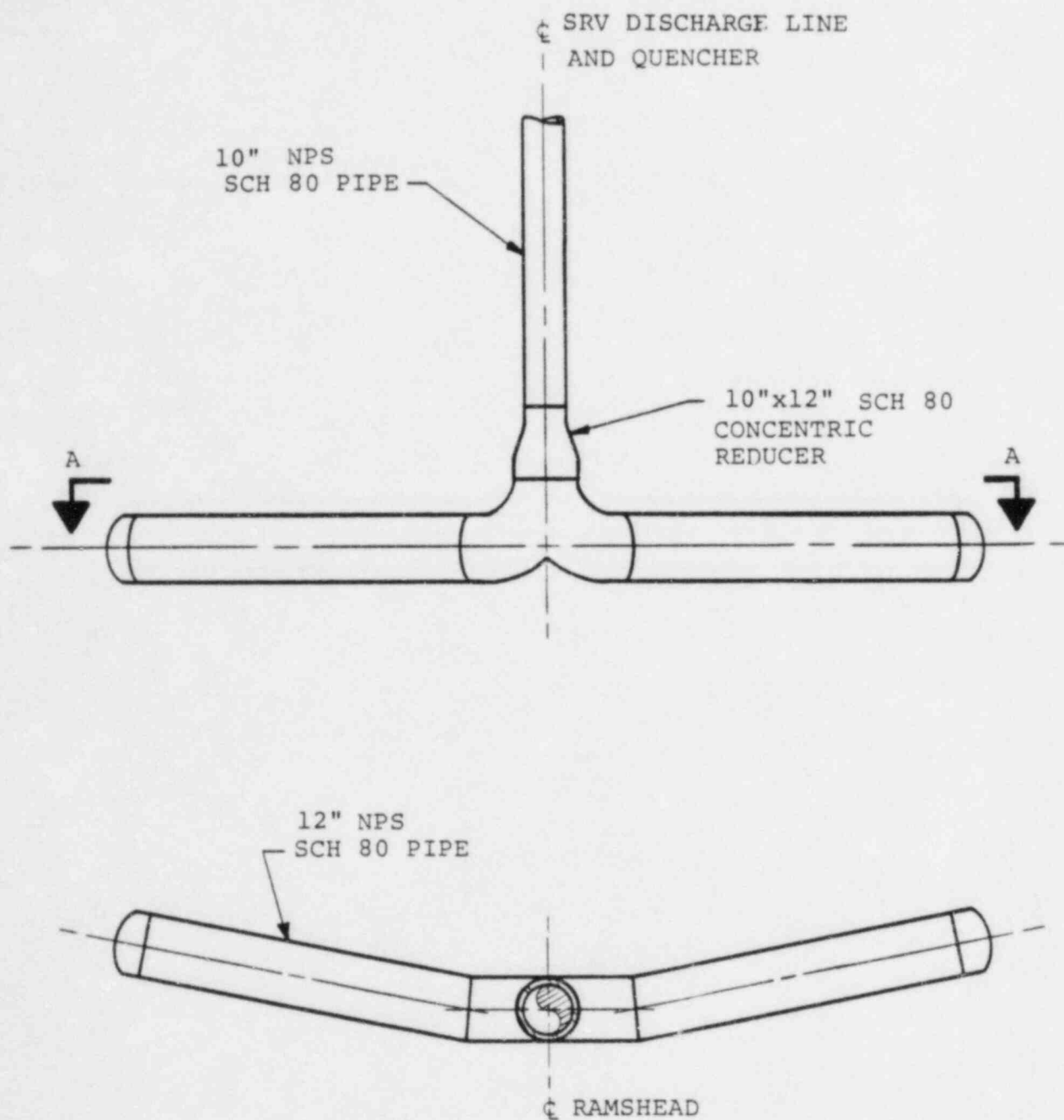
This section discusses the procedures used to determine loads resulting from the actuation of one or more SRV's.

When a SRV actuates, pressure and thrust loads are exerted on the SRVDL piping and the T-quencher discharge device. In addition, the expulsion of water followed by air into the suppression pool through the T-quencher results in pressure loads on the submerged portion of the torus shell and in drag loads on submerged structures.

The T-quencher utilized in Hope Creek is a standard Mark I T-quencher described in the load definition report. The T-quencher has 12", Schedule 80 arms which are mitered at the connection to the ramshead as described in Section 1-2.1.4. Since the T-quenchers for Hope Creek are located at the mitered joint, use of a mitered T-quencher results in symmetric torus shell loads. Figures 1-4.2-1 and 1-4.2-2 illustrate the geometry of the SRVDL, ramshead, and T-quencher connection and the hole distribution along a typical quencher arm.

Volume 5 of this PUAR provides a detailed description of the SRVDL, T-quencher, and their related support structures.

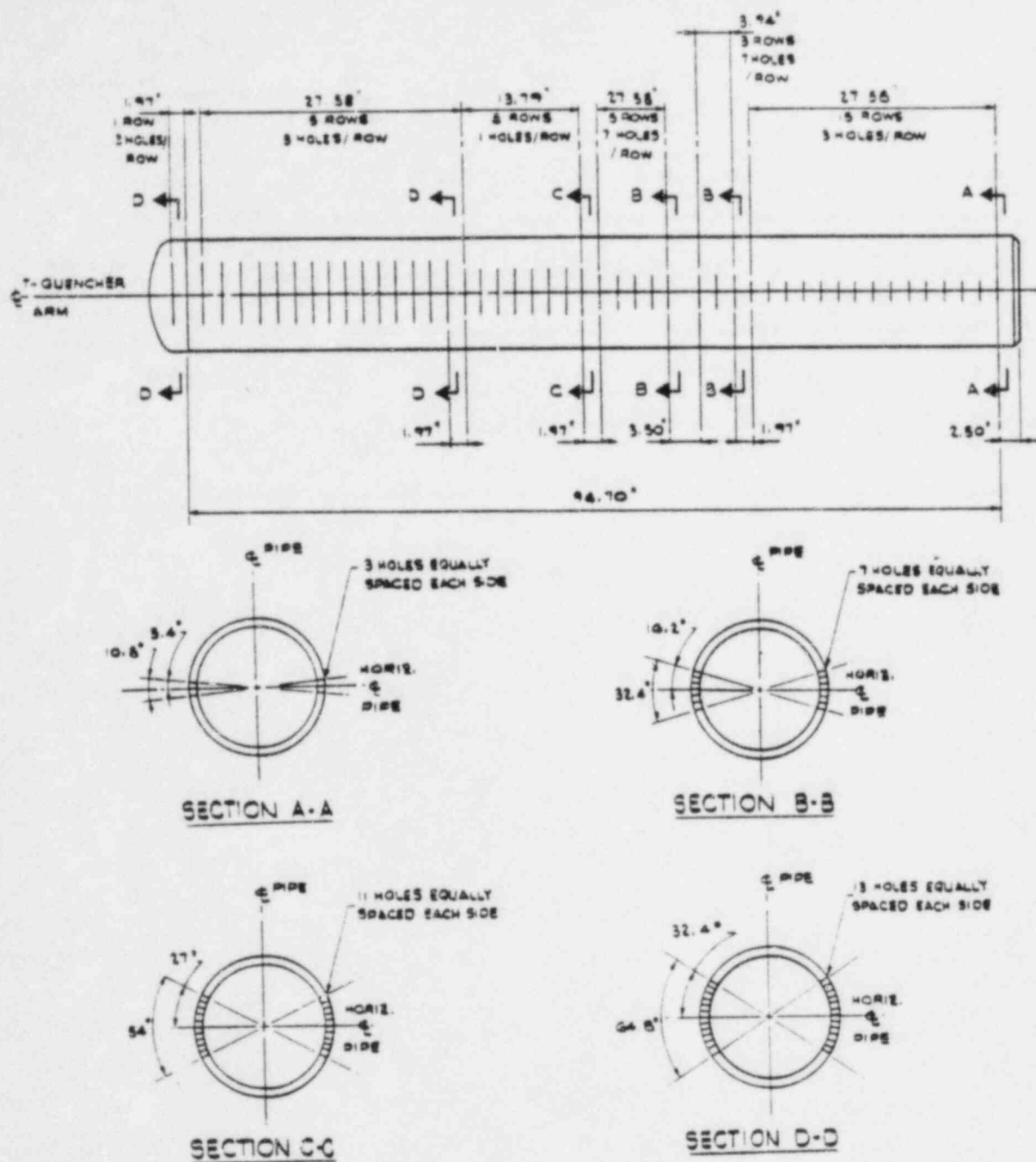
As specified in Section 2.13.9 of Appendix A of NUREG-0661, plant unique SRV testing at Hope Creek will be performed to confirm that the computed loadings and predicted structural responses for SRV discharge loads are conservative for Hope Creek.



VIEW A-A

Figure 1-4.2-1

T-QUENCHER AND SRV DISCHARGE LINE



NOTES:

1. ALL HOLE PATTERNS SYMMETRICAL ABOUT \bar{C} .
2. ALL HOLES ARE 0.391" IN DIAMETER.
3. ALL HOLE SPACINGS NOT DIMENSIONED ARE 1.97" CENTER TO CENTER.

Figure 1-4.2-2
ELEVATION AND SECTION VIEWS OF
T-QUENCHER ARM HOLE PATTERNS

1-4.2.1 SRV Actuation Cases

This section provides a discussion of SRV discharge cases considered for evaluations. The load cases summarized in Table 1-4.2-1 are described as follows.

Load Case A1.1 (Normal Operating Conditions (NOC), First Actuation)

The first actuation of a SRV may occur under normal operating conditions; i.e., the SRVDL is cold, there is air in the drywell, and the water in the SRV is at its normal operating level.

Load Case A1.2 (SBA/IBA, First Actuation)

First actuation of SRV(s) is assumed to occur at the predicted time of ADS actuation. At this time, the SRVDL is full of air at the pressure corresponding to the drywell pressure minus the vacuum breaker set point. The water level inside the line is depressed below the normal operating level because the drywell pressure is higher than the wetwell pressure

by a pressure differential equal to the down-comer submergence.

Load Case Al.3 (DBA, First Actuation)

The same assumptions are used as for Case Al.1, except for SRV flowrate. This load case is bounded by Case Al.1.

Load Case B (First Actuation, Leaking SRV)

First actuation of a SRV may occur under NOC for leaking safety relief valves. For T-quenchers, Load Case Al.1 bounds the leaking SRV load.

Load Case C3.1 (NOC, Subsequent Actuation, Normal Water Leg)

After the SRV is closed following a first actuation (Case Al.1), the steam in the line is condensed, causing a rapid pressure drop which draws water back into the line. At the same time, the vacuum breaker allows air from the drywell to enter the discharge line. The air repressurizes the line and the water

refloods to a point which is higher than its equilibrium height, and oscillates back to its equilibrium point. A subsequent actuation is assumed to occur after the water level oscillations have damped out and the water leg has returned to the normal water level.

Load Case C3.2 (SBA/IBA, Subsequent Actuation)

Following SRV closure after the first actuation (Case A1.2) in the SBA/IBA, the water refloods back into the line while air from the drywell flows through the vacuum breaker into the SRV discharge line. The SRV is assumed to actuate after the water level oscillations have damped out and the level has stabilized at a point determined by the drywell-to-wetwell ΔP minus the vacuum breaker set point.

Load Case C3.3 (SBA/IBA, Subsequent Actuation, Steam in SRVDL)

This case differs from the previous case in that during the reflood transient, steam, instead of air, flows through the vacuum

breaker. Thus, the line contains very little air and the loading imposed on the torus shell from this subsequent SRV actuation is bounded by Case C3.2.

The SRVDL water leg is assumed at its equilibrium height for all subsequent actuation SRV cases. The time after the first valve closure when the equilibrium height is reestablished is calculated using the LDR SRVDL reflood model. Hope Creek primary system transient analyses are used to confirm that more than the minimum required time is available for the SRVDL water leg to return to the equilibrium position. To further insure that the SRVDL water leg will be at its equilibrium height for all subsequent SRV actuation cases, Hope Creek will have delay logic on the two lowest-set relief valves to allow this water leg to clear after initial actuation. For the steam-in-the-drywell conditions, a steam-water convective heat transfer coefficient of 2×10^5 BTU/hr·ft²·°R is used. This conservative coefficient is based on the results of a literature survey on chugging and the downcomer water column rise characteristics during chugging in the Mark I Full-Scale Test Facility.

The number of SRV's predicted to actuate for each of the above conditions is maximized in performing the Hope Creek structural evaluations, as documented in the remaining PUAR volumes. Section 1-4.3 describes the other hydrodynamic loads which are combined with SRV loads.

Table 1-4.2-1

SRV LOAD CASE/INITIAL CONDITIONS

DESIGN INITIAL CONDITION, LOAD CASE	ANY ONE VALVE	ADS VALVES	MULTIPLE VALVES (1)
NOC, FIRST ACTUATION	A1.1		A3.2
SBA/IBA, FIRST ACTUATION	A1.2	A2.2	A3.2
DBA, FIRST ACTUATION ⁽²⁾	A1.3		
NOC, LEAKING SRV ⁽³⁾			B3.1 ⁽⁴⁾
NOC, SUBSEQUENT ACTUATION			C3.1
SBA/IBA, SUBSEQUENT ACTUATION, AIR IN SRVDL			C3.2
SBA/IBA, SUBSEQUENT ACTUATION, STEAM IN SRVDL			C3.3

NOTES:

1. THE NUMBER (ONE OR MORE) AND LOCATION OF VALVES ASSUMED TO ACTUATE ARE DETERMINED BY PLANT UNIQUE ANALYSIS.
2. THIS ACTUATION IS ASSUMED TO OCCUR COINCIDENT WITH THE POOL SWELL EVENT. ALTHOUGH SRV ACTUATION CAN OCCUR LATER IN THE DBA, THE RESULTING AIR LOADING ON THE TORUS SHELL IS NEGLIGIBLE SINCE THE AIR AND WATER INITIALLY IN THE LINE WILL BE CLEARED AS THE DRYWELL-TO-WETWELL ΔP INCREASES DURING THE DBA TRANSIENT.
3. THIS IS APPLICABLE TO RAMSHEAD DISCHARGE ONLY.
4. ONLY ONE VALVE OF THE MULTIPLE GROUP IS ASSUMED TO LEAK.

The flow of high pressure steam into the discharge line when a SRV opens results in the development of a pressure wave at the entrance to the line. During the early portion of this transient, a substantial pressure differential exists across the pressure wave. This pressure differential, plus momentum effects resulting from steam (or water in the initially submerged pipe runs) flowing through elbows in the line, produce transient thrust loads on the SRV discharge piping segments. These loads are considered in the evaluation of the SRV piping restraints, the SRV piping penetrations in the vent lines, and the T-quencher support system.

The LDR presents the bases, assumptions, and descriptions of the SRV discharge line clearing analytical model. The parameters affecting SRVDL clearing loads development are the SRVDL geometry, plant specific initial conditions for the SRV actuation cases, and the SRV mass flowrate. Table 1-4.2-2 presents plant specific initial conditions for various actuation cases. Table 1-4.2-3 presents common (but case-independent) SRVDL analysis input parameters. All calculation input procedures for

the SRVDL clearing model are consistent with the LDR.

The line clearing model is used to obtain transient values for each SRV actuation case for each SRVDL for the following parameters or loads.

- SRVDL Pressures and Temperatures
- Thrust Loads on SRVDL Piping Segments
- T-quencher Internal Discharge Pressure and Temperature
- Water Slug Mass Flowrate
- Water Clearing Time, Velocity, and Acceleration

The values obtained for T-quencher discharge pressure and water clearing time are used as input to evaluate the torus shell loads (Section 1-4.2.3) and SRV air bubble drag loads (Section 1-4.2.4) on submerged structures. The water slug mass flowrate and acceleration are used as inputs to calculations of SRV water jet loads on submerged structures (Section 1-4.2.4).

The water clearing thrust load along the axis of the T-quencher (due to the uneven flowsplit in the ramshead), and the thrust load perpendicular to the T-quencher arms (due to a skewed air-water interface) are calculated as specified in the LDR.

The calculation procedures, load definitions, and applications used for SRV water and air clearing thrust and all other SRV water clearing loads are in accordance with the LDR and Appendix A of NUREG-0661. The effects of SRV line clearing loads on the SRV piping and supports are evaluated in PUAR Volume 5.

Table 1-4.2-2

PLANT UNIQUE INITIAL
CONDITIONS FOR ACTUATION CASES
USED FOR SRVDL CLEARING TRANSIENT LOAD DEVELOPMENT

PARAMETER	CASE A1.1	CASE A1.2	CASE C3.1	CASE C3.2
PRESSURE IN THE WETWELL (psia)	15.45	35.357	15.45	35.357
PRESSURE IN THE DRYWELL (psia)	15.45	36.8	15.45	36.8
ΔP VACUUM BREAKER (psid)	0.3	0.3	0.3	0.3
INITIAL PIPE WALL TEMPERATURE IN THE WETWELL AIRSPACE (°F)	115°	340°	350°	350°
INITIAL PIPE WALL TEMPERATURE IN THE SUPPRESSION POOL (°F)	95°	112°	95°	112°
INITIAL AIR PRESSURE IN SRVDL (psia)	15.15	36.5	15.15	36.5
INITIAL AIR DENSITY IN SRVDL (lbm/ft ³)	0.0711	0.1231	0.0505	0.1216
INITIAL WATER VOLUME IN SRVDL AND T-QUENCHER (ft ³)	13.867	12.206	13.867	13.523

Table 1-4.2-3

SRVDL ANALYSIS PARAMETERS

PARAMETER	VALUE
DESIGN SRV FLOW RATE (lbm/sec)	306.59
STEAM LINE PRESSURE (psia)	1179
STEAM DENSITY IN THE STEAM LINE (lbm/ft ³)	2.701
RATIO OF AREAS OF DISCHARGE DEVICE EXIT TO TOTAL T-QUENCHER ARM	0.94

NOTES:

1. DESIGN FLOW RATE 22.5% ABOVE ASME FLOW RATE.
2. PRESSURE 3% ABOVE SET PRESSURE.

1-4.2.3 SRV Loads on the Torus Shell

Following an SRV actuation, the air mass in the SRVDL is expelled into the suppression pool, forming many small air bubbles. These bubbles then coalesce into four larger bubbles which expand and contract as they rise and break through the pool surface. The positive and negative dynamic pressures developed within these bubbles result in an oscillatory, attenuated pressure loading on the torus shell.

The analytical model which is used to predict air bubble and torus shell boundary pressures resulting from SRV discharge is similar to that described in Reference 14. The analytical model in Reference 14 was modified slightly to more closely bound the magnitudes and time characteristics of pressures observed in the Monticello test. Figure 1-4.2-3 shows a comparison of the shell pressure-time history measured during the Monticello test to the shell pressure-time history computed using the revised analytical model. The comparison is shown for shell pressures at the bottom of the torus beneath the quencher, where the highest shell pressures were observed. Figure 1-4.2-3 shows that

the predicted shell pressures envelop those observed in the Monticello test.

The pressure-time history generated using the analytical model discussed above is used to perform a forced vibration analysis of the suppression chamber. The phenomena associated with SRV discharge into the suppression pool are characteristic of an initial value or free vibration condition rather than a forced vibration condition. Correction factors are applied to convert the forced vibration response to a free vibration response.

The correction factors are developed using single degree-of-freedom analogs. The factors vary with the ratio of load frequency to structural frequency and are applied to the response (displacement, velocity, and acceleration) associated with each structural mode. Figure 1-4.2-4 shows the modal correction factors (MCF) which are used in the suppression chamber evaluation.

Table 1-4.2-4 shows a comparison of shell membrane stresses and column forces observed in the Monticello test with those values predicted using the analytical methods and correction factors

described above. The table shows that predicted forces and stresses conservatively bound the measured values at all locations. A series of in-plant tests will be performed at Hope Creek after fuel load. These tests are expected to provide additional confirmation that the computed loadings and predicted structural response due to SRV discharge are conservative.

Table 1-1.2-4

COMPARISON OF ANALYSIS AND MONTICELLO TEST RESULTS

QUANTITY	LOCATION	ANALYSIS	TEST	<u>ANALYSIS</u> <u>TEST</u>
SUPPRESSION CHAMBER SHELL MEMBRANE STRESSES (ksi)	MIDBAY 90° FROM BDC REACTOR SIDE	2.8	0.6	4.7
	MIDBAY 52.5° FROM BDC REACTOR SIDE	2.3	1.1	2.1
	MIDBAY 12.4° FROM BDC OPPOSITE REACTOR	2.2	1.4	1.6
	MIDBAY 12.4° FROM BDC REACTOR SIDE	2.1	1.7	1.2
	MIDBAY 52.5° FROM BDC OPPOSITE REACTOR	2.5	1.1	2.3
	1/4 BAY 12.4° FROM BDC OPPOSITE REACTOR	2.2	1.4	1.6
TORUS COLUMN UPLIFT LOADS (kips)	INSIDE COLUMN	123.9	49.0	2.5
	OUTSIDE COLUMN	157.8	52.5	3.0
TORUS COLUMN DOWN LOADS (kips)	INSIDE COLUMN	152.9	64.5	2.4
	OUTSIDE COLUMN	178.2	78.5	2.3

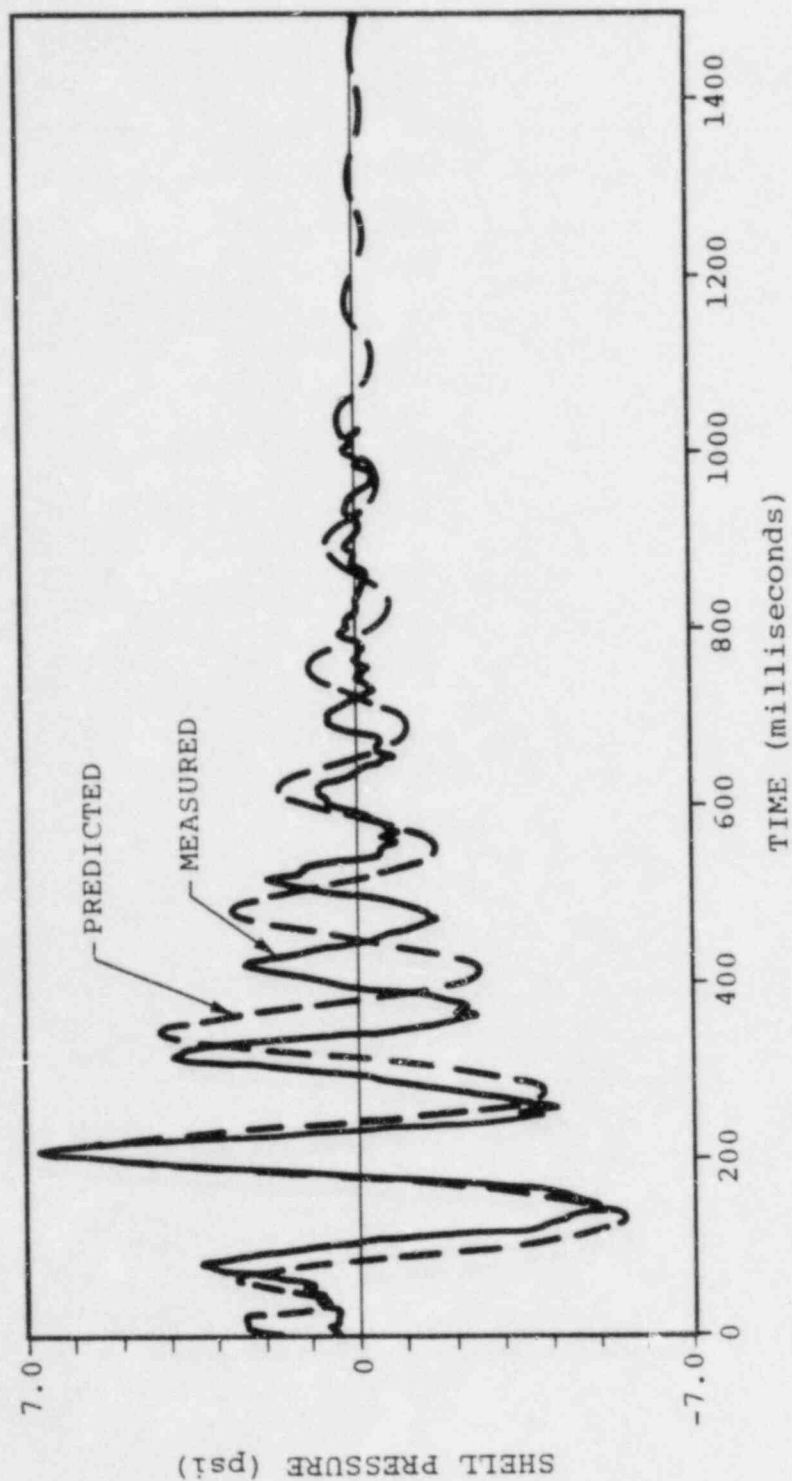


Figure 1-4.2-3

COMPARISON OF PREDICTED AND MEASURED SHELL PRESSURE
TIME-HISTORIES FOR MONTICELLO TEST 801

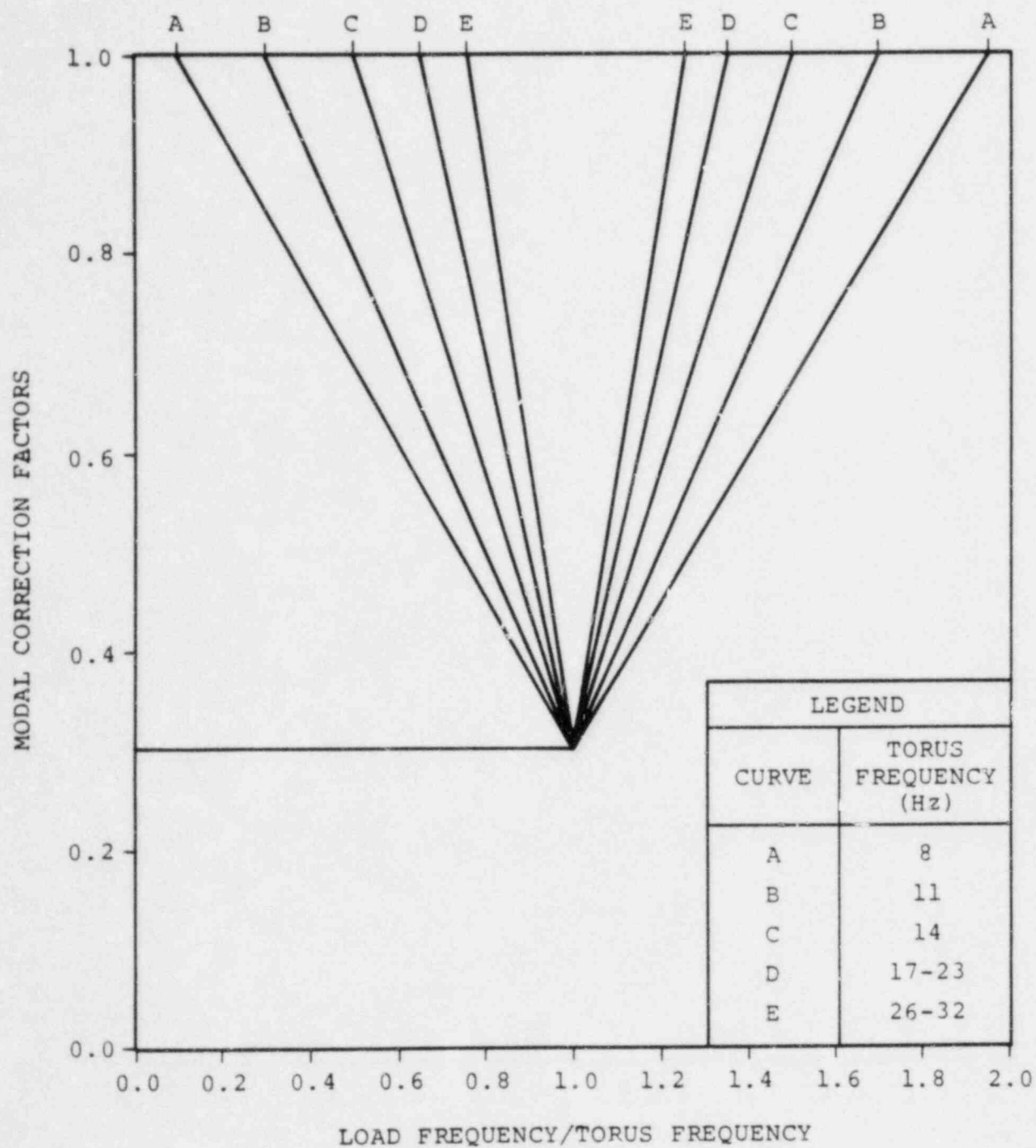


Figure 1-4.2-4

MODAL CORRECTION FACTORS FOR ANALYSIS
OF SRV DISCHARGE TORUS SHELL LOADS

1-4.2.4 SRV Loads on Submerged Structures

This section addresses the load definition procedures for determining SRV loads on submerged structures due to T-quencher water jets and air bubbles.

When a SRV is actuated, water initially contained in the submerged portion of the SRVDL is forced out of the T-quencher through holes in the arms, forming orifice jets. Some distance downstream, the orifice jets merge to form column jets. Further downstream, the column jets merge to form the quencher arm jets. As soon as the water flow through the arm hole ceases, the quencher arm jet velocity decreases rapidly and the jet penetrates a limited distance into the pool. The T-quencher water jets create drag loads on nearby submerged structures within the jet path.

Oscillating bubbles resulting from a SRV actuation create an unsteady three-dimensional flow field, and therefore induce acceleration and standard drag forces on the submerged structures in the suppression pool.

a. T-quencher Water Jet Loads

The T-quencher water jet model conservatively models the T-quencher water jet test data. The bases, justification, and assumptions for the Mark I T-quencher model are presented in Reference 1. The SRV T-quencher water jet analytical model calculation procedure and application are in accordance with Mark I LDR techniques. Figure 1-4.2-5 shows a plan view of the T-quencher arm jet sections.

b. SRV Bubble-Induced Drag Loads

The SRV bubble drag load development methodology, load definition, and application for the Hope Creek PUA are performed utilizing the T-quencher geometry shown in Figures 1-4.2-1 and 1-4.2-2. The techniques utilized in developing the SRV bubble drag loads are in accordance with the LDR and Appendix A of NUREG-0661. Dynamic load factors are derived from Monticello in-plant SRV test data.

A bubble pressure bounding factor based on Monticello test data in lieu of the LDR value

of 2.5 is utilized for Hope Creek SRV load development. A value of 1.75 produces results which bound the peak positive bubble pressure and maximum bubble pressure differential from the Monticello T-quencher test data. Using 1.75, the calculated values for Monticello are 9.9 psid and 18.1 psid, respectively. The predicted values correspond to the single valve actuation, normal water level, and cold pipe case listed in Table 3.2 of Reference 14.

For submerged structures with sharp corners such as T-beams, I-beams, etc., the acceleration drag volumes are calculated using the methodology in Section 1-4.1.5.

The effects of SRV loads on submerged structures are evaluated in PUAR volumes 2, 3, 5, and 6.

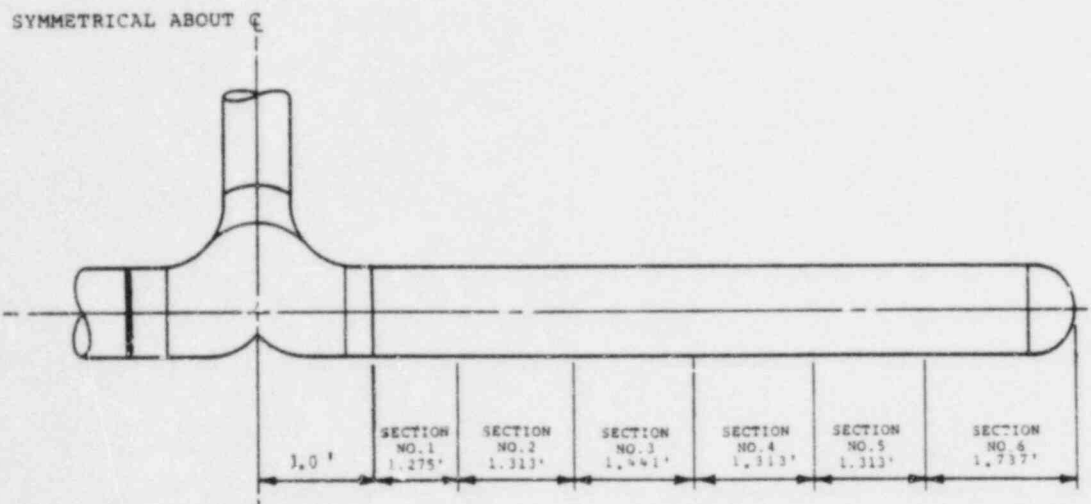


Figure 1-4.2-5

PLAN VIEW OF T-QUENCHER
ARM WATER JET SECTIONS

BPC-01-300-1
Revision 0

1-4.107

Not all of the suppression pool hydrodynamic loads discussed in this evaluation can occur at the same time. In addition, the load magnitudes and timing vary, depending on the accident scenario being considered. Therefore, it is necessary to construct a series of event combinations to describe the circumstances under which individual loads might combine.

Tables 1-3.2-1 and 1-3.2-2 show the event combinations used in the plant unique analysis. The combinations of load cases were determined from typical plant primary system and containment response analyses, with considerations for automatic actuation, manual actuation, and single active failures of the various systems in each event. This section describes the event sequences for the following postulated loss-of-coolant accidents.

- Design Basis Accident
- Intermediate Break Accident
- Small Break Accident

Table 1-4.3-1 identifies the SRV and LOCA loads which potentially affect structural components and identifies the appropriate section of this report defining the loads. For SRV piping and other structures within the wetwell, the locations of the structural components are considered to determine if any of the identified conditions affect the structures.

Table 1-4.3-1

SRV AND LOCA STRUCTURAL LOADS

LOADS	STRUCTURES							OTHER WETWELL INTERIOR STRUCTURES		
	TORUS SHELL	TORUS SUPPORT SYSTEM	MAIN VENTS	VENT HEADER	DOWNCOMERS	SRV PIPING	TORUS-ATTACHED PIPING	ABOVE NORM WATER LEVEL	ABOVE BOTTOM OF DOWNCOMERS AND BELOW NORM WATER LEVEL	BELOW BOTTOM OF DOWNCOMERS
1-4.1.1 CONTAINMENT PRESSURE AND TEMPERATURE RESPONSE	X	X	X	X	X	X	X	X	X	X
1-4.1.2 VENT SYSTEM DISCHARGE LOADS			X	X	X					
1-4.1.3 POOL SWELL LOADS ON THE TORUS SHELL	X	X								
1-4.1.4 POOL SWELL LOADS ON ELEVATED STRUCTURES										
1-4.1.4.1 IMPACT AND DRAG LOADS ON THE VENT SYSTEM			X	X	X					
1-4.1.4.2 IMPACT AND DRAG LOADS ON OTHER STRUCTURES			X			X	X	X		
1-4.1.4.3 POOL SWELL FROTH IMPINGEMENT LOADS			X					X		
1-4.1.4.4 POOL FALLBACK LOADS						X	X	X	X	
1-4.1.5 LOCA WATERJET LOADS ON SUBMERGED STRUCTURES						X	X			X
1-4.1.6 LOCA BUBBLE-INDUCED LOADS ON SUBMERGED STRUCTURES						X	X			X
1-4.1.7 CONDENSATION OSCILLATION LOADS										
1-4.1.7.1 CO LOADS ON THE TORUS SHELL	X	X								
1-4.1.7.2 CO LOADS ON THE DOWNCOMERS AND VENT SYSTEM			X	X	X					
1-4.1.7.3 CO LOADS ON SUBMERGED STRUCTURES						X	X		X	X
1-4.1.8 CHUGGING LOADS										
1-4.1.8.1 CHUGGING LOADS ON THE TORUS SHELL	X	X								
1-4.1.8.2 CHUGGING DOWNCOMER LATERAL LOADS				X	X					
1-4.1.8.3 CHUGGING LOADS ON SUBMERGED STRUCTURES						X	X		X	X
1-4.2 SAFETY RELIEF VALVE DISCHARGE LOADS										
1-4.2.2 SRV DISCHARGE LINE CLEARING LOADS						X				
1-4.2.3 SRV LOADS ON THE TORUS SHELL	X	X								
1-4.2.4 SRV LOADS ON SUBMERGED STRUCTURES					X	X	X		X	X

The postulated DBA for the Mark I containment evaluation is the instantaneous guillotine rupture of the largest pipe in the primary system (the recirculation line). Figures 1-4.3-1 through 1-4.3-3 present the load combinations for the DBA. Table 1-4.3-2 presents the nomenclature for these figures. The bar charts for the DBA show the loading condition combinations for postulated breaks large enough to produce significant pool swell. The length of the bars in the figures indicates the time periods during which the loading conditions may occur. Loads are considered to act simultaneously on a structure at a specific time if the loading condition bars overlap at that time. For SRV discharge, the loads may occur at any time during the indicated time period. The assumption of combining a SRV discharge with the DBA is beyond the design basis for Hope Creek. Therefore, the DBA and SRV load combination is evaluated only to demonstrate containment structural capability. Table 1-4.3-3 shows the SRV discharge loading conditions.

Table 1-4.3-2

EVENT TIMING NOMENCLATURE

TIME	DESCRIPTION
t_1	THE ONSET OF CONDENSATION OSCILLATION
t_2	THE BEGINNING OF CHUGGING
t_3	THE END OF CHUGGING
t_4	TIME OF COMPLETE REACTOR DEPRESSURIZATION
t_{ADS}	ADS ACTUATION ON HIGH DRYWELL PRESSURE AND LOW REACTOR WATER LEVEL. THE ADS IS ASSUMED TO BE ACTUATED BY THE OPERATOR FOR THE SBA.

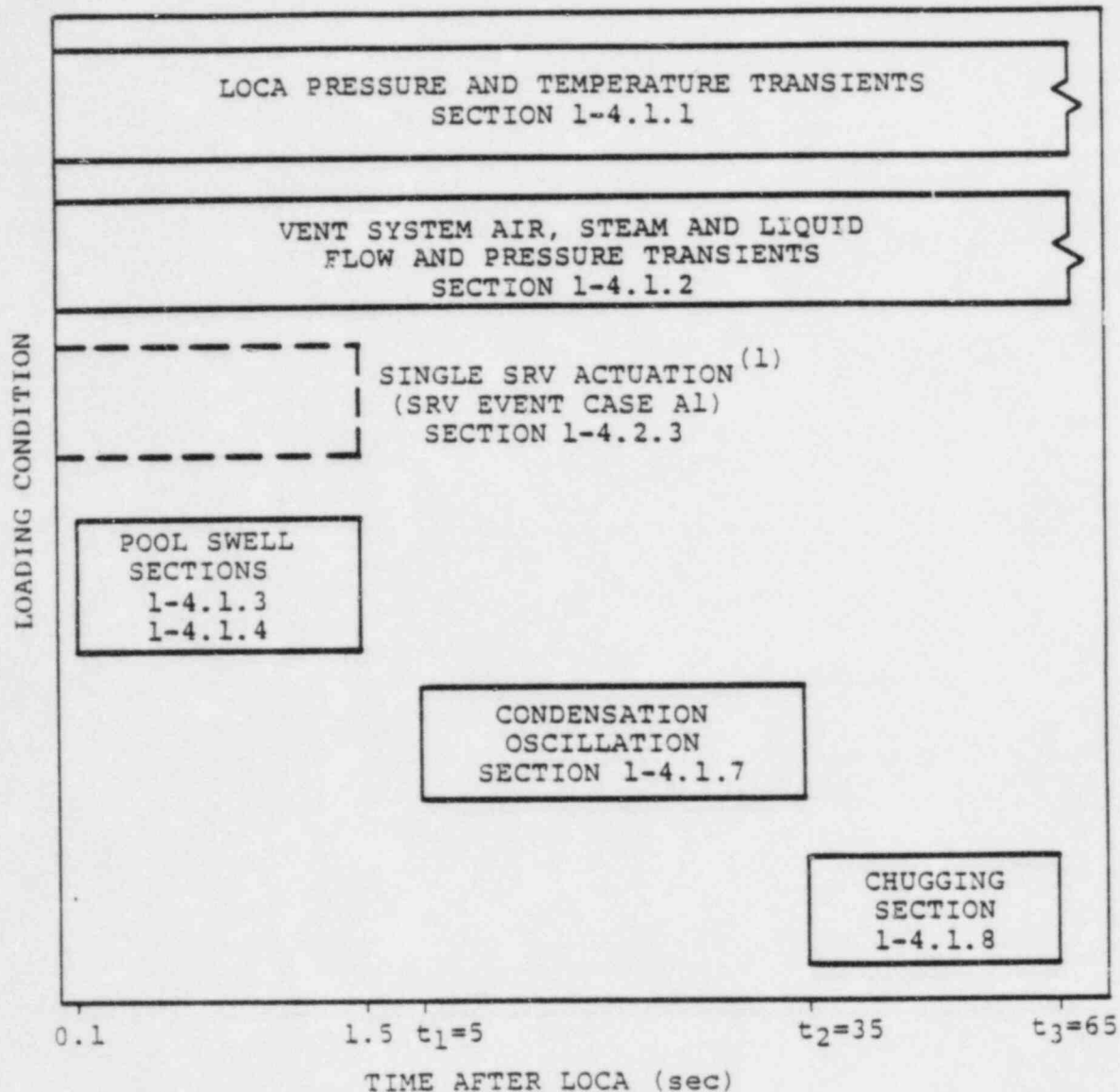
Table 1-4.3-3

SRV DISCHARGE LOAD CASES
FOR MARK I STRUCTURAL ANALYSIS

INITIAL CONDITIONS	ANY ONE VALVE	ADS VALVES	MULTIPLE VALVES (1)
FIRST ACTUATION	A 1	A 2	A 3
FIRST ACTUATION, LEAKING SRV(2)			B 3
SUBSEQUENT ACTUATION			C 3

NOTES:

1. THE NUMBER (ONE OR MORE) AND LOCATION OF SRV's ASSUMED TO ACTUATE ARE DETERMINED BY PLANT UNIQUE ANALYSES.
2. THE LOADS FOR T-QUENCHER DISCHARGE DEVICES ARE NOT AFFECTED BY LEAKING SRV's. NO SRV's ARE CONSIDERED TO LEAK PRIOR TO A LOCA.



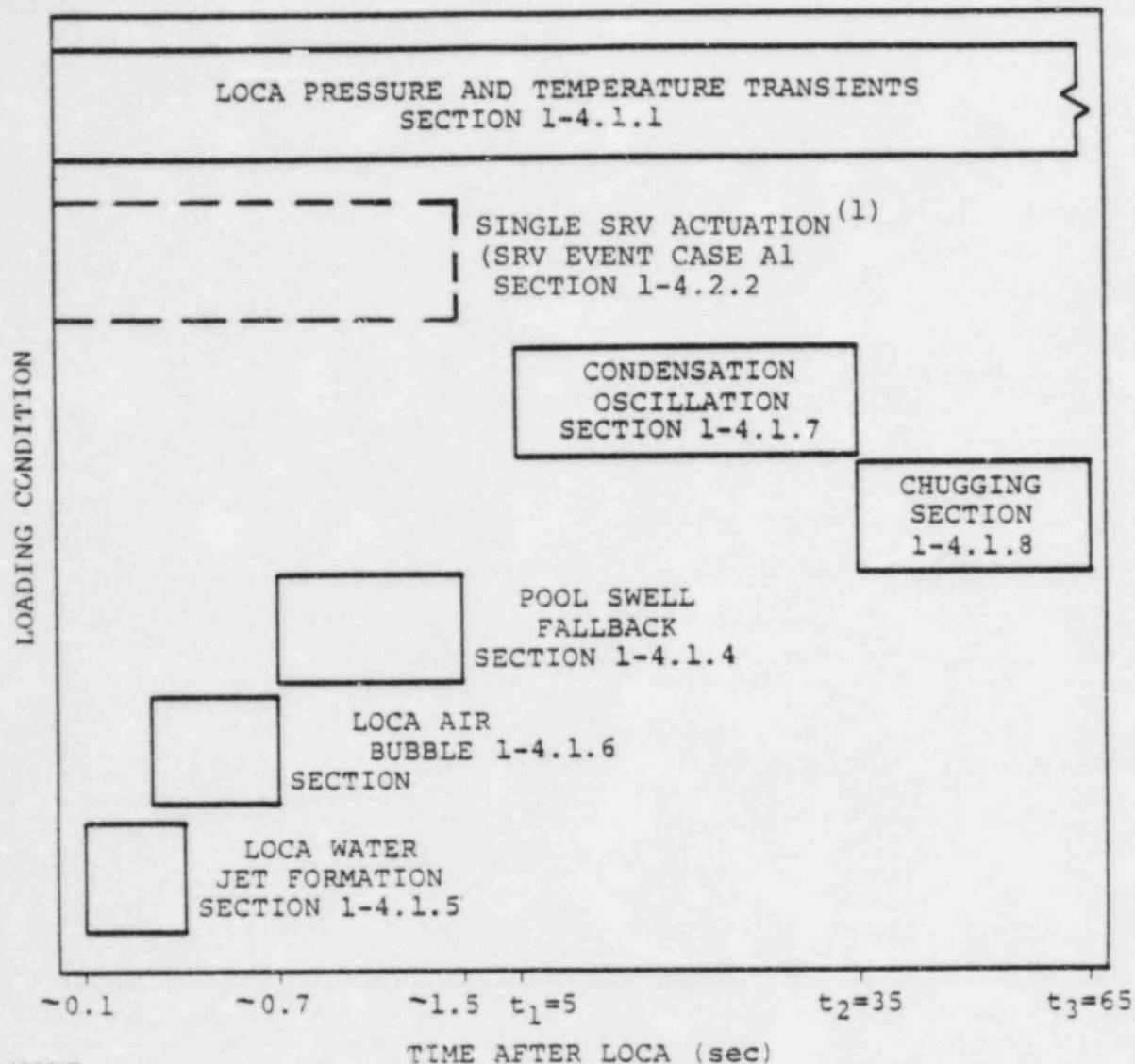
NOTE:

1. THIS ACTUATION IS ASSUMED TO OCCUR COINCIDENT WITH THE POOL SWELL EVENT. ALTHOUGH SRV ACTUATION CAN OCCUR LATER IN THE DBA, THE RESULTING AIR LOADING ON THE TORUS SHELL IS NEGLIGIBLE, SINCE THE AIR AND WATER INITIALLY IN THE LINE WILL BE CLEARED AS THE DRYWELL-TO-WETWELL ΔP INCREASES DURING THE DBA TRANSIENT.

Figure 1-4.3-1

LOADING CONDITION COMBINATIONS FOR THE VENT HEADER,
MAIN VENTS, DOWNCOMERS, AND TORUS SHELL DURING A DBA

BPC-01-300-1
Revision 0

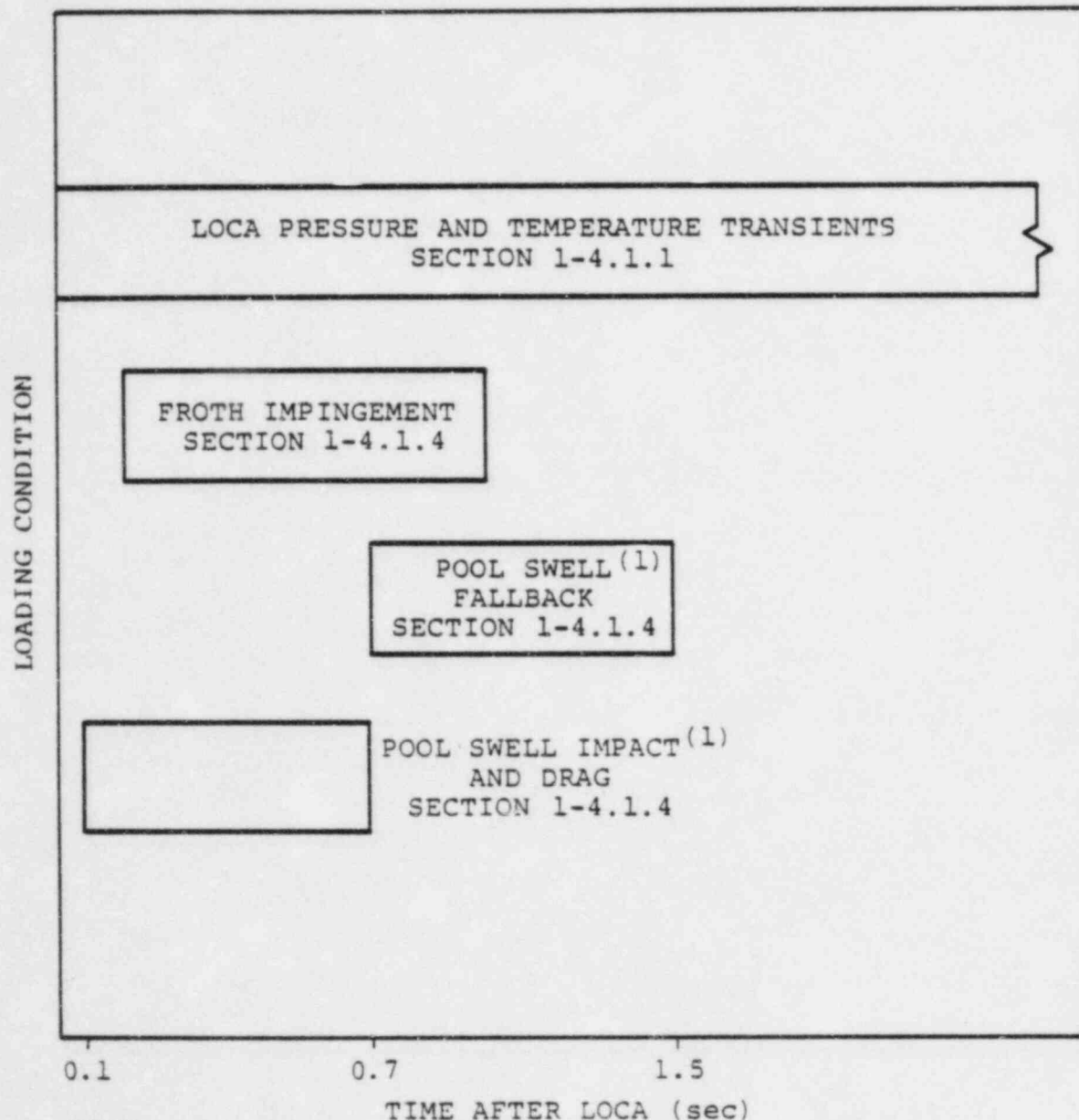


NOTE:

1. THIS ACTUATION IS ASSUMED TO OCCUR COINCIDENT WITH THE POOL SWELL EVENT. ALTHOUGH SRV ACTUATION CAN OCCUR LATER IN THE DBA, THE RESULTING AIR LOADING ON THE TORUS SHELL IS NEGLIGIBLE, SINCE THE AIR AND WATER INITIALLY IN THE LINE WILL BE CLEARED AS THE DRYWELL-TO-WETWELL ΔP INCREASES DURING THE DBA TRANSIENT.

Figure 1-4.3-2

LOADING CONDITION COMBINATIONS FOR SUBMERGED
STRUCTURES DURING A DBA



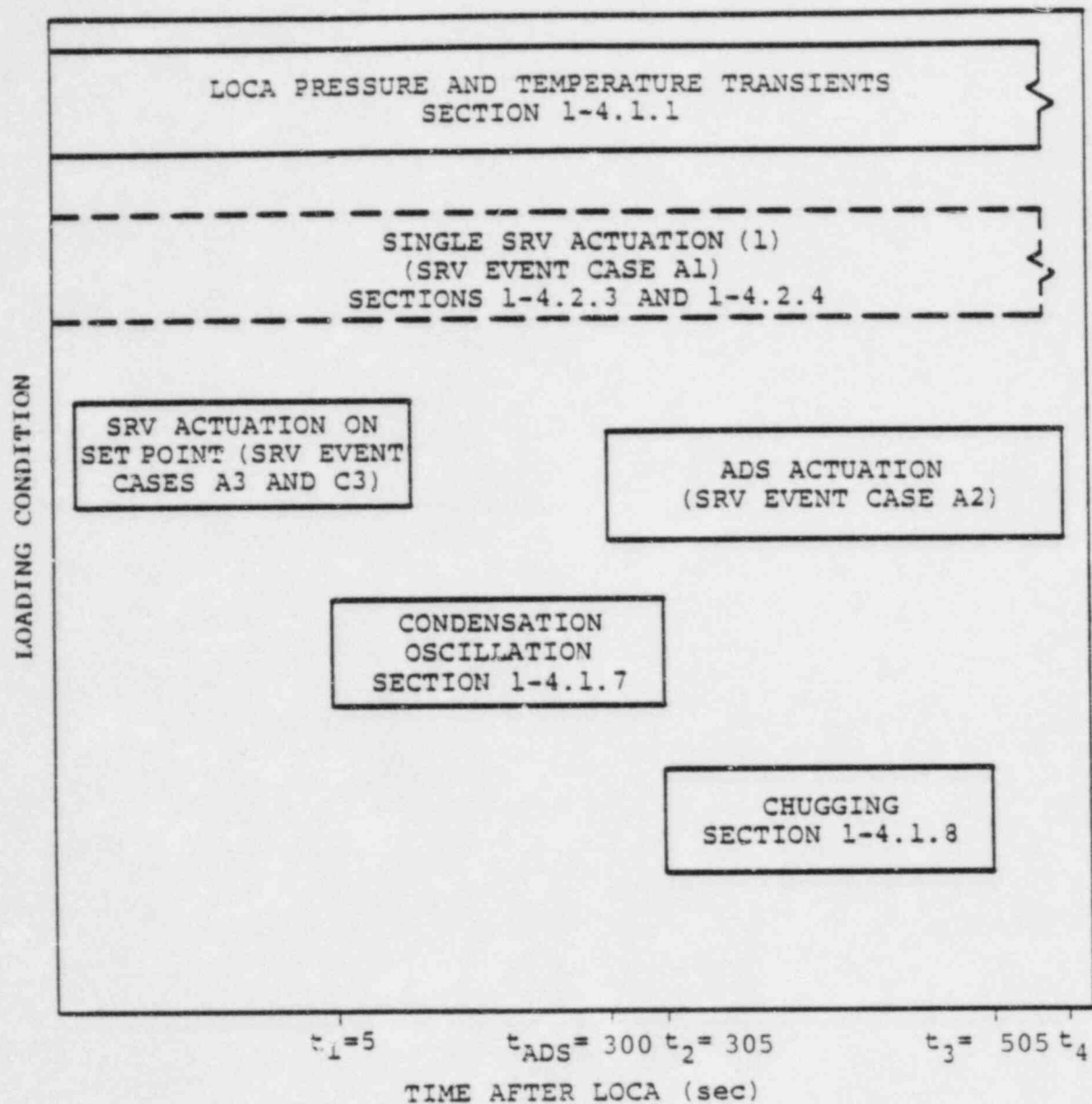
NOTE:

1. STRUCTURES ARE BELOW MAXIMUM POOL SWELL HEIGHT.

Figure 1-4.3-3

LOADING CONDITION COMBINATIONS FOR
STRUCTURES ABOVE SUPPRESSION POOL DURING A DBA

The bar chart in Figure 1-4.3-4 shows conditions for a break size large enough such that the HPCI system cannot prevent ADS actuation on low-water level, but for break sizes smaller than that which would produce significant pool swell loads. A break size of 0.1 ft^2 is assumed for an IBA. Table 1-4.3-3 shows SRV discharge loading conditions. The IBA break is too small to cause significant pool swell.



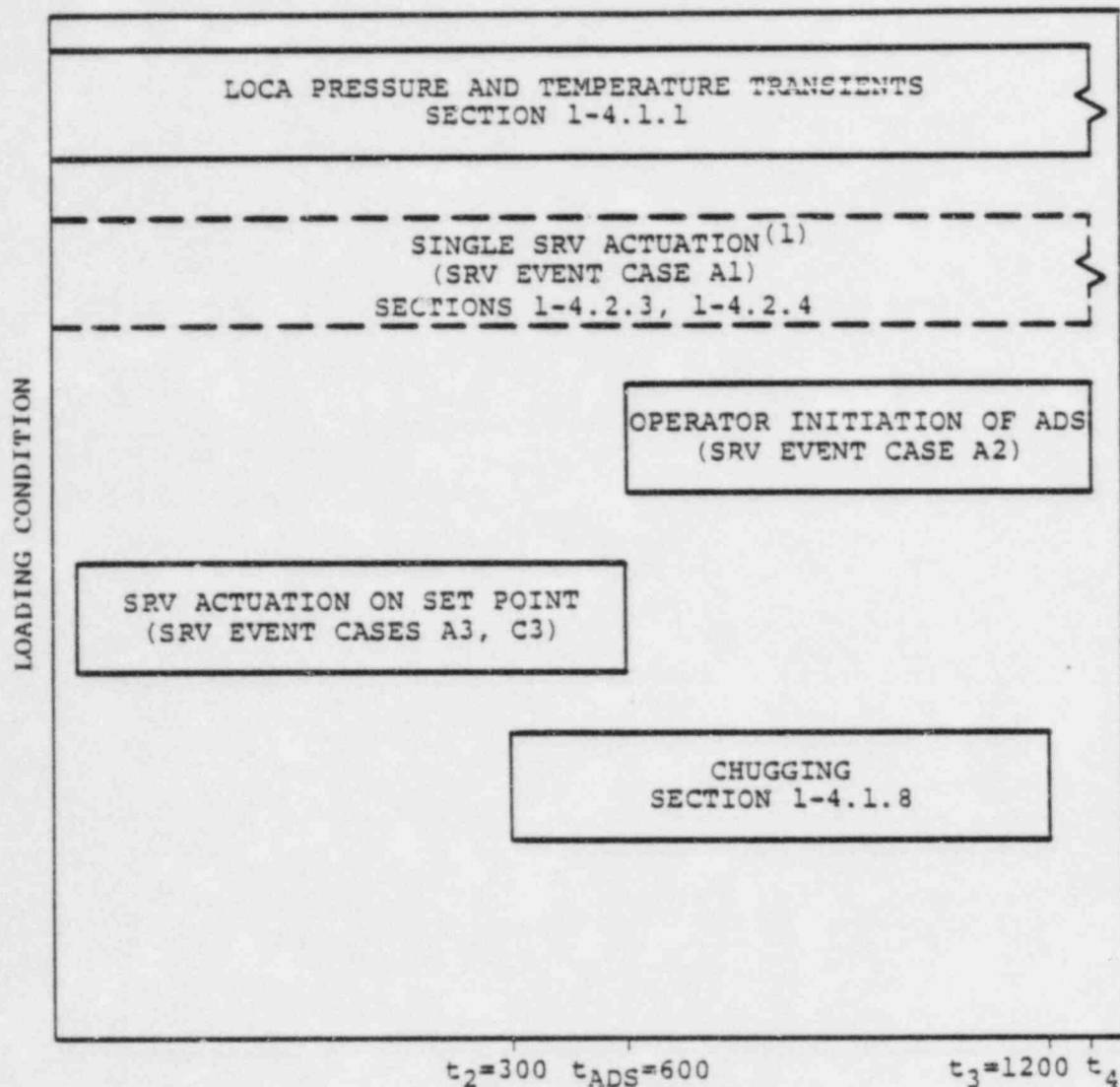
NOTE:

1. LOADING NOT COMBINED WITH OTHER SRV CASES.

Figure 1-4.3-4

LOADING CONDITION COMBINATIONS FOR THE
VENT HEADER, MAIN VENTS, DOWNCOMERS, TORUS SHELL,
AND SUBMERGED STRUCTURES DURING AN IBA

The bar chart in Figure 1-4.3-5 shows conditions for a break size equal to 0.01 ft^2 . For a SBA, the HPCI system would be able to maintain the water level and the reactor would be depressurized by means of operator initiation of the automatic depressurization system. Table 1-4.3-3 identifies the SRV discharge loading conditions. The SBA break is too small to cause significant pool swell, and CO does not occur during a SBA. The ADS is assumed to be initiated by the operator 10 minutes after the SBA begins. With the concurrence of the NRC (Reference 16), the procedures which the operator will use to perform this action are being developed as part of the Emergency Procedures Guidelines.



TIME AFTER LOCA (sec)

NOTE:

1. LOADING NOT COMBINED WITH OTHER SRV CASES.

Figure 1-4.3-5

LOADING CONDITION COMBINATIONS FOR THE VENT HEADER,
MAIN VENTS, DOWNCOMERS, TORUS SHELL, AND
SUBMERGED STRUCTURES DURING A SBA

LIST OF REFERENCES

1. "Mark I Containment Program Load Definition Report," General Electric Company, NEDO-21888, Revision 2, November 1981.
2. "Mark I Containment Program Structural Acceptance Criteria Plant-Unique Analysis Applications Guide," Task Number 3.1.3, Mark I Owners Group, General Electric Company, NEDO-24583, Revision 1, July 1979.
3. "Mark I Containment Long-Term Program," Safety Evaluation Report, USNRC, NUREG-0661, July 1980; Supplement 1, August 1982.
4. "Final Safety Analysis Report (FSAR)," Hope Creek Generating Station, Public Service Electric and Gas Company, October 1983.
5. Regulatory Guide 1.61, "Damping Values for Seismic Design of Nuclear Power Plants," U.S. Nuclear Regulatory Commission Office of Standards Development, Revision 0, October 1973.
6. "The General Electric Pressure Suppression Containment Analytical Model," General Electric Company, NEDO-10320, April 1971; Supplement 1, May 1971; Supplement 2, January 1973.
7. "Mark I Containment Program Plant Unique Load Definition," Hope Creek Generating Station, General Electric Company, NEDO-24579, Revision 1, January 1982.
8. "Mark I Containment Program Quarter-Scale Plant Unique Tests, Task Number 5.5.3, Series 2," General Electric Company, NEDE-21944-P, Volumes 1-4, April 1979.
9. Patton, K.T., "Tables of Hydrodynamic Mass Factors for Translational Motion," ASME Manuscript, Chicago, November 7-11, 1965.
10. Miller, R.R., "The Effects of Frequency and Amplitude of Oscillation on the Hydrodynamic Masses of Irregularly-Shaped Bodies," MS Thesis, University of Rhode Island, Kingston, R.I., 1965.

11. Fitzsimmons, G. W. et al., "Mark I Containment Program Full-Scale Test Program Final Report, Task Number 5.11," General Electric Company, NEDE-24539-P, April 1979.
12. "Mark I Containment Program Letter Reports MI-LR-81-01 and MI-LR-81-01-P, Supplemental Full-Scale Condensation Test Results and Load Confirmation-Proprietary and Nonproprietary Information," General Electric Company, May 6, 1981.
13. "Mark I Containment Program - Full-Scale Test Program - Evaluation of Supplemental Tests," General Electric Company, NEDO-24539, Supplement 1, July 1981.
14. Hsiao, W. T. and Valandani, P., "Mark I Containment Program Analytical Model for Computing Air Bubble and Boundary Pressures Resulting from an SRV Discharge Through a T-Quencher Device," General Electric Company, NEDE-21878-P, August 1979.
15. Letter from T. A. Ippolito (NRC) to J. F. Quirk (GE) dated October 16, 1981.